



Title	Studies on immunosuppression caused by prostaglandin E2 during chronic infections of cattle
Author(s)	佐治木, 大和
Citation	北海道大学. 博士(獣医学) 甲第14554号
Issue Date	2021-03-25
DOI	10.14943/doctoral.k14554
Doc URL	http://hdl.handle.net/2115/81760
Type	theses (doctoral)
File Information	Yamato_Sajiki.pdf



[Instructions for use](#)

**Studies on immunosuppression caused by
prostaglandin E₂ during chronic infections of cattle**

牛慢性感染症における
プロスタグランジン E₂ を介した免疫抑制に関する研究

Yamato SAJIKI

CONTENTS

CONTENTS-----	2
ABBREVIATIONS-----	4
NOTES-----	6

PREFACE-----	7
--------------	---

CHAPTER I

The suppression of Th1 immune responses by prostaglandin E₂ in cattle infected with *Mycobacterium avium* subsp. *paratuberculosis*

INTRODUCTION-----	14
MATERIALS AND METHODS-----	16
RESULTS-----	22
DISCUSSION-----	33
SUMMARY-----	35

CHAPTER II

Antiviral efficacy of COX-2 inhibitor combined with anti-PD-L1 antibody in bovine leukemia virus infection

INTRODUCTION-----	37
MATERIALS AND METHODS-----	38
RESULTS-----	44
DISCUSSION-----	57
SUMMARY-----	60

CHAPTER III

The enhancement of immunotherapeutic efficacy of anti-PD-L1 antibody in combination with an EP4 antagonist

INTRODUCTION-----	62
MATERIALS AND METHODS-----	64
RESULTS-----	70
DISCUSSION-----	82
SUMMARY-----	84

CONCLUSION -----	85
AKNOWLEDGEMENTS -----	87
REFERENCES -----	89
SUMMARY IN JAPANESE -----	105

ABBREVIATIONS

Ab	antibody
AL	aleukemic
APC	allophycocyanin
BLV	bovine leukemia virus
B-PPD	purified protein derivative from <i>M. bovis</i> BCG strain
BSA	bovine serum albumin
cAMP	cyclic adenosine monophosphate
CFSE	carboxyfluorescein diacetate succinimidyl ester
chAb	chimeric antibody
Con A	concanavalin A
COX	cyclooxygenase
CRE	cAMP-response element
CTL	cytotoxic T cell
Cy	cyanin
DC	dendritic cell
DMSO	dimethyl sulfoxide
EBL	enzootic bovine leukosis
ELISA	enzyme-linked immunosorbent assay
EP	E prostanoid
FCS	fetal calf serum
FITC	fluorescein isothiocyanate
FLK	fetal lamb kidney
Foxp3	forkhead box P3
HIV	human immunodeficiency virus
HPGD	15-hydroxyprostaglandin dehydrogenase
IFN	interferon
IL	interleukin
J-PPD	Johnin purified protein derivative
LAG-3	lymphocyte activation gene 3
LTR	long terminal repeat
mAb	monoclonal antibody
MAP	<i>Mycobacterium avium</i> subsp. <i>paratuberculosis</i>
MDSC	myeloid-derived suppressor cell
NF-κB	nuclear factor-kappa B

NK	natural killer
PBMC	peripheral blood mononuclear cell
PBS	phosphate buffered saline
PCR	polymerase chain reaction
PD	programmed death
PD-L1	PD-ligand 1
PE	phycoerythrin
PerCP	peridinin chlorophyll protein
PGE ₂	prostaglandin E ₂
PKA	protein kinase A
PL	persistent lymphocytosis
qPCR	quantitative polymerase chain reaction
STAT3	signal transducer and activation of transcription 3
TGF	transforming growth factor
Th	T helper
Tim-3	T cell immunoglobulin and mucin domain-3
TNF	tumor necrosis factor
TNFR _{II}	TNF receptor type II
Treg	regulatory T

NOTES

The contents of Chapters I and II have been published in *Infection and Immunity* and *The Journal of Immunology*.

Sajiki Y, Konnai K, Okagawa T, Nishimori A, Maekawa N, Goto S, Ikebuchi R, Nagata R, Kawaji S, Kagawa Y, Yamada S, Kato Y, Nakajima C, Suzuki Y, Murata S, Mori Y, Ohashi K. 2018. Prostaglandin E₂ induction suppresses the Th1 immune responses in cattle with Johne's disease. *Infect Immun* **86**: e00910–17.

Sajiki Y, Konnai S, Okagawa T, Nishimori A, Maekawa N, Goto S, Watari K, Minato E, Kobayashi A, Kohara J, Yamada S, Kaneko MK, Kato Y, Takahashi H, Terasaki H, Takeda A, Yamamoto K, Toda M, Suzuki Y, Murata S, Ohashi K. 2019. Prostaglandin E₂-induced immune exhaustion and enhancement of antiviral effects by anti-PD-L1 antibody combined with COX-2 inhibitor in bovine leukemia virus infection. *J Immunol* **203**: 1313–1324.

The contents of Chapter III have been published in *ImmunoHorizons*.

Sajiki Y, Konnai S, Cai Z, Takada K, Okagawa T, Maekawa N, Fujisawa S, Kato Y, Suzuki Y, Murata S, Ohashi K. 2020. Enhanced immunotherapeutic efficacy of anti-PD-L1 antibody in combination with an EP4 antagonist. *ImmunoHorizons* **4**: 837–850.

PREFACE

Immune system is essential to distinguish self from non-self, and is an organization of cells and molecules which have specialized roles in defending against invaders, such as pathogens. Generally, cell-mediated immunity plays a central role in the protection against cancers and infections. However, a number of pathogens, which cause chronic infections, evade the immune response of the host via multiple mechanisms [Alcami and Koszinowski, 2000; Finlay and McFadden, 2006]. T-cell exhaustion is a well-known mechanism of immune evasion in chronic infections and cancers [Wherry, 2011]. During chronic infections and cancers, CD8⁺ cytotoxic T cells (CTLs) gradually differentiate into an exhausted state which is characterized by the accumulation of immunoinhibitory receptors, such as programmed death (PD)-1, on the cell surface and by the decrease in effector functions, such as the production of T helper 1 (Th1) cytokines and cytotoxicity [Wherry and Kurachi, 2015; McLane *et al.*, 2019]. PD-1 is identified as one of the markers of exhausted T cells in chronic disease states, and causes the dysfunction of antigen-specific T cells via the interaction with its ligands, PD-ligand 1 (PD-L1) and PD-L2 (Figure 1A) [Okazaki and Honjo, 2007]. Numerous studies have reported the association of T-cell exhaustion with the progression of cancers, such as melanoma and chronic lymphocytic leukemia [Lee *et al.*, 1999; Riches *et al.*, 2013; Thommen and Schumacher, 2018] and chronic infections, such as hepatitis B virus infection and human immunodeficiency virus (HIV) infection [Ye *et al.*, 2015; Fenwick *et al.*, 2019]. Therefore, overcoming T-cell exhaustion has become a promising therapeutic strategy for the treatment of patients with cancers [Pauken and Wherry, 2015; Wang *et al.*, 2018a]. The blockade of the PD-1/PD-L1 interaction using a specific antibody (Ab) reinvigorates T-cell responses against tumor antigens in murine and human studies (Figure 1B) [Iwai *et al.*, 2002; Blank *et al.*, 2006]. In addition, previous studies have shown that an anti-PD-1 monoclonal Ab (mAb), nivolumab, demonstrates antitumor efficacy in part of patients with melanoma and other cancers [Topalian *et al.*, 2012; Larkin *et al.*, 2015]. Furthermore, anti-PD-1/PD-L1 mAbs including nivolumab are now clinically approved in many countries. The prognosis of patients with several cancers, especially melanoma has strikingly improved by using these Abs for the treatment [Seidel *et al.*, 2018]. However, a significant proportion of the patients remains less responsive, and the objective response rates are generally 10%–30% [Iwai *et al.*, 2017; Gong *et al.*, 2018]. Thus, understanding how to prevent T-cell exhaustion or to efficiently reactivate T-cell function is the most pressing question in the fields of immunology and oncology.

In bovine research, several studies have described the suppression of T-cell responses during chronic diseases including Johne's disease [Stabel, 2006; Sohal *et al.*, 2008] and bovine leukemia virus (BLV) infection [Orlik and Splitter, 1996; Kabeya *et al.*, 2001; Frie and Coussens, 2015]. Johne's disease is a chronic granulomatous enteritis of ruminants caused by the bacteria *Mycobacterium avium* subsp. *paratuberculosis* (MAP), and is characterized by untreatable chronic diarrhea, severe weight loss, and eventual death [Rathnaiah *et al.*, 2017]. This disease is prevalent in many countries including Japan, and is of particular concern to the global livestock industry because of economic and production losses, the cost of diagnosis, and the lack of effective therapeutic methods [Li *et al.*, 2016]. Fecal–oral transmission is the primary mechanism for the transfer of MAP. Transmission via contaminated colostrum and milk from the infected animals also occurs frequently, because calves under 6 months of age are the most susceptible animals in a herd due to the incomplete development of their immune systems [Harris and Barletta, 2001; Windsor and Whittington, 2010]. In cattle, the infected animals progress to the clinical stage after a latent period of generally 2–3 years following infection. Once clinical symptoms develop, no treatment method is available. Therefore, the development of a novel control strategy against this disease is strongly required. Several studies have demonstrated that Th1 response, especially interferon (IFN)- γ production, is important for the control of disease progression [Bassey and Collins, 1997; Burrells *et al.*, 1998; Weiss *et al.*, 2006]. However, the suppression of Th1 response is frequently observed in cattle with Johne's disease [Stabel, 2006; Sohal *et al.*, 2008]. A previous study has revealed the association of the suppression of MAP-specific Th1 response with immunoinhibitory molecules during Johne's disease. The upregulation of immunoinhibitory molecules, such as PD-1, PD-L1, and lymphocyte activation gene 3 (LAG-3) was observed in peripheral immune cells in MAP-infected cattle. Additionally, PD-L1 expression was also upregulated in the ileum of naturally infected cattle with clinical diarrhea. Furthermore, the blockade of these inhibitory molecules using specific mAbs reactivated MAP-specific Th1 responses *in vitro* [Okagawa *et al.*, 2016a]. These results suggest that the suppression of MAP-specific Th1 response is caused by T-cell exhaustion mediated with immunoinhibitory molecules.

BLV is a member of the genus *Deltaretrovirus*, the family *Retroviridae*, and is closely related to human T-cell leukemia virus type 1 [Sagata *et al.*, 1985]. BLV commonly infects host B cells and causes enzootic bovine leukosis (EBL) after a long latent period of 3–5 years. During BLV infection, the majority of infected cattle is asymptomatic carriers which are called aleukemic (AL). Approximately 30% of infected cattle show persistent lymphocytosis (PL) characterized by the polyclonal expansion of

BLV-infected B cells in the peripheral blood. Further, less than 5% of infected cattle develop EBL characterized by B-cell lymphosarcoma [Schwartz and Levy, 1994]. BLV is transmitted both horizontally and vertically. Horizontal transmission occurs through blood containing BLV-positive cells and blood-sucking insects [Rodríguez *et al.*, 2011; Ooshiro *et al.*, 2013]. Vertical transmission occurs *in utero*, in the birth canal, and via colostrum and milk [Rodríguez *et al.*, 2011; Mekata *et al.*, 2015a; Sajiki *et al.*, 2017]. BLV infection is highly prevalent in Japan and many other countries. A previous study has investigated that the seroprevalence of BLV infection among dairy cattle in Japan is more than 40% [Murakami *et al.*, 2013]. Although only a quite small proportion of infected animals develops lethal lymphosarcoma, BLV infection causes economic losses in the livestock industry. Several studies have shown the association of BLV-infected cattle with the decrease in milk production [Norby *et al.*, 2016; Yang *et al.*, 2016]. Additionally, previous studies have reported that the suppression of immune responses is frequently observed in BLV-infected cattle and is associated with the disease progression and susceptibility to other infections [Kabeya *et al.*, 2001; Ohira *et al.*, 2016; Konnai *et al.*, 2017]. A previous study has demonstrated that the number of regulatory T (Treg) cells, an immunosuppressive subpopulation of T cells, is increased in BLV-infected cattle, possibly leading to increased susceptibility to other infections including opportunistic infections [Ohira *et al.*, 2016]. The same report has also suggested that transforming growth factor (TGF)- β 1 secreted from Treg cells is one of the factors involving in the suppression of Th1 response [Ohira *et al.*, 2016]. In addition, previous studies have shown the association of the PD-1/PD-L1 pathway with the suppression of Th1 response in BLV-infected cattle [Konnai *et al.*, 2017]. The expression of PD-1 and PD-L1 was upregulated in immune cells of BLV-infected cattle, and negative correlations were observed between PD-L1 expression and *IFN- γ* expression in BLV-infected animals [Ikebuchi *et al.*, 2011, 2013]. Furthermore, the blockade of the PD-1/PD-L1 pathway using specific mAbs reinvigorated Th1 responses in peripheral blood mononuclear cell (PBMC)-cultures *in vitro*, and the administration of anti-bovine PD-1/PD-L1 Abs into BLV-infected cattle reduced BLV proviral loads [Ikebuchi *et al.*, 2011, 2013; Okagawa *et al.*, 2017; Nishimori *et al.*, 2017], suggesting that the therapeutic strategies targeting the PD-1/PD-L1 pathway have a potential for the prevention of disease progression in BLV infection.

The immunosuppression caused by the PD-1/PD-L1 pathway is observed in not only these diseases but also other bovine chronic diseases, such as bovine anaplasmosis and mycoplasmosis [Okagawa *et al.*, 2016b; Goto *et al.*, 2017]. Thus, it is considered as a common mechanism for the immune evasion of pathogens in chronic diseases of cattle.

However, the molecular mechanism for the upregulation of these immunoinhibitory molecules during bovine chronic infections has not been fully elucidated.

Prostaglandins are synthesized from arachidonic acid which is released from plasma membranes by phospholipases. The synthesis of prostaglandins is mediated by several enzymes, such as cyclooxygenase (COX)-1 and COX-2 [Phipps *et al.*, 1991]. Prostaglandins are involved in the regulation of many physiological processes including inflammation and immune responses [Hirata and Narumiya, 2012; Ricciotti and FitzGerald, 2013]. Among prostaglandins, prostaglandin E₂ (PGE₂) is notably a well-known inflammatory mediator, whereas it also has an immunosuppressive function [Hirata and Narumiya, 2012]. PGE₂ exerts inhibitory effects on dendritic cells (DCs) and macrophages through the inhibition of tumor necrosis factor (TNF)- α and interleukin (IL)-12 secretion and the increase in IL-10 production. Among the four PGE₂ receptors, E prostanoid (EP) 1–EP4, these inhibitory effects are mediated by EP2 and EP4 [Nataraj *et al.*, 2001; Harizi *et al.*, 2003; Vassiliou *et al.*, 2003; Kalinski, 2012]. Additionally, PGE₂ indirectly affects T-cell priming and proliferation through DC modulation, and it also regulates T-cell proliferation and differentiation directly by binding to the receptors on T cells (Figure 1A) [Yao *et al.*, 2009]. In contrast, COX-2 inhibitors activate immune responses including T-cell responses in humans and mice by reducing PGE₂ synthesis (Figure 1B) [Stolina *et al.*, 2000; Pettersen *et al.*, 2011]. Interestingly, several recent studies in human and murine research have revealed that PGE₂ exerts immunosuppressive functions via immunoinhibitory molecules including PD-1 and PD-L1. PGE₂ increases the expression of PD-L1 in myeloid-derived suppressor cells (MDSCs) and tumor-associated macrophages in a murine tumor model [Prima *et al.*, 2016]. PGE₂ upregulates the expression of PD-1 in tumor infiltrating T cells obtained from patients with lung cancer via EP2 and EP4 receptors [Wang *et al.*, 2018b]. Furthermore, PGE₂ induces the expression of T cell immunoglobulin and mucin domain-3 (Tim-3), which is another immunoinhibitory receptor on T cells, via EP4 in a human T cell line [Yun *et al.*, 2019]. Thus, these results suggest that PGE₂ is an inducer of immunoinhibitory molecules. However, in the field of veterinary medicine, the immunosuppressive function of PGE₂ and its association with the upregulation of immunoinhibitory molecules are still unknown.

In this study, to examine whether PGE₂ has suppressive effects on bovine immune cells, the functional analysis of PGE₂ using bovine PBMCs was performed in Chapter I. Next, to determine the association of PGE₂ with the progression of bovine chronic infections, the kinetic analysis of PGE₂ was conducted in Johne's disease and BLV infection in Chapters I and II. Then, to demonstrate the effects of PGE₂ inhibition on Th1

responses, the functional analysis of a COX-2 inhibitor, meloxicam, was performed using PBMCs from MAP- or BLV-infected cattle *in vitro* in Chapters I and II. Additionally, the antiviral effect of the COX-2 inhibitor and/or anti-PD-L1 Ab *in vivo* was examined using BLV-infected cattle in Chapter II. Finally, to elucidate the underlying mechanism of the effect of the combined treatment tested in Chapter II, the role of PGE₂ under the treatment with anti-PD-L1 Ab was examined in Chapter III. The effects of the combined treatment of anti-PD-L1 Ab with EP4 blockade were also analyzed using bovine immune cells and a murine tumor model in Chapter III.

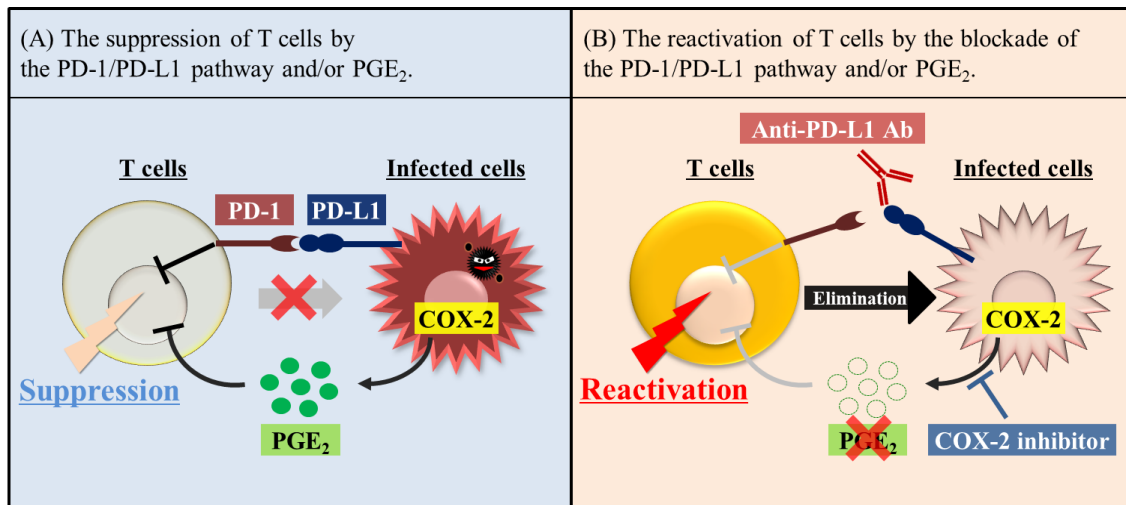


Figure 1. The suppression of T-cell activity by the PD-1/PD-L1 pathway and PGE₂ in humans and mice. (A) The mechanism of immune evasion during chronic infections. PD-1 is an immunoinhibitory receptor expressed on T cells and interacts with PD-L1 expressed on the infected cells. PGE₂ is a lipid mediator synthesized in part by COX-2. Both the PD-1/PD-L1 pathway and PGE₂ suppress effector function of T cells. (B) Reactivation of T cells by PD-L1 blockade and COX-2 inhibition. Treatment with anti-PD-L1 Ab and/or COX-2 inhibitor restores the effector function, leading to the elimination of pathogens.

CHAPTER I

The suppression of Th1 immune responses by prostaglandin E₂ in cattle infected with *Mycobacterium avium* subsp. *paratuberculosis*

INTRODUCTION

Johne's disease, which is caused by MAP, is a chronic enteritis of ruminants [Rathnaiah *et al.*, 2017], and is prevalent in many countries, including Japan [Li *et al.*, 2016]. The clinical signs of Johne's disease include chronic diarrhea, severe weight loss, reduced milk production, and mortality [Rathnaiah *et al.*, 2017]. In the early stage of infection, Th1 responses are strongly induced by MAP-infected macrophages which produce several cytokines, such as IFN- γ and IL-12, and enhance bactericidal activity of macrophages [Stabel, 2006; Khalifeh *et al.*, 2009]. The Th1 responses gradually decline during the late subclinical stage, contributing to the progression to clinical disease [Bassey and Collins, 1997; Burrells *et al.*, 1998; Weiss *et al.*, 2006]. Thus, Th1 immune response plays an essential role in the prevention from the disease progression.

Immunoinhibitory receptors, PD-1 and LAG-3, are important for the inhibition of excessive immune responses as a negative-feedback system via interactions with their ligands, PD-L1 and major histocompatibility complex class II, respectively [Okazaki and Honjo, 2007; Sierro *et al.*, 2011]. These immunoinhibitory molecules are associated with the functional exhaustion of antigen-specific T cells during chronic infections [Keir *et al.*, 2008; Wherry, 2011]. A previous study reported that the upregulation of PD-1 and LAG-3 was observed on T cells during the subclinical stage of MAP-infected cattle [Okagawa *et al.*, 2016a]. Additionally, the blockade of PD-1 and LAG-3 using specific Abs enhanced MAP-specific Th1 immune responses in PBMC cultures [Okagawa *et al.*, 2016a]. Therefore, MAP-specific Th1 response is considered to be suppressed, at least in part, via the induction of immunoinhibitory molecules on T cells in MAP-infected cattle. However, the mechanism for the upregulation of these molecules during this infection remains unclear.

PGE₂ is one of the inflammatory mediators and is synthesized from arachidonic acid by several enzymes, such as COX-1 and COX-2 [Phipps *et al.*, 1991]. COX-1 is a constitutive enzyme that is expressed in many tissues, whereas COX-2 is an inducible enzyme [Morita, 2002]. The expression of COX-2 is induced by several factors, such as inflammatory cytokines and subsequent activation of nuclear factor-kappa B (NF- κ B) [Subbaramaiah *et al.*, 1996]. PGE₂ has suppressive effects on immune cells, such as T cells, DCs, natural killer (NK) cells, and macrophages, via its receptors EP2 and EP4 [Kalinski, 2012]. Previous studies in humans have shown that PGE₂ suppresses Th1 response and inhibits DC differentiation. In addition, PGE₂ induces several suppressive subpopulations of immune cells, including Treg cells, MDSCs, and M2 macrophages [Betz and Fox, 1991; Wang and DuBois, 2013, 2016]. Interestingly, several recent studies

have demonstrated the association of PGE₂ with the expression of immunoinhibitory molecules. PGE₂ upregulated PD-L1 expression in MDSCs and tumor-associated macrophages in a tumor model of mice [Prima *et al.*, 2016]. Additionally, COX-2 expression was positively correlated with PD-L1 expression in human melanoma cells [Botti *et al.*, 2017]. Furthermore, the receptors EP2 and EP4 were upregulated on CD8⁺ CTLs, leading to the impairment of CTL function and survival in a murine model of chronic infection [Chen *et al.*, 2015]. Importantly, the dual blockade of the PD-1/PD-L1 pathway and PGE₂ enhanced antiviral immune responses [Chen *et al.*, 2015]. However, in the veterinary field, little information is available on the immunosuppression caused by PGE₂ and its association with PD-1/PD-L1 upregulation.

In this chapter, the immunosuppressive function of PGE₂ was examined using bovine PBMCs *in vitro*, and PGE₂ kinetics in cattle with Johne's disease were analyzed. Additionally, to evaluate whether a COX-2 inhibitor, which blocks PGE₂ production, activates MAP-specific Th1 responses, *in vitro* cultures were performed using PBMCs derived from MAP-infected cattle.

MATERIALS AND METHODS

Bovine samples

Blood samples from MAP-uninfected Holstein cattle were collected at dairy farms in Hokkaido, Japan. Informed consent was obtained from all owners of cattle sampled in Chapter I. All experimental procedures using bovine samples were carried out following approval from the local committee for animal studies at Hokkaido University (approval number: 17-0024). Seven Holstein calves (male, 3–4 weeks of age) were orally inoculated with intestinal tissue homogenate from a MAP-infected cow containing MAP (6.8×10^6 CFU) once daily for 20 days. All calves experimentally infected with MAP were kept in a biosafety level 2 animal facility at the National Institute of Animal Health, Japan, and did not show any clinical symptoms. Blood samples from MAP-infected cattle were collected from these experimentally infected cattle. Serum samples were obtained from uninfected and MAP naturally-infected cattle, and were stored at -30°C until use in the experiments. All animal experiments using samples from MAP-infected cattle were approved by the National Institute of Animal Health Ethics Committee (approval number: 17-077).

Cell preparation

PBMCs were prepared from blood samples by density gradient centrifugation on Percoll (GE Healthcare, Little Chalfont, UK), and were cultured in RPMI 1640 medium (Sigma-Aldrich, St. Louis, MO, USA) containing 10% heat-inactivated fetal calf serum (FCS; Thermo Fisher Scientific, Waltham, MA, USA), 100 U/mL penicillin (Thermo Fisher Scientific), 100 $\mu\text{g}/\text{mL}$ streptomycin (Thermo Fisher Scientific), and 2 mM L-glutamine (Thermo Fisher Scientific) using 96-well culture plates (Corning Inc., Corning, NY, USA) at 37°C in a 5% CO_2 atmosphere. The *in vitro* cultures using PBMCs from animals experimentally infected with MAP were performed using samples taken at various time points from 82 to 120 weeks post-first inoculation.

Enzyme-linked immunosorbent assay (ELISA)

To determine the concentrations of IFN- γ , TNF- α , and PGE₂ in culture supernatants and sera, ELISA was performed by using Bovine IFN- γ ELISA Development Kit (Mabtech, Nacka Strand, Sweden), Bovine TNF- α Do-It-Yourself ELISA (Kingfisher Biotech, St. Paul, MN, USA), and Prostaglandin E₂ Express ELISA Kit (Cayman Chemical, Ann Arbor, MI, USA), respectively, according to the manufacturers' protocols.

Quantitative polymerase chain reaction (qPCR)

Total RNA was extracted from the cultured PBMCs using TRI Reagent (Molecular Research Center, Cincinnati, OH, USA) following the manufacturer's instructions. cDNA synthesis from the total RNA obtained was conducted using PrimeScript reverse transcriptase (Takara Bio, Otsu, Japan) following the manufacturer's instructions. To quantitate the mRNA expression of *COX2*, *PD-L1*, *signal transducer and activation of transcription 3 (STAT3)*, *forkhead box P3 (Foxp3)*, and several cytokines in PBMCs, qPCR was performed using a LightCycler 480 system II (Roche Diagnostics, Mannheim, Germany) and SYBR Premix DimerEraser (TaKaRa Bio) following the manufacturers' instructions. The *GAPDH* and *ACTB* genes were used as reference genes. Primers used in Chapter I are shown in Table I-1.

Flow cytometry

For all staining procedures, Fc blocking was firstly performed by incubating collected cells in phosphate buffered saline (PBS, pH 7.2) containing 10% heat-inactivated goat serum (Thermo Fisher Scientific) for 15 min at 25°C to prevent nonspecific reactions.

For carboxyfluorescein diacetate succinimidyl ester (CFSE) staining, the cells were stained with Alexa Fluor 647-labeled anti-bovine CD4 mAb (CC30; Bio-Rad, Hercules, CA, USA), peridinin chlorophyll protein (PerCP)/cyanin (Cy) 5.5-conjugated anti-bovine CD8 mAb (CC63; Bio-Rad), and phycoerythrin (PE)/Cy7-conjugated anti-bovine IgM mAb (IL-A30; Bio-Rad) for 25 min at 25°C. CC30 was pre-labeled with a Zenon Alexa Fluor 647 mouse IgG₁ labeling kit (Thermo Fisher Scientific). CC63 and IL-A30 were conjugated using Lightning-Link antibody labeling kits (Innova Biosciences, Cambridge, UK). The stained cells were washed twice with PBS containing 1% bovine serum albumin (BSA, Sigma-Aldrich), and then were analyzed by FACS Verse (BD Biosciences, San Jose, CA, USA).

For PD-L1 expression, the cells were stained with anti-bovine PD-L1 mAb (4G12, rat IgG_{2a}) [Ikebuchi *et al.*, 2014] or rat IgG_{2a} isotype control (R35-95; BD Biosciences) for 25 min at 25°C. To analyze PD-L1 expression on T cells and B cells, the cells were then washed twice with PBS containing 1% BSA and stained with PE-labeled anti-bovine CD3 mAb (MM1A; Washington State University Monoclonal Antibody Center, Pullman, WA, USA), fluorescein isothiocyanate (FITC)-conjugated anti-bovine CD4 mAb (CC8; Bio-Rad), PerCP/Cy5.5-conjugated anti-bovine CD8 mAb (CC63), PE/Cy7-conjugated anti-bovine IgM mAb (IL-A30), and allophycocyanin (APC)-conjugated anti-rat immunoglobulin antibody (Southern Biotech, Birmingham, AL, USA) for 25 min at 25°C. MM1A was pre-labeled with the Zenon R-PE mouse IgG₁ labeling kit (Thermo Fisher

Scientific). To detect PD-L1 expression on CD14⁺ cells, the cells were stained with PerCP/Cy5.5-conjugated anti-bovine CD14 mAb (CAM36A; Washington State University Monoclonal Antibody Center) and APC-conjugated anti-rat immunoglobulin antibody for 25 min at 25°C. CAM36A was conjugated using the Lightning-Link antibody labeling kit. After final staining, the cells were washed twice with PBS containing 1% BSA, and then were analyzed by FACS Verse.

For PD-1 and LAG-3 expression, collected cells were stained with anti-bovine PD-1 mAb (5D2, rat IgG_{2a}) [Ikebuchi *et al.*, 2013] or anti-bovine LAG-3 mAb (71-2D8, rat IgG₁) [Okagawa *et al.*, 2016a] for 25 min at 25°C. Rat IgG_{2a} (R35-95) or rat IgG₁ isotype control (R3-34; BD Biosciences) was used as an isotype control, respectively. The cells were then washed twice with PBS containing 1% BSA and stained with following Abs; PerCP/Cy5.5-conjugated anti-bovine CD3 mAb (MM1A), FITC-conjugated anti-bovine CD4 mAb (CC8), PE-conjugated anti-bovine CD8 mAb (CC63), PE/Cy7-conjugated anti-bovine IgM mAb (IL-A30), and APC-conjugated anti-rat immunoglobulin antibody for 25 min at 25°C. The stained cells were washed with PBS containing with 1% BSA, and then were analyzed by FACS Verse.

PBMC culture

To examine suppressive effects of PGE₂ on bovine immune cells, PBMCs from uninfected cattle were cultured with 2,500 nM of PGE₂ (Cayman Chemical) for 24 h. PBMCs from uninfected cattle were labeled with 2 μM of CFSE (Sigma-Aldrich) and cultured with 2.5 to 2,500 nM of PGE₂ in the presence of 1 μg/mL of anti-bovine CD3 mAb (MM1A) and 1 μg/mL of anti-bovine CD28 mAb (CC220; Bio-Rad) for 72 h.

To examine whether the stimulation of MAP antigen induces the expression of immunoinhibitory molecules and PGE₂ production, PBMCs from MAP-infected and uninfected cattle were cultured for 24 or 120 h with or without 1 μM of meloxicam (Sigma-Aldrich), a COX-2 inhibitor. Dimethyl sulfoxide (DMSO, Nacalai Tesque, Kyoto, Japan) was used as a vehicle control. Cultures were stimulated by adding 1 μg/mL of Johnin purified protein derivative (J-PPD).

To examine whether the inhibition of PGE₂ production activates MAP-specific Th1 responses, PBMCs from MAP-infected cattle were labeled with CFSE and cultured for 120 h with 1 μM of meloxicam and/or 10 μg/mL of anti-bovine PD-L1 mAb (4G12) in the presence of 1 μg/mL of J-PPD. DMSO and rat IgG (Sigma-Aldrich) were used as negative controls. 1 μg/mL of purified protein derivative from *M. bovis* BCG strain (B-PPD) was used as a control antigen.

Immunohistochemical staining

The sections of ileum tissues were collected from cattle naturally or experimentally infected with MAP (animals #I-1 and #I-2) and an uninfected cow (animal #I-3). The MAP naturally-infected animal (animal #I-1) showed clinical symptoms of Johne's disease. The MAP experimentally-infected animal (animal #I-2) showed bacterial shedding in feces (Table I-2) and clinical symptoms. The collected tissues were fixed by formalin, embedded into paraffin wax, and cut into 4-mm-thick sections. The sections were deparaffinized in xylene on the slide glass. Antigen retrieval was performed for 10 min in citrate buffer (0.37 g/mL citric acid and 2.4 g/mL trisodium citrate dihydrate) by microwave heating. The sections were incubated for 15 min in methanol containing 0.3% hydrogen peroxide to block endogenous peroxidase activity. The staining was then performed for 30 min using following Abs; anti-bovine PD-L1 mAb (6C11-3A11) [Ikebuchi *et al.*, 2014], anti-prostaglandin E₂ antibody (Abcam, Cambridge, UK), and anti-prostaglandin E receptor EP2 antibody (EPR8030 (B); Abcam). The reactivity of anti-bovine PD-L1 mAb (6C11-3A11) with bovine PD-L1 was confirmed by flow cytometric analysis using Chinese hamster ovary cells expressing bovine PD-L1 (data not shown). The sections were washed twice with PBS and incubated for 30 min with Histofine simple stain MAX PO (rat) (Nichirei, Tokyo, Japan). 3-diaminobenzidine tetrahydrochloride was used to visualize the positive staining. Additionally, Ziehl-Neelsen staining was carried out to detect acid-fast bacilli in these tissues.

Statistical analyses

In Figure I-4A, statistical significance was analyzed using the Mann-Whitney *U* test. In the other figures, statistical significances were analyzed using the Wilcoxon signed-rank test for comparing two-group and the Steel-Dwass test for comparing multiple groups. All statistical tests were performed using with the MEPHAS program (<http://www.gen-info.osaka-u.ac.jp/MEPHAS/>). For all tests, $p < 0.05$ was considered statistically significant.

Table I-1. Primers used in Chapter I.

Gene	Primer sequence (5'–3')
<i>IFN-γ</i>	F: ATA ACC AGG TCA TTC AAA GG R: ATT CTG ACT TCT CTT CCG CT
<i>TNF-α</i>	F: TAA CAA GCC AGT AGC CCA CG R: GCAAGG GCT CTT GAT GGC AGA
<i>IL-2</i>	F: TTT TAC GTG CCC AAG GTT AA R: CGT TTA CTG TTG CAT CAT CA
<i>IL-10</i>	F: TGC TGG ATG ACT TTA AGG G R: AGG GCA GAA AGC GAT GAC A
<i>STAT3</i>	F: ATG GAA ACA ACC AGT CGG TGA R: TTT CTG CAC ATA CTC CAT CGC T
<i>TGF-β1</i>	F: CTG CTG AGG CTC AAG TTA AAA GTG R: CAG CCG GTT GCT GAG GTA G
<i>Foxp3</i>	F: CAC AAC CTG AGC CTG CAC AA R: TCT TGC GGA ACT CAAACT CAT C
<i>PD-L1</i>	F: GGG GGT TTA CTG TTG CTT GA R: GCC ACT CAG GAC TTG GTG AT
<i>COX2</i>	F: ACG TTT TCT CGT GAA GCC CT R: TCT ACC AGA AGG GCG GGA TA
<i>ACTB</i>	F: TCT TCC AGC CTT CCT TCC TG R: ACC GTG TTG GCG TAG AGG TC
<i>GAPDH</i>	F: GGC GTG AAC CAC GAG AAG TAT AA R: CCC TCC ACG ATG CCAAAG T

F: forward, R: reverse.

Table I-2. The bacterial load in fecal and tissue samples at necropsy.

Animal	Status	Fecal MAP DNA (pg)	MAP DNA in ileum tissue (pg)
#I-1	Natural infection	N.A.	N.A.
#I-2	Experimental infection	0.589	26.8
#I-3	Uninfected control	N.D.	N.D.

N.D.: not detected, N.A.: not available.

The results of #I-2 have been published in a previous paper [Okagawa *et al.*, 2016a].

RESULTS

The suppression of bovine immune responses by PGE₂

To examine whether PGE₂ has suppressive effects on bovine immune responses, the expression of genes related to T-cell responses was assayed by qPCR. PGE₂ treatment downregulated the gene expression of Th1 cytokines, *IFN-γ*, *TNF-α*, and *IL-2*, *in vitro* (Figures I-1A–C). In contrast, PGE₂ treatment upregulated the gene expression of *IL-10*, *STAT3*, *TGF-β1*, and *Foxp3*, which are involved in the suppression of T-cell responses (Figures I-1D–G). Additionally, treatment with PGE₂ inhibited the proliferation of CD4⁺ and CD8⁺ cells in a dose-dependent manner (Figures I-2A and B), and decreased the production of Th1 cytokines, such as IFN-γ and TNF-α (Figures I-2C and D). Furthermore, treatment with PGE₂ significantly upregulated the expression of PD-L1 in PBMCs (Figures I-3A and B). Taken together, these results suggest that PGE₂ suppresses bovine immune responses, especially Th1 responses, *in vitro*.

Kinetic analysis of PGE₂ in MAP-infected cattle

Previous studies have shown the association of PGE₂ with the progression of several chronic infections in humans [Dumais *et al.*, 1998, 2002; Waris and Siddiqui, 2005]. To demonstrate the association of PGE₂ with the progression of MAP infection, serum PGE₂ concentrations were firstly measured by ELISA. As shown in Figure I-4A, serum PGE₂ concentrations in MAP naturally-infected cattle were significantly higher than those in uninfected cattle (Figure I-4A). The stimulation by J-PPD induced *COX2* expression in PBMCs from MAP-infected animals (Figure I-4B). In addition, J-PPD stimulation promoted PGE₂ secretion from PBMCs of MAP-infected cattle but not from PBMCs of uninfected cattle, and J-PPD induced-PGE₂ production was suppressed by the treatment with the COX-2 inhibitor, meloxicam, (Figure I-4C). Taken together, these results suggest that the COX-2–PGE₂ pathway is activated by the stimulation with MAP antigens in PBMCs from MAP-infected animals.

Upregulation of immunoinhibitory molecule expression by J-PPD stimulation

The expression of immunoinhibitory molecules was then analyzed in the presence of J-PPD. The stimulation by J-PPD significantly upregulated PD-L1 expression in PBMCs from MAP-infected cattle at both protein and mRNA levels compared to that in PBMCs from uninfected cattle (Figures I-5A and B). Further analysis by flow cytometry revealed that J-PPD stimulation also increased PD-L1 expression in CD4⁺ and CD8⁺ T cells, B cells, and CD14⁺ cells (Figures I-5C–F). The expression of PD-1 and LAG-3 was also

examined in the presence of J-PPD by flow cytometry. J-PPD stimulation induced both PD-1 and LAG-3 expression in CD4⁺ and CD8⁺ T cells (Figures I-6A–D). Collectively, these results suggest the stimulation of MAP antigens strongly upregulates the expression of these inhibitory molecules in PBMCs of MAP-infected cattle *in vitro*.

Expression analysis of PGE₂, EP2, PD-L1 in MAP-infected cells of the ileum

It has been previously reported that PD-L1 is expressed in MAP-infected macrophages in the ileum [Okagawa *et al.*, 2016a]. In the present study, the expression of PGE₂, EP2, and PD-L1 in the ileum from cattle with Johne's disease was examined by immunohistochemical staining. The ileum tissues from MAP-infected cattle (animals #I-1 and #I-2) but not from an uninfected cow (animals #I-3) expressed PGE₂ (Figure I-7A), and both MAP-infected and uninfected animals (animals #I-1–#I-3) expressed EP2, a PGE₂ receptor (Figure I-7B). Interestingly, both PD-L1⁺ cells and MAP-infected cells were observed in the same lesion (Figures I-7C and D). These results suggest that PGE₂ and PD-L1 are involved in the immunosuppression in infected lesions of cattle with Johne's disease.

The activation of MAP-specific Th1 responses by the combined treatment of the COX-2 inhibitor and anti-PD-L1 Ab

To examine whether the inhibition of PGE₂ production by the COX-2 inhibitor activates Th1 responses in MAP-infected cattle, PBMCs from MAP-infected cattle were cultured with the COX-2 inhibitor in the presence of J-PPD. Treatment with the COX-2 inhibitor increased the proliferation of CD8⁺ cells and Th1 cytokine production from PBMCs *in vitro* (Figures I-8A–C). Next, the effects of PD-L1 blockade on Th1 responses in MAP-infected cattle were evaluated. The blockade of the PD-1/PD-L1 pathway using anti-bovine PD-L1 mAb also increased the proliferation of CD8⁺ cells and IFN- γ production from PBMCs of MAP-infected cattle (Figures I-8D and E). Finally, whether the combined treatment of the COX-2 inhibitor with anti-PD-L1 Ab enhances MAP-specific Th1 responses was examined *in vitro*. The proliferation of CD8⁺ cells was significantly enhanced in the group treated with the COX-2 inhibitor and anti-bovine PD-L1 mAb compared to the control group (Figure I-9A). The stimulation with a control antigen, B-PPD, had no effect in each group (Figure I-9A). In addition, the combined treatment tended to increase IFN- γ production responded to J-PPD (Figure I-9B), although the difference was not statistically significant. These data show that the combined treatment could be a novel strategy to prevent the progression of MAP infection.

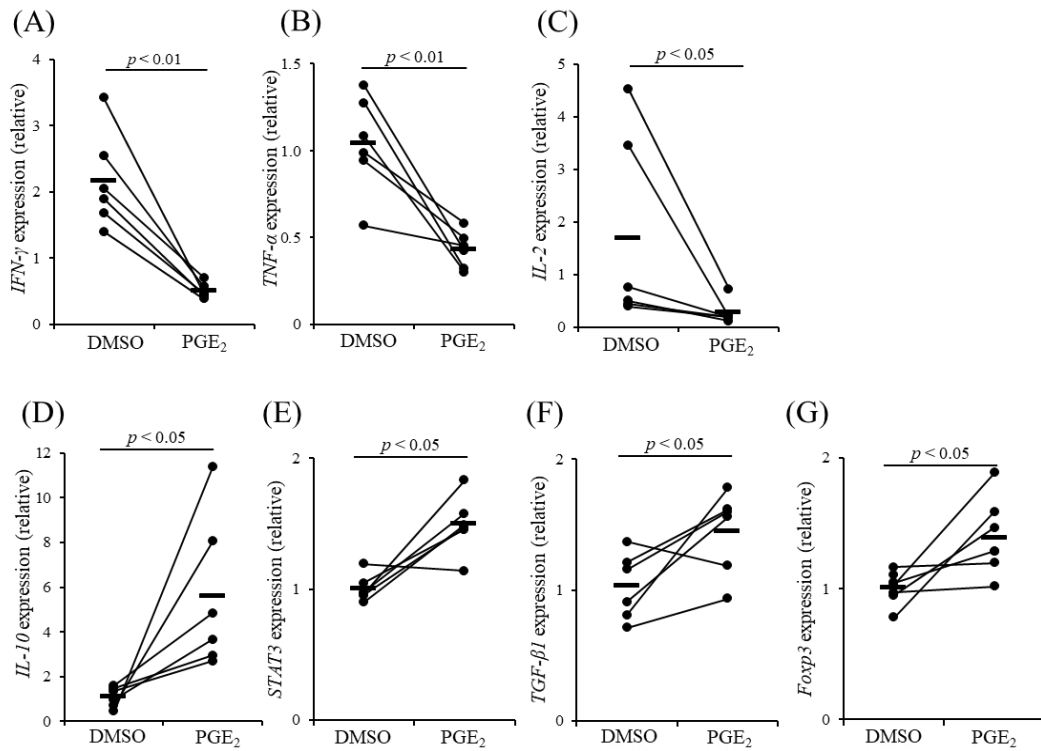


Figure I-1. The effects of PGE₂ on the expression of genes related to T-cell responses. (A–G) PBMCs from uninfected cattle ($n = 6$) were cultivated with 2,500 nM of PGE₂ for 24 h. The expression of *IFN- γ* (A), *TNF- α* (B), *IL-2* (C), *IL-10* (D), *STAT3* (E), *TGF- β 1* (F), and *Foxp3* (G) was measured by qPCR. Statistical analysis was performed using the Wilcoxon signed-rank test.

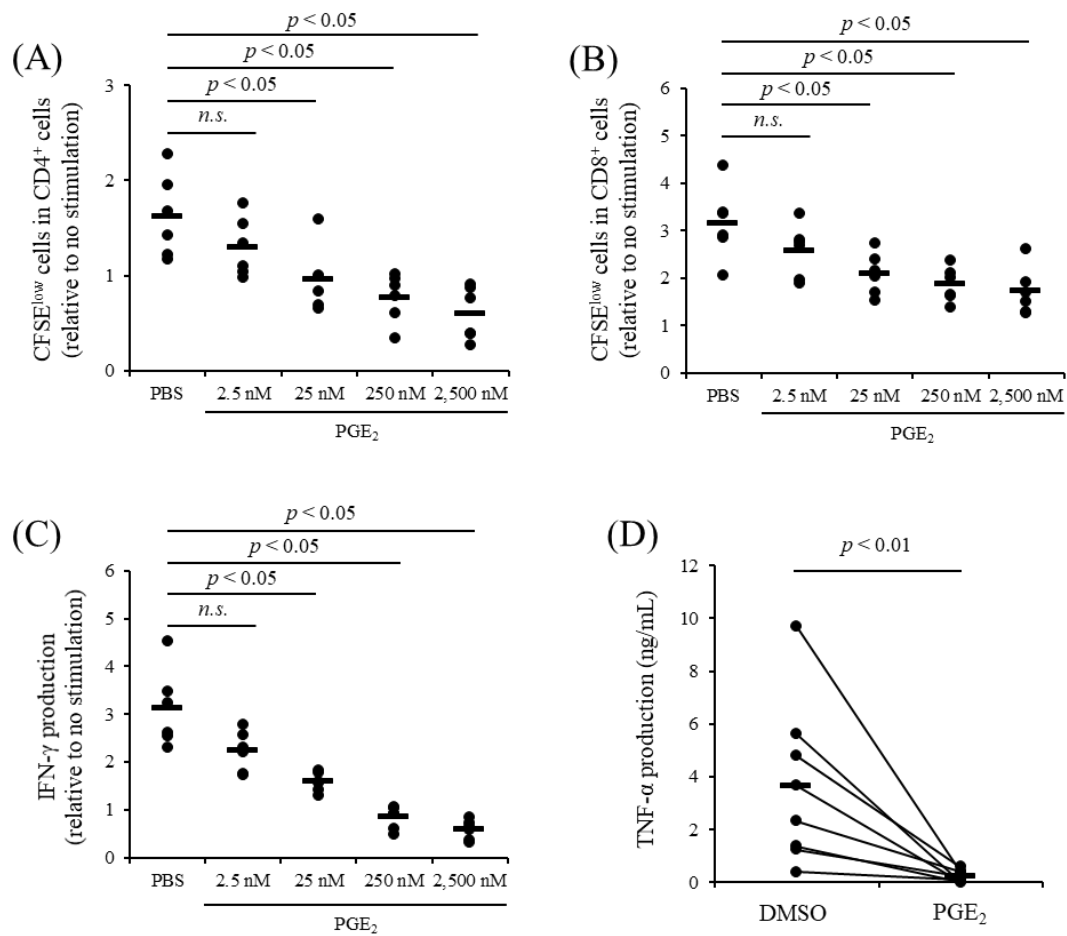


Figure I-2. The suppression of bovine Th1 responses by PGE₂. (A–D) PBMCs from uninfected cattle (A–C: $n = 6$) were cultured with each concentration of PGE₂. In Figure D, PBMCs from uninfected cattle ($n = 8$) were cultured with 2,500 nM of PGE₂. The cultures were stimulated by anti-bovine CD3 and anti-bovine CD28 mAbs for 72 h. The proliferation of CD4⁺ (A) and CD8⁺ (B) cells was analyzed by flow cytometry, and IFN- γ (C) and TNF- α (D) concentrations in culture supernatants were measured by ELISA. Statistical analysis was performed using the Steel-Dwass test (A–C) and the Wilcoxon signed-rank test (D). *n.s.*: not significant.

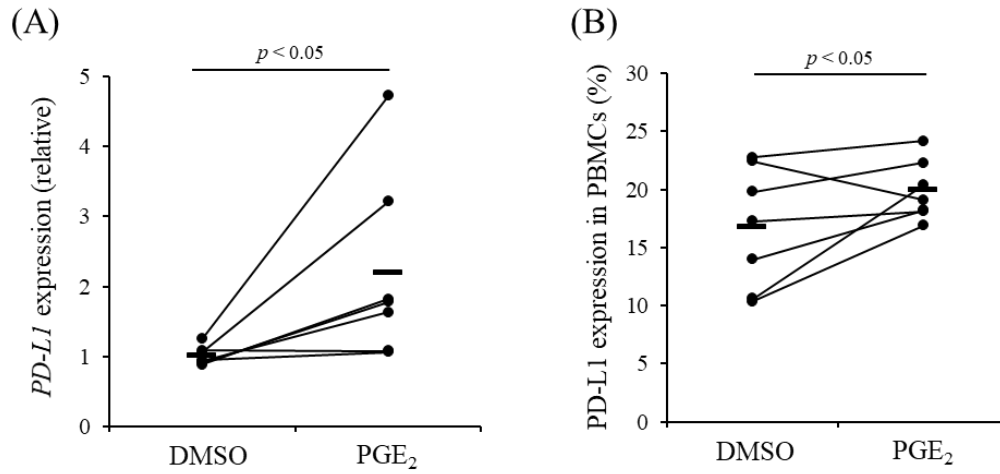


Figure I-3. The upregulation of PD-L1 expression by PGE₂. (A and B) PBMCs from uninfected cattle ($n = 7$) were cultured with 2,500 nM of PGE₂ for 24 h. PD-L1 expression was measured at mRNA (A) and protein (B) levels by qPCR and flow cytometry, respectively. Statistical analysis was performed by the Wilcoxon signed-rank test.

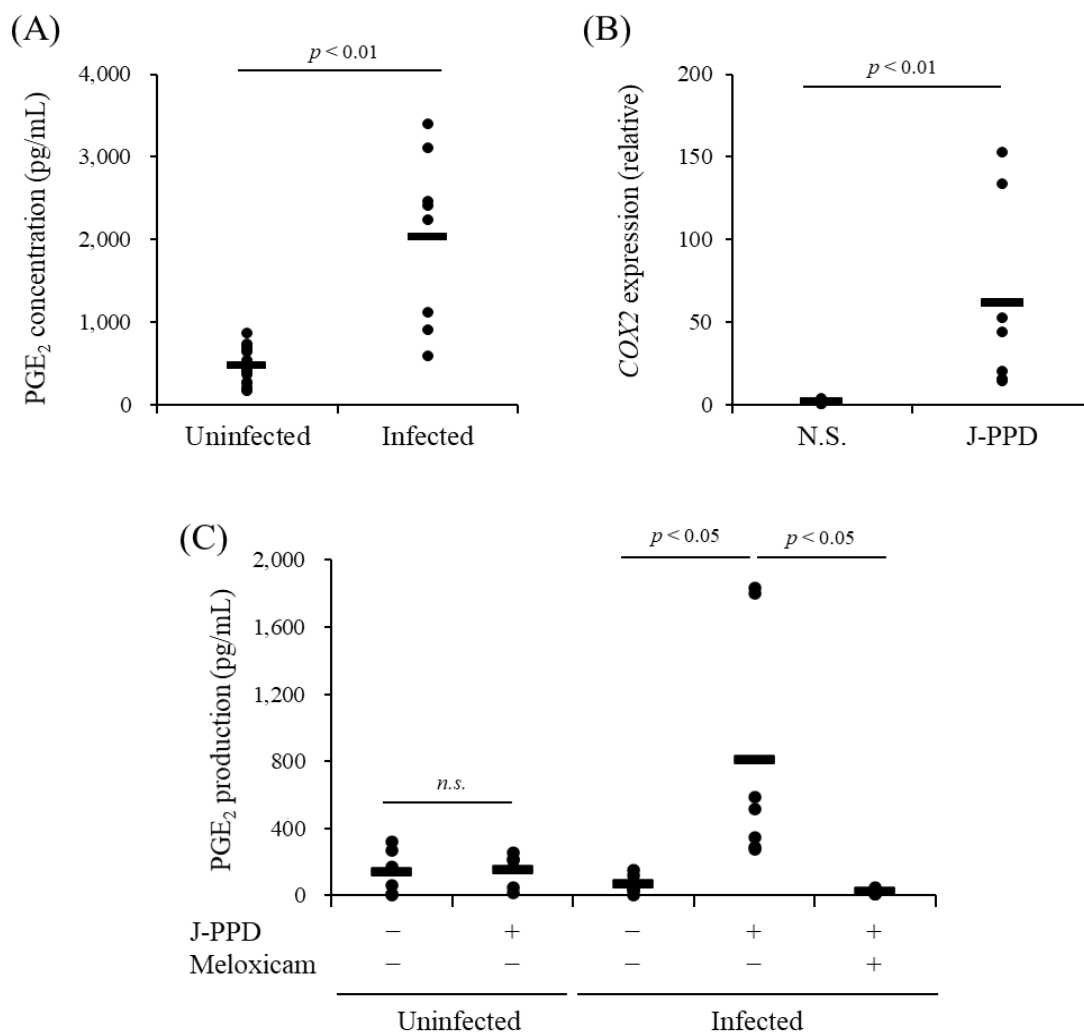


Figure I-4. Kinetic analysis of PGE₂ in MAP-infected cattle. (A) Serum concentrations of PGE₂ in uninfected ($n = 16$) or MAP naturally-infected cattle ($n = 8$) were determined by ELISA. (B) PBMCs from MAP-infected cattle ($n = 7$) were cultured with J-PPD for 120 h, and COX-2 expression was measured by qPCR. (C) PBMCs from uninfected ($n = 6$) and MAP-infected cattle ($n = 7$) were cultured with or without 1 μ M of a COX-2 inhibitor, meloxicam, in the presence of J-PPD for 120 h. PGE₂ concentrations in culture supernatants were determined by ELISA. (A–C) Statistical analysis was performed by the Mann-Whitney U test (A), the Wilcoxon signed-rank test (B), and the Steel-Dwass test (C). Uninfected: MAP-uninfected cattle, Infected: MAP-infected cattle, N.S.: no stimulation.

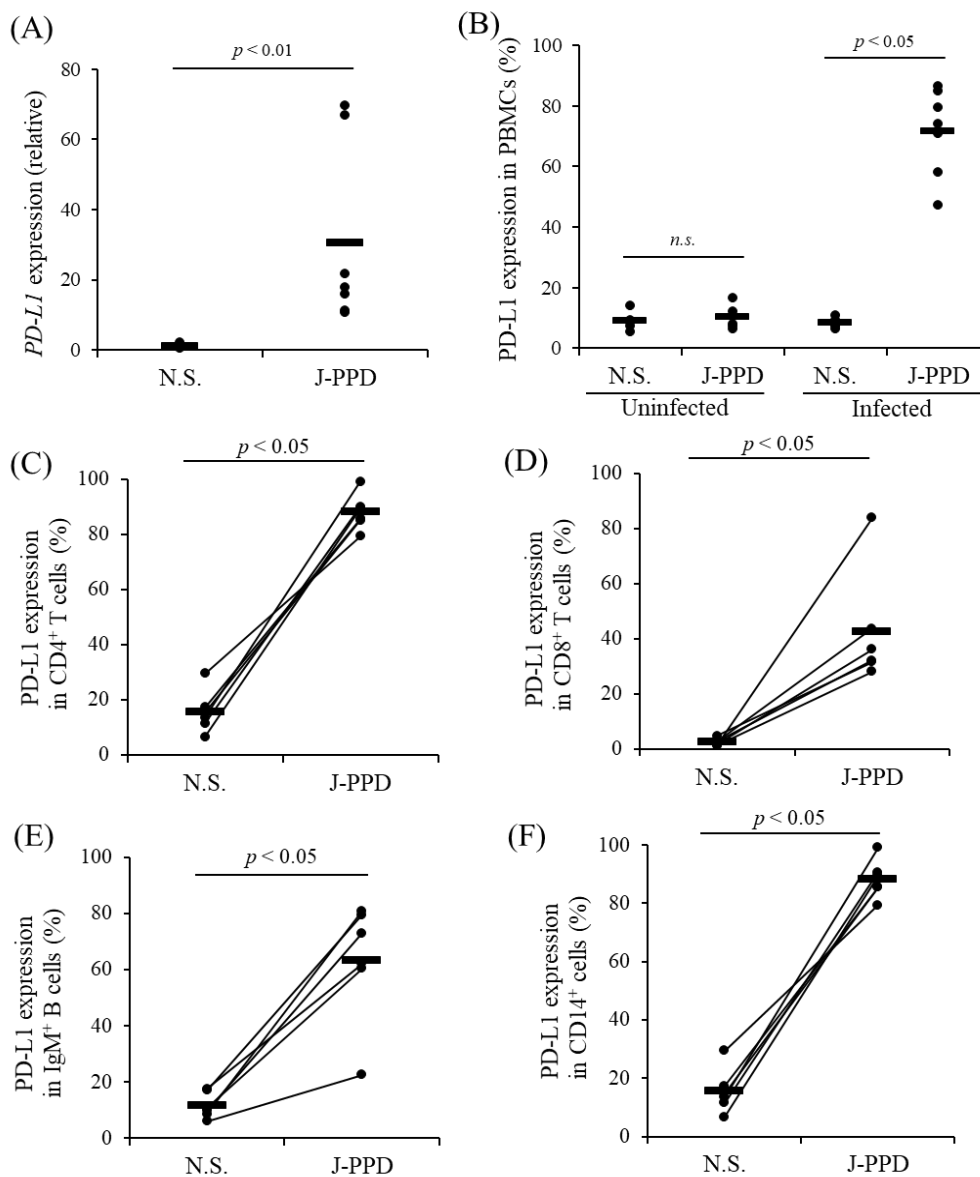


Figure I-5. The increase in PD-L1 expression on immune cells by J-PPD. (A–F) PBMCs from uninfected and MAP-infected cattle were cultured in the presence of J-PPD for 24 h. (A) The expression of *PD-L1* gene in PBMCs from the infected cattle was analyzed by qPCR. (B) The expression of PD-L1 in PBMCs from both uninfected and MAP-infected cattle was measured by flow cytometry. (C–F) PD-L1 expression in CD4⁺ T cells (C), CD8⁺ T cells (D), B cells (E), and CD14⁺ cells (F) of MAP-infected cattle was measured by flow cytometry. (A–F) Statistical analysis was performed by the Wilcoxon signed-rank test.

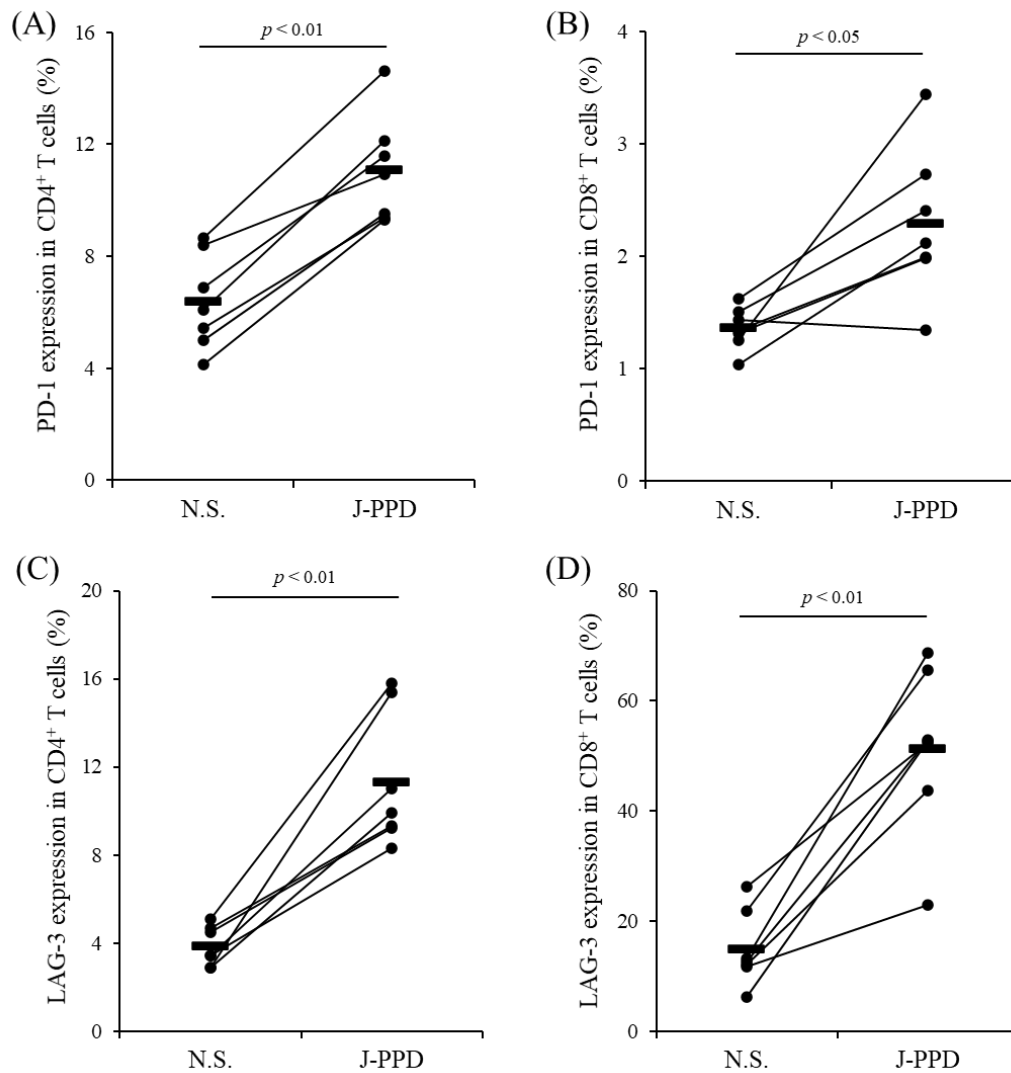


Figure I-6. The increase in PD-1 and LAG-3 expression on T cells by J-PPD. (A–D) PBMCs from MAP-infected cattle ($n = 7$) were cultured in the presence of J-PPD for 24 h. Flow cytometric analyses were performed to measure PD-1 (A and B) and LAG-3 (C and D) expression in CD4⁺ and CD8⁺ T cells. (A–D) Statistical analysis was performed by the Wilcoxon signed-rank test.

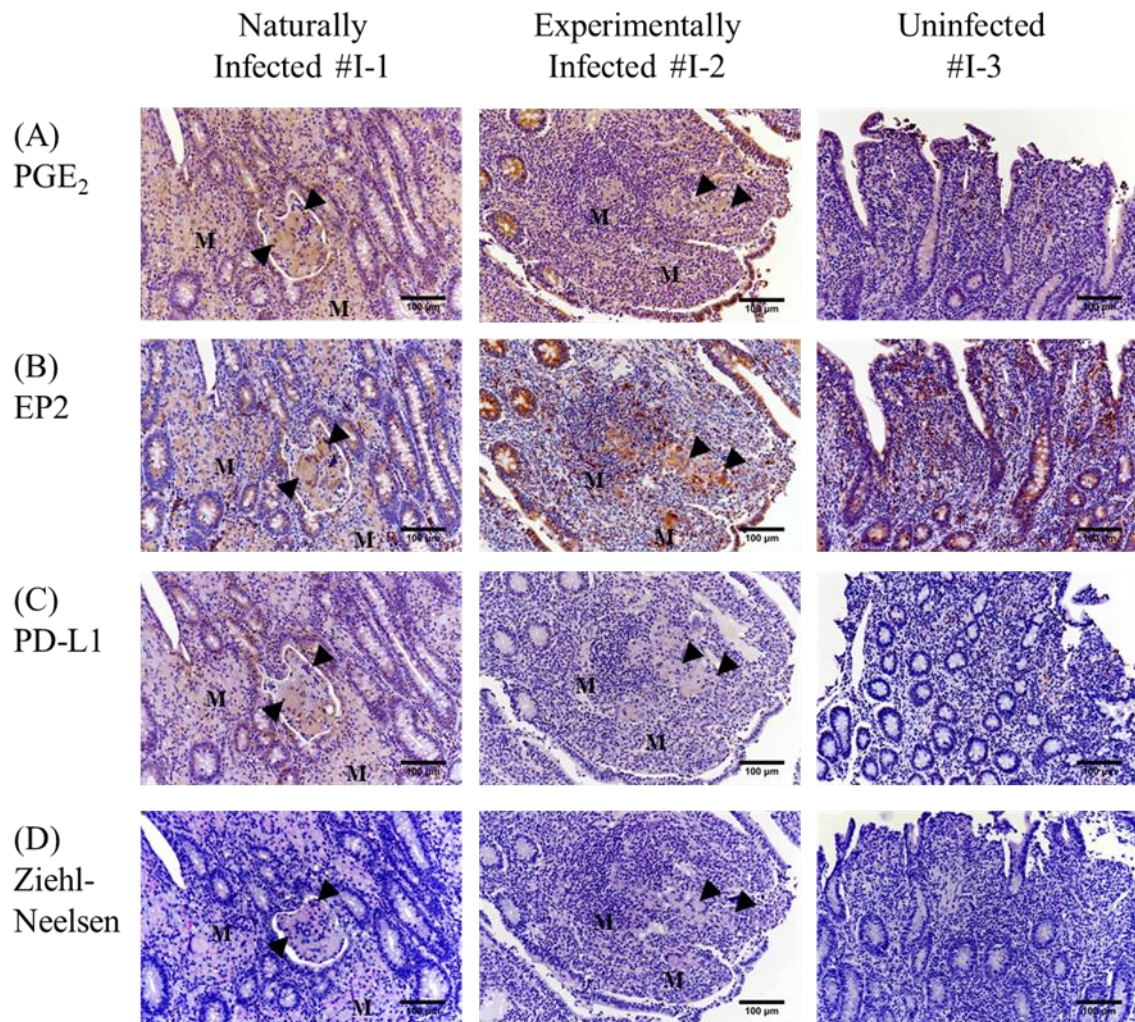


Figure I-7. The expression of PGE₂, EP2, and PD-L1 and the localization of MAP in the ileal tissues from cattle with Johne’s disease. (A–C) Immunohistochemical staining was performed using the ileal tissues obtained from cattle naturally or experimentally infected with MAP (animals #I-1 and #I-2) and an uninfected cow (animal #I-3) to detect PGE₂ (A), EP2 (B), and PD-L1 (C). (D) Ziehl-Neelsen staining in the ileal tissues of MAP-infected and uninfected cattle (animals #I-1–#I-3) was performed to detect acid-fast bacilli. Arrowheads indicate MAP-infected Langhans giant cells, and “M” indicates the accumulation of MAP-infected macrophages.

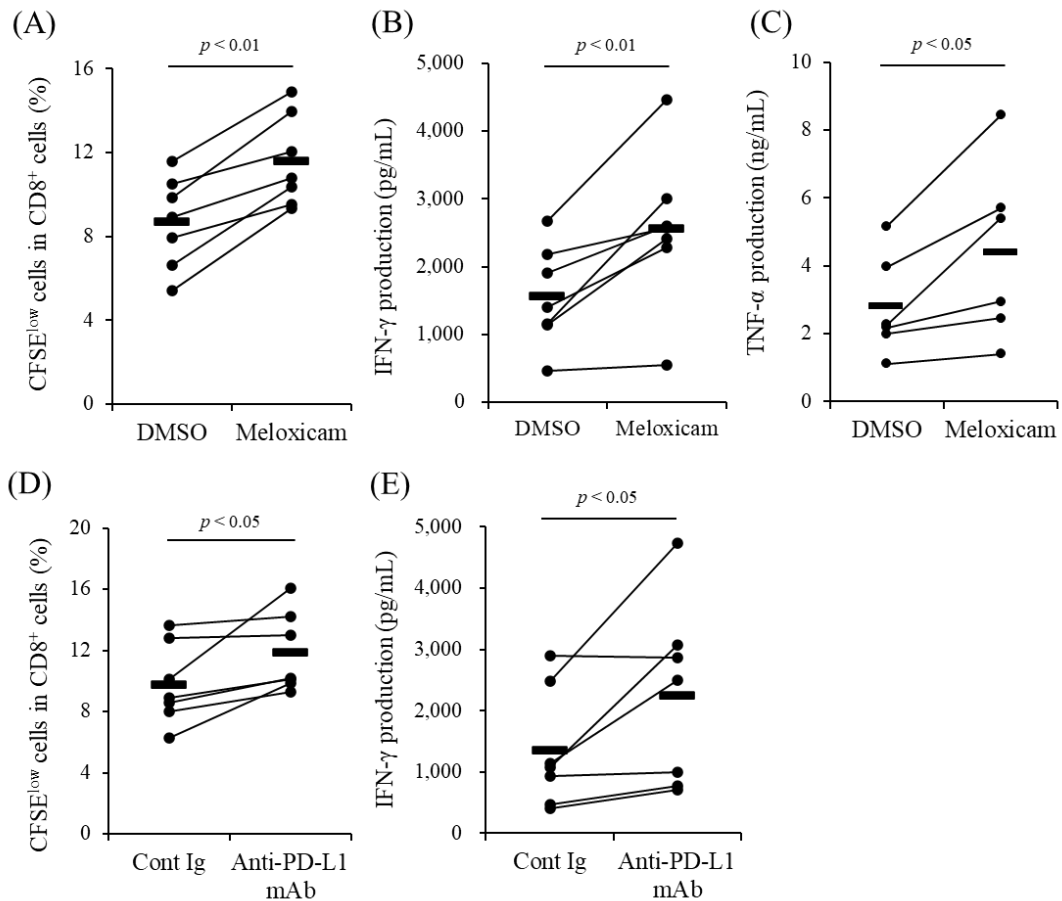


Figure I-8. The activation of Th1 responses by treatment with the COX-2 inhibitor or anti-PD-L1 Ab. (A–C) PBMCs from MAP-infected cattle (A and B: $n = 7$, C: $n = 6$) were cultured with 1 μM of the COX-2 inhibitor in the presence of J-PPD for 120 h. (A) CD8⁺ cell proliferation was assayed by flow cytometry. (B and C) IFN- γ (B) and TNF- α (C) concentrations in culture supernatants were measured by ELISA. (D and E) PBMCs from MAP-infected cattle ($n = 7$) were cultured with 10 $\mu\text{g}/\text{mL}$ of anti-bovine PD-L1 mAb (4G12) in the presence of J-PPD for 120 h. CD8⁺ cell proliferation (D) and IFN- γ production (E) were analyzed by flow cytometry and ELISA, respectively. (A–E) Statistical analysis was performed by the Wilcoxon signed-rank test. Cont Ig: rat control IgG.

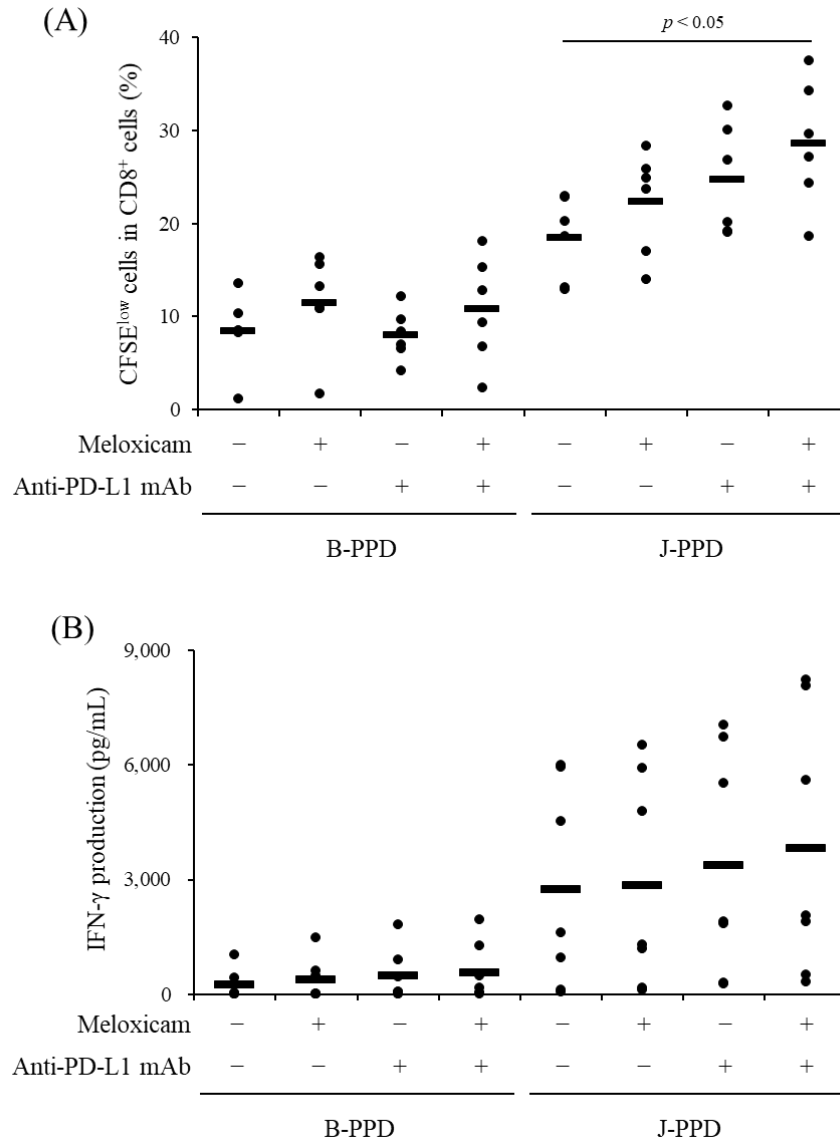


Figure I-9. The enhancement of Th1 responses by the combined treatment of the COX-2 inhibitor with anti-PD-L1 Ab. (A and B) PBMCs from MAP-infected cattle were cultured with 1 μ M of the COX-inhibitor and 10 μ g/mL of anti-bovine PD-L1 mAb (4G12) in the presence of J-PPD or B-PPD for 120 h. CD8⁺ cell proliferation (A) and IFN- γ production (B) were analyzed by flow cytometry and ELISA, respectively. Statistical analysis was performed by the Steel-Dwass test.

DISCUSSION

During the late subclinical stage of MAP infection, a decline in MAP-specific Th1 response contributes to bacterial growth and progression to the clinical stage because Th1 response, especially IFN- γ production, plays an essential role in the control of MAP infection [Bassey and Collins, 1997; Burrells *et al.*, 1998; Weiss *et al.*, 2006]. In addition, MAP infection induces the production of IL-10, which is an immunosuppressive cytokine and activates STAT3, contributing to immunosuppression and bacterial persistence [Weiss *et al.*, 2005; Hussain *et al.*, 2016]. As shown in Chapter I, serum PGE₂ concentrations were increased in MAP-infected cattle, and treatment with PGE₂ suppressed Th1 responses, such as T-cell proliferation and Th1 cytokine production, in cattle. In addition, PGE₂ treatment upregulated the expression of *IL-10* and *STAT-3* genes in PBMCs. Thus, these data suggest that PGE₂ is associated with the progression of Johne's disease by suppressing Th1 response and inducing IL-10 production. Furthermore, several studies have previously shown the involvement of PGE₂ in other mycobacterial infections [Edwards *et al.*, 1986; Chen *et al.*, 2008], but the role of PGE₂ in these infections was not demonstrated. The data shown in this chapter could be important for the understanding of the role of PGE₂ during mycobacterial infections.

J-PPD stimulation promoted PGE₂ production from PBMCs of MAP-infected cattle by increasing *COX2* expression. Previous reports have shown that J-PPD stimulation induces the secretion of IFN- γ and TNF- α from MAP-specific CD4⁺ T cells in PBMC cultures [Coussens, 2004; Stabel, 2006; Sohal *et al.*, 2008]. Inflammatory cytokines including TNF- α are important factors to induce *COX2* transcription via NF- κ B activation in a human cell line [Jobin *et al.*, 1998]. In mouse macrophages, NF- κ B activation by IFN- γ -induced TNF is involved in the transcriptional control of *COX2* expression [Viladell Sol and Fresno, 2005]. Taken together, TNF- α secretion may be involved in the induction of *COX2* expression in macrophages via the TNF- α -NF- κ B axis, leading to the increase in PGE₂ production in PBMC cultures stimulated with J-PPD.

A previous study has shown the association of immunoinhibitory molecules with the loss of functional Th1 responses during this infection [Okagawa *et al.*, 2016a], although the mechanism for the upregulation of these inhibitory molecules is still unclear. Here, the results in this chapter revealed that the treatment with PGE₂ *in vitro* induced PD-L1 expression. The expression of *IL-10* and *STAT3* genes was also upregulated by PGE₂ treatment. A previous study has shown that PD-L1 expression is decreased by the inhibition of STAT3 activity in non-small-cell lung cancer [Abdelhamed *et al.*, 2016]. Therefore, PGE₂-mediated PD-L1 upregulation might be caused via the activation of IL-

10–STAT3 signaling. This study also revealed that PGE₂ was expressed in MAP-infected macrophages and Langhans giant cells in the ileum tissues obtained from cattle at the clinical stages of Johne's disease. Interestingly, PD-L1 expression was also observed in MAP-infected macrophages in the same lesions. These findings suggest that PGE₂ is an inducer of PD-L1 via IL-10–STAT3 signaling, leading to the immunosuppression and the formation of pathological lesions in the intestinal tissues of animals with Johne's disease. However, the detailed roles of PGE₂ in the formation of pathological lesions during Johne's disease are still unclear. Thus, additional experiments are needed to elucidate the mechanism in detail.

In Chapter I, the treatment with the COX-2 inhibitor *in vitro* activated Th1 responses, such as CD8⁺ T-cell proliferation and IFN- γ production, in the presence of J-PPD stimulation. Additionally, the combination of the COX-2 inhibitor with anti-bovine PD-L1 Ab enhanced MAP-specific Th1 responses *in vitro*, although the difference was not statistically significant in the case of IFN- γ production, possibly due to the limited number of tested samples. Previous studies have demonstrated that CD8⁺ CTLs and macrophages, which are activated by Th1 cytokines, play a key role in the killing of intracellular MAP [Coussens, 2004; Stabel, 2006; Sohal *et al.*, 2008]. Therefore, the treatment of the COX-2 inhibitor with or without anti-PD-L1 Ab could be a novel control method to prevent the progression of this disease. Additionally, previous studies have shown that the upregulation of immunoinhibitory molecules is observed in other bovine infections, such as BLV infection and bovine mycoplasmosis [Ikebuchi *et al.*, 2011, 2013; Goto *et al.*, 2017, Konnai *et al.*, 2017]. However, no study has demonstrated the association of PGE₂ with other chronic infections in cattle. Future studies will be required to examine the clinical efficacy of the treatment with the COX-2 inhibitor in MAP-infected cattle, and the involvement of PGE₂ in the pathogenesis of other bovine infections.

SUMMARY

Johne's disease, which is caused by MAP infection, is a bovine chronic enteritis and endemic in many countries including Japan. The upregulation of immunoinhibitory molecule, such as PD-1 and PD-L1, was observed during MAP infection. However, the detailed mechanism of immunosuppression has not been fully elucidated. PGE₂ is known to have suppressive effects on immune cells in humans and mice, but little information is available on its suppressive effects in the field of veterinary medicine.

In this chapter, the functional analysis of PGE₂ using bovine PBMCs and kinetic analysis of PGE₂ in MAP-infected cattle were performed to examine whether PGE₂ is involved in the immunosuppression observed during Johne's disease. Treatment of PBMCs with PGE₂ suppressed bovine Th1 responses, such as T-cell proliferation and Th1 cytokine production, and increased the expression of PD-L1. Serum PGE₂ concentrations were increased in cattle with Johne's disease, and PGE₂ expression was upregulated in ileum tissues derived from cattle with Johne's disease. Additionally, the stimulation of J-PPD induced *COX2* gene expression, PGE₂ secretion, and the expression of immunoinhibitory molecules in PBMCs of MAP-infected cattle *in vitro*. Hence, these results suggest that the PGE₂ pathway regulates MAP-specific Th1 responses. Furthermore, the inhibition of PGE₂ production by the COX-2 inhibitor activated MAP-specific Th1 responses *in vitro*. The combined treatment of the COX-2 inhibitor with anti-bovine PD-L1 Ab enhanced MAP-specific Th1 responses, suggesting its therapeutic potential for Johne's disease. Further studies to evaluate the therapeutic efficacy in MAP-infected animals will open up new avenues for the development of a novel control strategy against Johne's disease.

CHAPTER II

Antiviral efficacy of COX-2 inhibitor combined with anti-PD-L1 antibody in bovine leukemia virus infection

INTRODUCTION

BLV belongs to the family of *Retroviridae*, persistently infects B cells of cattle, and causes EBL after a long latent period. The majority of the infected cattle is asymptomatic carriers of the virus called AL. Approximately 30% of the infected cattle show PL, and only 1%–5% of the infected cattle develop EBL characterized by fatal lymphosarcoma [Schwartz and Levy, 1994]. The prevalence of this infection is high in Japan and many other countries, and the seroprevalence of BLV in Japan is increasing due to the lack of an effective treatment [Murakami *et al.*, 2013]. Therefore, the development of a novel therapy for BLV infection is strongly needed for the continuous supply of livestock production.

During BLV infection, the suppression of CD4⁺ T-cell proliferation and cytotoxic immune responses to BLV antigens contributes to the disease progression [Orlik and Splitter, 1996; Kabeya *et al.*, 2001]. These studies suggest that BLV-specific Th1 response plays a central role in the control of BLV infection. Previous studies have revealed the detailed mechanisms of BLV-specific Th1 suppression during BLV infection. The expression of immunoinhibitory molecules, including PD-1 and PD-L1, was upregulated, leading to the suppression of BLV-specific Th1 responses and the promotion of disease progression [Ikebuchi *et al.*, 2010, 2011; Konnai *et al.*, 2017]. Furthermore, the treatment with anti-PD-1/PD-L1 Abs *in vivo* decreased BLV proviral loads in the infected cattle [Nishimori *et al.*, 2017; Okagawa *et al.*, 2017]. These results suggest that treatment targeting PD-1 and PD-L1 has a potential as a new therapeutic method for BLV infection. However, it is still unclear how these immunoinhibitory molecules are upregulated in BLV-infected cattle.

In Chapter I, PGE₂ was shown to suppress Th1 responses and induced PD-L1 expression in bovine immune cells *in vitro*. Additionally, PGE₂ was upregulated in cattle with Johne's disease, and PGE₂ inhibition enhanced T-cell proliferation and Th1 cytokine production in response to J-PPD stimulation. These results suggest that PGE₂ is an inducer of PD-L1 expression, and causes the suppression of Th1 responses during Johne's disease.

However, little is known on the roles of PGE₂ in BLV infection. Thus, in Chapter II, PGE₂ kinetics were analyzed in BLV-infected cattle to elucidate the role of PGE₂ in the suppression of Th1 responses during this infection. In addition, the effects of the COX-2 inhibitor on Th1 responses and BLV proviral loads were evaluated *in vitro* and *in vivo*, respectively. Finally, the combined treatment of the COX-2 inhibitor with anti-PD-L1 Ab was tested whether this treatment enhances antiviral effects in BLV-infected cattle.

MATERIALS AND METHODS

Animals

Blood samples from uninfected and BLV-infected cattle were collected at dairy farms in Hokkaido, Japan. Informed consent was obtained from all owners of cattle sampled in Chapter II. BLV infection was diagnosed by a commercial ELISA (JNC, Tokyo, Japan) and nested polymerase chain reaction (PCR) targeting the BLV long terminal repeat (LTR) using genomic DNA extracted from whole blood samples by Wizard Genomic DNA Purification Kit (Promega, Madison, WI, USA). Primers were LTR1 5'-TGT ATG AAA GAT CAT GCC GAC-3' and LTR533 5'-AAT TGT TTG CCG GTC TCT-3' for the initial PCR, and LTR256 5'-GAG CTC TCT TGC TCC CGA GAC-3' and LTR453 5'-GAA ACA AAC GCG GGT GCA AGC CAG-3' for the second PCR. The numbers of leukocytes in peripheral blood of BLV-infected cattle were counted using a Celltac α MEK-6450 automatic hematology analyzer (Nihon Kohden, Tokyo, Japan), and animals were diagnosed with PL when the lymphocyte counts were more than 7,500 cells/ μ L. The serum or plasma samples from uninfected and BLV-infected cattle were collected for the measurement of PGE₂ concentrations by ELISA as described in Chapter I. All experimental procedures using bovine samples were carried out following approval from the local committee for animal studies at Hokkaido University (approval number: 17-0024) and the Ethics Committee of the Animal Research Center, Agricultural Research Department, Hokkaido Research Organization (approval number: 1703).

Cell preparation

PBMCs of uninfected and BLV-infected cattle were separated as described in Chapter I of this study. The isolation of CD14⁺ and CD21⁺ cells was performed by using PBMCs by magnetic sorting. Briefly, PBMCs were incubated with anti-bovine CD14 mAb (CAM36A) or anti-bovine CD21 mAb (GB25A; Washington State University Monoclonal Antibody Center), and then, the isolation was carried out using BD IMagnet Cell Separation System (BD Bioscience) or autoMACS Pro (Miltenyi Biotec, Bergisch Gladbach, Germany). The purity of each population (> 90%) was examined using FACS Verse. CD14 and CD21 were used as markers of monocytes and B cells, respectively. PBMCs, CD14⁺ cells, and CD21⁺ cells were cultured in RPMI 1640 medium containing 10% heat-inactivated FCS, 100 U/mL penicillin, 100 μ g/mL streptomycin, and 2 mM L-glutamine using 96-well culture plates as described in Chapter I.

qPCR

Total RNA extraction and cDNA synthesis were performed as described in Chapter I. To quantitate the mRNA expression of *COX2*, *15-hydroxyprostaglandin dehydrogenase (HPGD)*, *EP2*, *EP4*, *IFN- γ* , *env*, *G4*, and *R3* in PBMCs and each subpopulation (CD14⁺ and CD21⁺), qPCR was performed as described in Chapter I. *ACTB* and *GAPDH* were used as reference genes. Primers used in Chapter II are shown in Table II-1.

To measure BLV proviral loads in the infected animals, qPCR was performed using genomic DNA extracted from PBMCs by Wizard Genomic DNA Purification Kit. The DNA concentrations were measured using NanoDrop 8000 Spectrophotometer (Thermo Fisher Scientific). Amplification was performed with a reaction mixture including 5 μ L of 2 \times Cycleave PCR Reaction Mix SP (Takara Bio), 0.5 μ L of Probe/Primer Mix for BLV (Takara Bio), 1 μ L of template DNA, and 3.5 μ L of RNase-free distilled water (Takara Bio) using LightCycler 480 System II. The condition was 95°C for 10 s, followed by amplification of the template for 55 cycles at 95°C for 5 s and 64°C for 30 s. Calibration curves were generated to calculate the BLV provirus copy numbers by using Serial dilutions of BLV Positive Control (Takara Bio). The indicated values are the numbers of copies per 50 ng of genomic DNA.

Cell culture

To examine the effects of PGE₂ signaling on the expression of viral genes, PBMCs from BLV-infected cattle were cultured with 1 μ M of PGE₂, 1 μ g/mL of EP2 agonist (Butaprost (free acid); Cayman Chemical), or 1 μ g/mL of EP4 agonist (Revinprost; Cayman Chemical) for 72 h.

To examine whether BLV antigens induce the production of PGE₂, PBMCs from uninfected and BLV-infected cattle were cultured in the presence of a BLV antigen, fetal lamb kidney (FLK)-BLV (2% heat-inactivated culture supernatant of FLK-BLV cells), for 144 h. To evaluate the capacity of PGE₂ production, PBMCs, CD14⁺ cells, and CD21⁺ cells were separately incubated without stimulation for 72 h.

To examine the effects of PGE₂ inhibition and/or PD-L1 blockade, PBMCs from BLV-infected cattle were labeled with CFSE and cultured with 1 μ M of the COX-2 inhibitor, meloxicam, and/or 10 μ g/mL of anti-bovine PD-L1 Ab in the presence of FLK-BLV for 144 h. In this assay, two types of anti-bovine PD-L1 Abs, anti-bovine PD-L1 rat mAb (4G12) and anti-bovine PD-L1 rat-bovine chimeric Ab (chAb, Boch4G12) [Nishimori *et al.*, 2017], were used to evaluate the combination effect. DMSO was used as a vehicle control of the COX-2 inhibitor. Rat IgG and bovine IgG were used as control Abs of anti-bovine PD-L1 Abs. FLK (2% heat-inactivated culture supernatants of FLK cells) was used as a control antigen.

Immunohistochemical staining

The sections of superficial cervical lymph nodes from an uninfected Holstein cow (female, 75 months of age) and periocular mass lesions from an EBL Holstein cow (female, 24 months of age) were collected, and the expression of PGE₂ and PD-L1 was analyzed by immunohistochemical staining as described in Chapter I. The cow exhibiting tumors was diagnosed with EBL as described in a previous report [Ikebuchi *et al.*, 2013]. The tumor mass lesion was confirmed as B-cell lymphoma by immunohistochemical staining with an anti-CD20 polyclonal Ab (Thermo Fisher Scientific) (data not shown).

COX-2 inhibitor administration

To analyze the antiviral efficacy of COX-2 inhibition, three BLV-infected cattle (animals #II-1–#II-3, Table II-2) were subcutaneously administered with 0.5 mg/kg of meloxicam (Metacam; Boehringer Ingelheim, Ingelheim, Germany) once a week for a total of nine times (animals #II-1 and #II-2) or a total of five times (animal #II-3). These animals were kept at the three different locations: in a private dairy farm (Shibecha, Hokkaido, Japan), a biosafety level I animal facility at the Animal Research Center, Agricultural Research Department, Hokkaido Research Organization (Shintoku, Hokkaido, Japan), and an animal facility at the Faculty of Veterinary Medicine, Hokkaido University. Blood collections from animals #II-1–#II-3 were conducted at least once per week during the observation period of 12 weeks (84 days).

Anti-bovine PD-L1 Ab administration

To analyze the antiviral efficacy of PD-L1 blockade, a BLV naturally-infected cow (animal #II-5, Table II-2) was intravenously administered with 1 mg/kg of anti-bovine PD-L1 chAb (Boch4G12). As a control, another BLV naturally-infected cow (animal #II-4, Table II-2) was intravenously administered with saline. Both animals (animals #II-4 and #II-5) were kept in a private dairy farm in Hokkaido, Japan. Blood collections from these animals were conducted at least once per week during the observation period of 9 weeks (63 days).

The evaluation of the combined COX-2 inhibition and PD-L1 blockade *in vivo*

To examine the antiviral efficacy of the combination treatment, two BLV-infected cattle (animals #II-3 and #II-6, Table II-2) were intravenously administered with 1 mg/kg of anti-bovine PD-L1 chAb (Boch4G12), and then, animal #II-3 was subcutaneously co-administered with 0.5 mg/kg of Metacam three times at weekly intervals. Both animals

were kept in the animal facility at the Faculty of Veterinary Medicine, Hokkaido University. Animal #II-3 was also used for COX-2 inhibitor administration as described above, and was administered with Boch4G12 after a long interval (118 days) from the final administration of the COX-2 inhibitor. Blood collections from these animals were conducted at least once per week during the observation period of 7 weeks (49 days).

Statistical analyses

In Figures II-9 and 10, statistical significances were analyzed using the Dunnett test. In other figures, statistical significances were analyzed using the Wilcoxon signed-rank test for comparing two-group and the Steel-Dwass test for comparing multiple groups, and correlations were analyzed using the Spearman correlation. All statistical tests were performed using with the MEPHAS program (<http://www.gen-info.osaka-u.ac.jp/MEPHAS/>). For all tests, $p < 0.05$ was considered statistically significant.

Table II-1. Primers used in Chapter II.

Gene	Primer sequence (5'–3')
<i>IFN-γ</i>	F: ATA ACC AGG TCA TTC AAA GG R: ATT CTG ACT TCT CTT CCG CT
<i>COX2</i>	F: ACG TTT TCT CGT GAA GCC CT R: TCT ACC AGA AGG GCG GGA TA
<i>EP4</i>	F: GTG ACC ATC GCC ACC TAC TT R: CTC ATC GCA CAG ATG ATG CT
<i>EP2</i>	F: CTCTGCTGTCGGGTTTCATTA R: CTACCCTCCTCAAAGGTCAATC
<i>HPGD</i>	F: GAA TCT CGA AGC AGG TGT CA R: CCA GCT TTC CAA AGT GGT CT
<i>gp51</i>	F: ACC TTT CTG TGC CAA GTC R: ATC GGG GCT CGC AAT CAT A
<i>G4</i>	F: TTC GGC GCC CAG CCA CAT C R: GTC GTT ATC AGG TAA TGG ATC CCG A
<i>R3</i>	F: GAT CAT CAG ATG GGT CCT GAT GAA C R: GCT GCT GGA TGT GGC TGG AAT GTC
<i>ACTB</i>	F: TCT TCC AGC CTT CCT TCC TG R: ACC GTG TTG GCG TAG AGG TC
<i>GAPDH</i>	F: GGC GTG AAC CAC GAG AAG TAT AA R: CCC TCC ACG ATG CCAAAG T

F: forward, R: reverse.

Table II-2. Information of cattle used in clinical studies of Chapter II.

Animal	#II-1	#II-2	#II-3 (Clinical study of the COX-2 inhibitor)	#II-4	#II-5	#II-6	#II-3 (Clinical study of the combined treatment)
Age	43 months old	96 months old	47 months old	19 months old	13 months old	76 months old	52 months old
Breed	Holstein	Holstein	Holstein	Holstein	Holstein	Holstein	Holstein
Sex	female	female	female	female	female	female	female
Body weight	749 kg	736 kg	759 kg	433 kg	295 kg	799 kg	799 kg
Administration dose (Boch4G12)				Saline 50 mL, <i>i.v.</i>	1 mg/kg, <i>i.v.</i>	1 mg/kg, <i>i.v.</i>	1 mg/kg, <i>i.v.</i>
Administration dose (Metacam)	0.5 mg/kg, once a week, totally 9 times, <i>s.c.</i>	0.5 mg/kg, once a week, totally 9 times, <i>s.c.</i>	0.5 mg/kg, once a week, totally 5 times, <i>s.c.</i>				0.5 mg/kg, once a week, totally 3 times, <i>s.c.</i>

RESULTS

Kinetic analysis of PGE₂ in BLV-infected cattle

To determine whether PGE₂-induced immunosuppression is a common feature of bovine chronic infections, the PGE₂ kinetics were analyzed in BLV-infected animals. Compared to uninfected cattle, the plasma concentrations of PGE₂ were increased in AL and PL cattle (Figure II-1A). Additionally, the PGE₂ concentrations were positively correlated with the lymphocyte numbers, BLV proviral loads, and PD-L1 expression in IgM⁺ B cells in BLV-infected cattle (Figures II-1B–E). Furthermore, the results of immunohistochemical staining showed that B-cell lymphoma tissues from EBL cattle strongly expressed both PGE₂ and PD-L1 (Figures II-2A and B). These results suggest that PGE₂ production appears to be increased with the disease progression of BLV infection. To examine the major source of PGE₂ production in the peripheral blood of BLV-infected cattle, *COX2* expression was quantitated in PBMCs and each cell population (CD14⁺ and CD21⁺). Consistent with the results of PGE₂ concentrations in the plasma, *COX2* expression in PL cattle was higher than that in uninfected and AL cattle (Figures II-3A–C). Compared to CD21⁺ cell cultures, the culture supernatants of CD14⁺ cell cultures contained the high concentration of PGE₂ (Figure II-3D). Thus, CD14⁺ cells might be the predominant source of PGE₂ in BLV-infected cattle. Finally, the expression of *EP4*, *EP2*, and *HPGD* genes was analyzed in PBMCs of uninfected and BLV-infected cattle, and it was revealed that the expression of PGE₂ receptors *EP4* and *EP2* was upregulated in PL cattle (Figure II-4A and B). In contrast, the gene expression of *HPGD*, which is an enzyme involving in PGE₂ catabolism, was downregulated in PL cattle and was negatively correlated with BLV proviral loads and PGE₂ concentrations in BLV-infected cattle (Figures II-4C–E). Collectively, these results suggest the association of PGE₂ with disease progression in BLV-infected cattle.

Upregulation of PGE₂ by stimulation with BLV antigens

The production of PGE₂ was analyzed in the presence of BLV antigens. FLK-BLV exposure induced PGE₂ production from PBMCs of AL and PL cattle, but not from those of uninfected cattle (Figures II-5A–C). Additionally, this induction of PGE₂ secretion was significantly inhibited by the treatment with the COX-2 inhibitor (Figures II-5B and C). Therefore, these observations suggest that the stimulation by BLV antigens activates the COX-2–PGE₂ pathway in the infected cattle.

Upregulation of *env*, *G4*, and *R3* viral genes by PGE₂

It has been previously reported that PGE₂ induces the expression of BLV viral genes, such as *tax* [Pyeon *et al.*, 2000]. To elucidate the effects of PGE₂ on viral gene expression, PBMCs of BLV-infected cattle were cultured with PGE₂. The results by qPCR showed that mRNA expression of *env*, *G4*, and *R3* was promoted by the treatment with PGE₂ *in vitro* (Figures II-6A–C). Additionally, PBMCs from BLV-infected cattle were cultured with EP2 or EP4 agonist, both of which induced the expression of these viral genes (Figures II-6D–F), suggesting the regulation of viral gene expression via the PGE₂/EP2 and/or PGE₂/EP4 signaling.

The activation of BLV-specific Th1 responses by the combined treatment of the COX-2 inhibitor and anti-PD-L1 Ab

In Chapter I, the treatment with the COX-2 inhibitor activated MAP-specific Th1 responses *in vitro*. Here, to examine whether the COX-2 inhibition activates Th1 responses in BLV-infected cattle, PBMCs from BLV-infected cattle were cultured with the COX-2 inhibitor in the presence of FLK-BLV. The treatment with the COX-2 inhibitor increased the proliferation of CD4⁺ and CD8⁺ cells and Th1 cytokine production from PBMCs *in vitro* (Figures II-7A–D). In addition, the combined treatment of the COX-2 inhibitor with anti-bovine PD-L1 mAb significantly increased the proliferation rate of CD4⁺ and CD8⁺ cells and IFN- γ production in the presence of FLK-BLV, whereas the stimulation by FLK had no effect in either group (Figures II-8A–C). Similarly, the combined treatment with anti-bovine PD-L1 chAb, Boch4G12, also significantly increased BLV-specific T-cell proliferation and IFN- γ production compared to the other treatment groups (Figures II-8D–F). Therefore, these data suggest that the combination treatment enhances BLV-specific Th1 responses *in vitro*.

Antiviral efficacy of the COX-2 inhibitor in BLV-infected cattle

Next, the administration of the COX-2 inhibitor was conducted to demonstrate the antiviral efficacy in BLV-infected cattle. In this chapter, BLV-infected cattle (animals #II-1–#II-3) were subcutaneously administered with 0.5 mg/kg of Metacam nine (animals #II-1 and #II-2) or five (animal #II-3) times at weekly intervals. Surprisingly, the proviral loads of COX-2 inhibitor-treated BLV-infected cattle (animals #II-1–#II-3) significantly fell during the observation periods, compared to the proviral loads at day 0 (Figures II-9A–C). To examine whether the administration enhances Th1 responses in these animals, IFN- γ expression was quantitated at several time points, days 0, 1, 7, 21, and 56. Compared to day 0, IFN- γ expression levels were increased at days 7, 21, and 56 (Figure II-9D). Thus, these results suggest that treatment with the COX-2 inhibitor exerts Th1-

mediated antiviral effects against BLV *in vivo*.

Antiviral efficacy of anti-PD-L1 chAb in BLV-infected cattle

A previous study has shown the antiviral activity of anti-bovine PD-L1 chAb Boch4G12 in a calf experimentally infected with BLV [Nishimori *et al.*, 2017]. In this chapter, a BLV naturally-infected cow (animal #II-5) was intravenously administered with 1 mg/kg of Boch4G12. As a control, another naturally infected cow (animal #II-4) was administered with saline. Although the proviral loads of animal #II-4 continued to rise, the proviral loads in animal #II-5 were significantly reduced after the administration (Figures II-10A and B). Thus, PD-L1 inhibition shows antiviral effects on cattle naturally infected with BLV.

Antiviral efficacy of the combined treatment of the COX-2 inhibitor with anti-PD-L1 Ab

Finally, to examine the efficacy of the combined treatment, BLV-infected cattle (animals #II-3 and #II-6) were intravenously administered with 1 mg/kg of Boch4G12. Animal #II-3 was subcutaneously co-administered with 0.5 mg/kg of Metacam once a week for a total of three times. The treatment with Boch4G12 alone did not show antiviral effects in BLV-infected cattle with high proviral loads (Figure II-10C). Remarkably, the proviral loads of animal #II-3 were significantly reduced (nearly 80% at day 14) following the combined treatment (Figure II-10D), suggesting its potential as a novel therapeutic strategy for BLV infection.

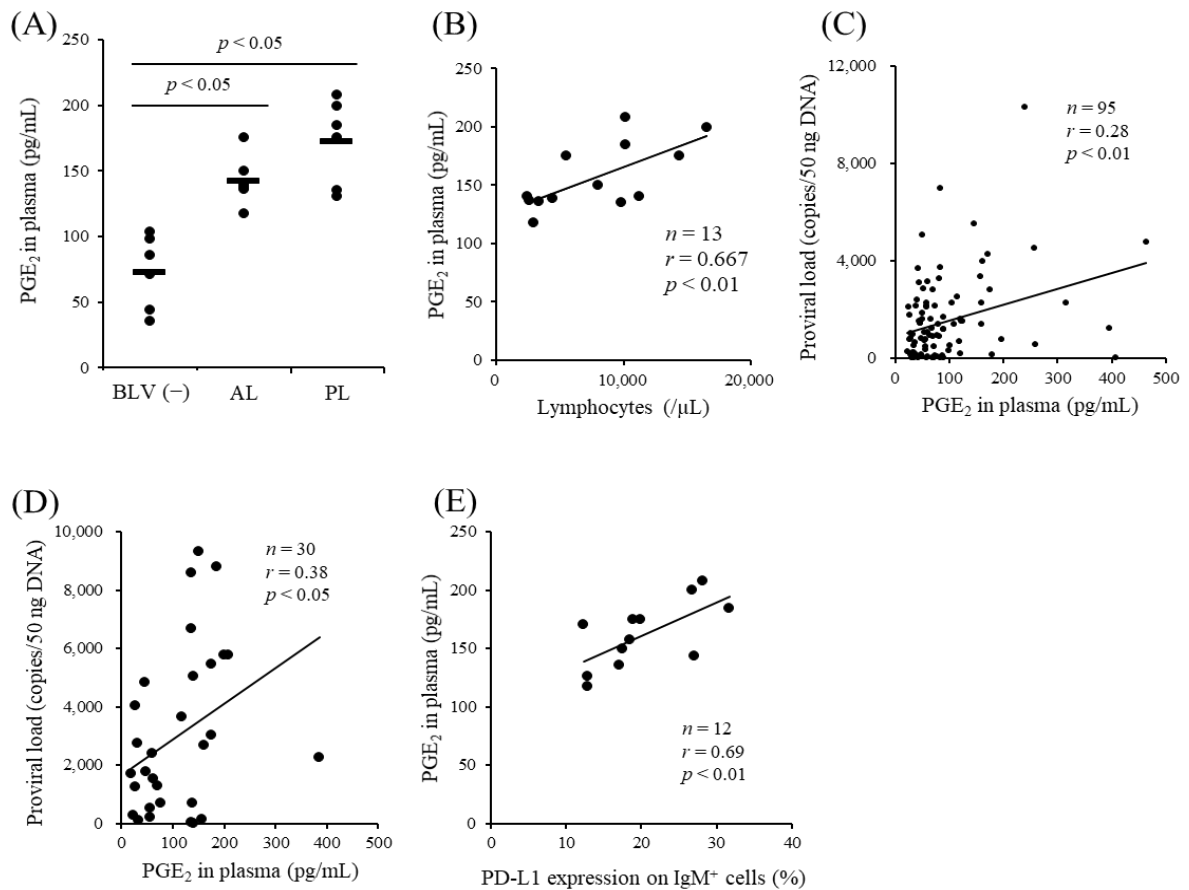


Figure II-1. Kinetic analysis of PGE₂ in BLV-infected cattle. (A) Plasma PGE₂ concentrations in uninfected ($n = 6$) and BLV-infected cattle (AL: $n = 7$, PL: $n = 6$) were measured by ELISA. Statistical analysis was performed by the Steel-Dwass test. (B–E) Positive correlations between the lymphocyte numbers (B), BLV proviral loads (C: Japanese black cattle and first filial of Japanese black/Holstein cattle, D: Holstein cattle), or PD-L1 expression in IgM⁺ cells (E) and plasma PGE₂ concentrations in BLV-infected cattle. Correlation statistics were analyzed by the Spearman correlation. BLV (-): BLV-uninfected cattle.

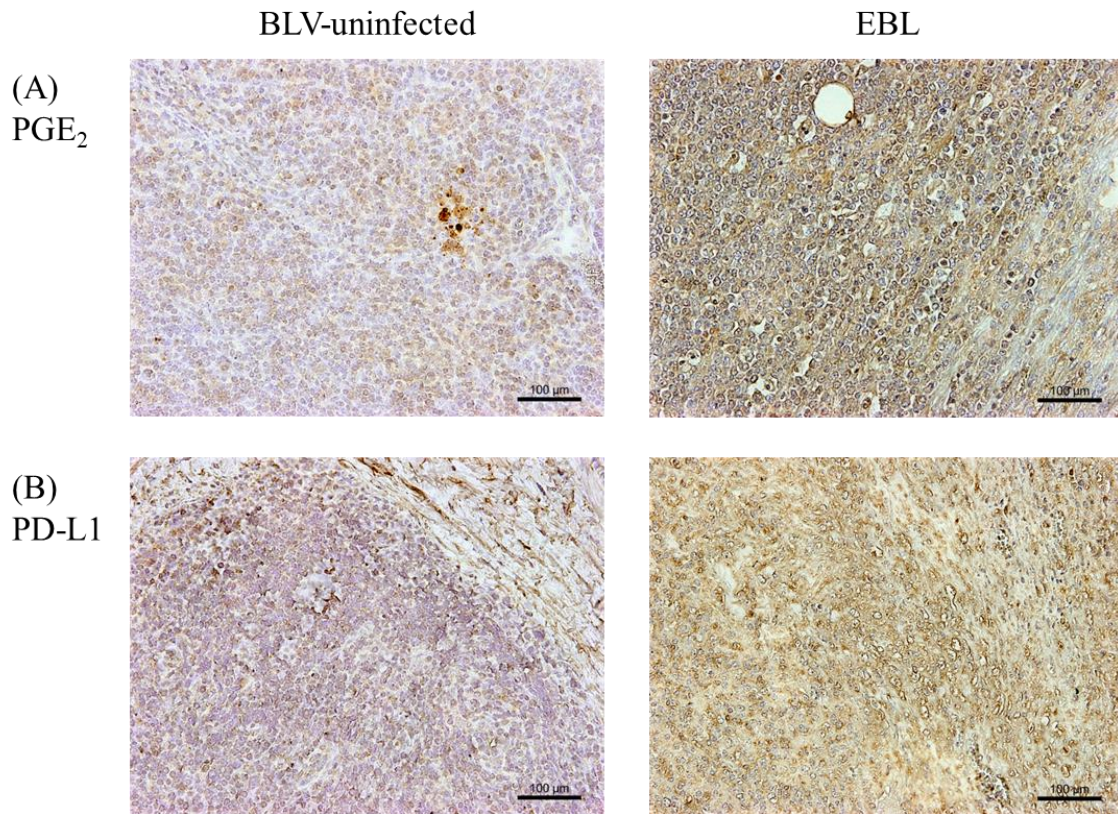


Figure II-2. PGE₂ and PD-L1 expression in tumor tissues of cattle with EBL. (A and B) The expression of PGE₂ (A) and PD-L1 (B) in lymph nodes from uninfected cattle and tumor tissues from EBL cattle was examined by immunohistochemical staining.

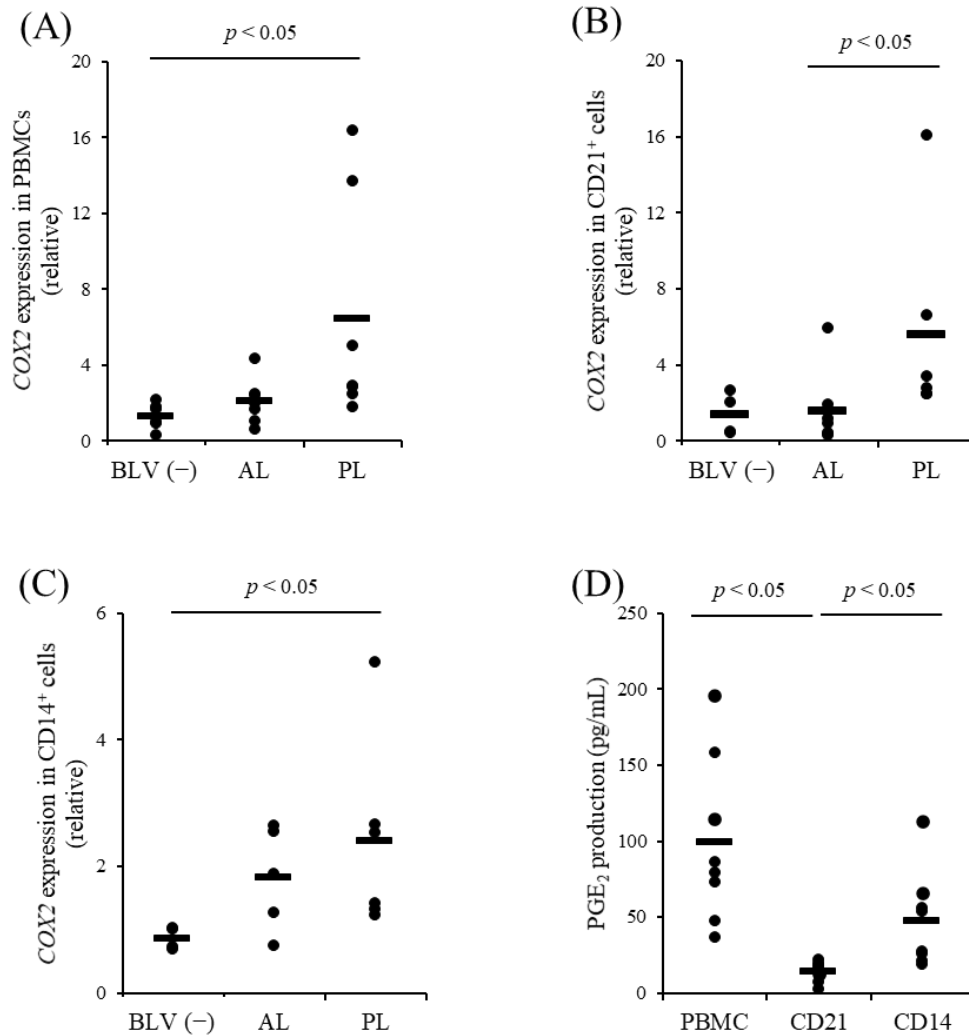


Figure II-3. *COX2* expression in cattle infected with BLV. (A–C) *COX2* expression in PBMCs ($n = 7$ each), CD21⁺ cells [BLV (-): $n = 4$, AL: $n = 7$, PL: $n = 6$], and CD14⁺ cells [BLV (-): $n = 4$, AL: $n = 5$, PL: $n = 6$] was analyzed by qPCR. (D) PGE₂ production from PBMCs, CD21⁺ cells, or CD14⁺ cells was assayed by ELISA ($n = 8$ each). (A–D) Statistical analysis was performed by the Steel-Dwass test.

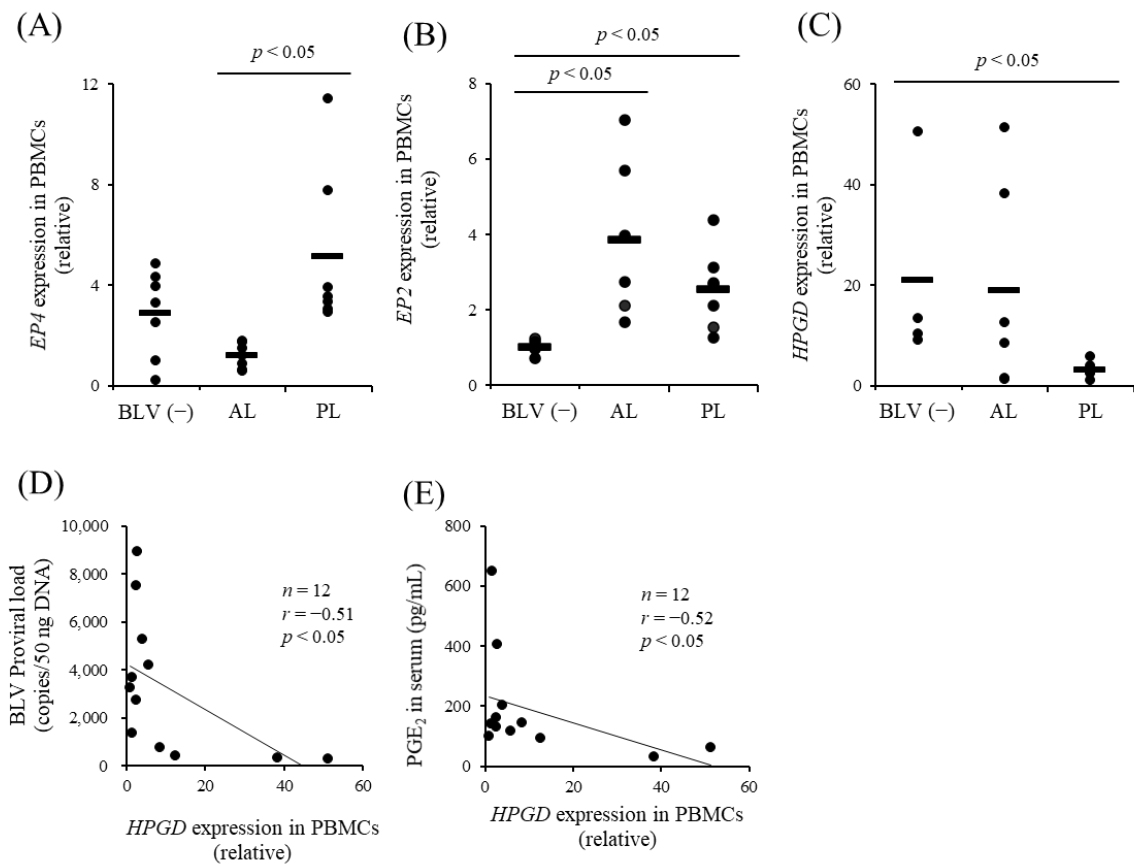


Figure II-4. *EP4*, *EP2*, and *HPGD* expression in BLV-infected cattle. (A–C) The expression of *EP4* ($n = 7$ each), *EP2* [BLV (-): $n = 6$, AL: $n = 6$, PL: $n = 7$], and *HPGD* [BLV (-): $n = 4$, AL: $n = 6$, PL: $n = 6$] in PBMCs was analyzed by qPCR. Statistical analysis was performed by the Steel-Dwass test. (D and E) Negative correlations between BLV proviral loads (D) or serum PGE_2 concentrations (E) and *HPGD* expression in PBMCs from BLV-infected cattle ($n = 12$). Correlation statistics were analyzed by the Spearman correlation.

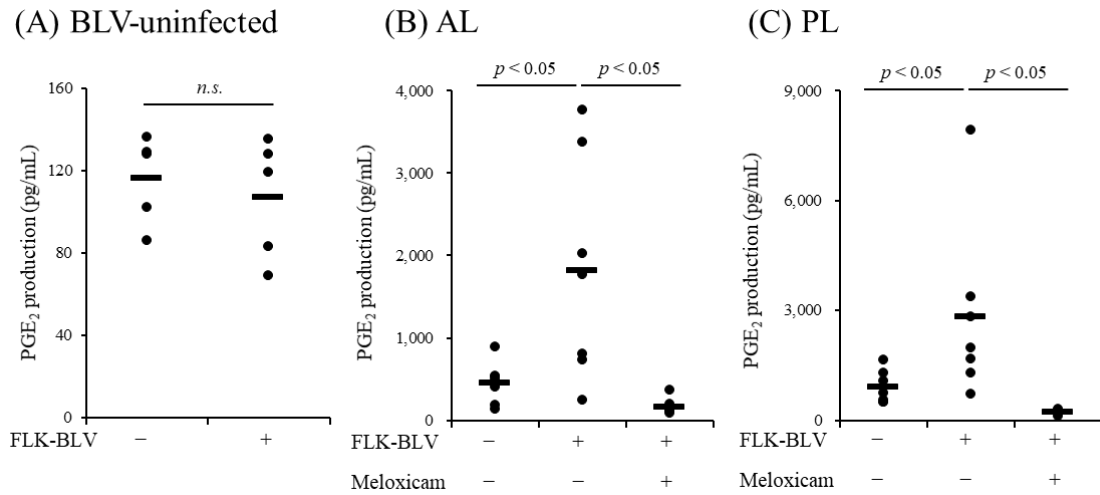


Figure II-5. The upregulation of PGE₂ secretion by FLK-BLV. (A–C) PBMCs from uninfected (A, $n = 5$), AL (B, $n = 7$), and PL (C, $n = 7$) cattle were cultured with or without 1 μ M of the COX-2 inhibitor, meloxicam, in the presence of FLK-BLV for 144 h. PGE₂ concentrations in culture supernatants were measured by ELISA. Statistical analysis was performed by the Wilcoxon signed-rank test (A) and the Steel-Dwass test (B and C).

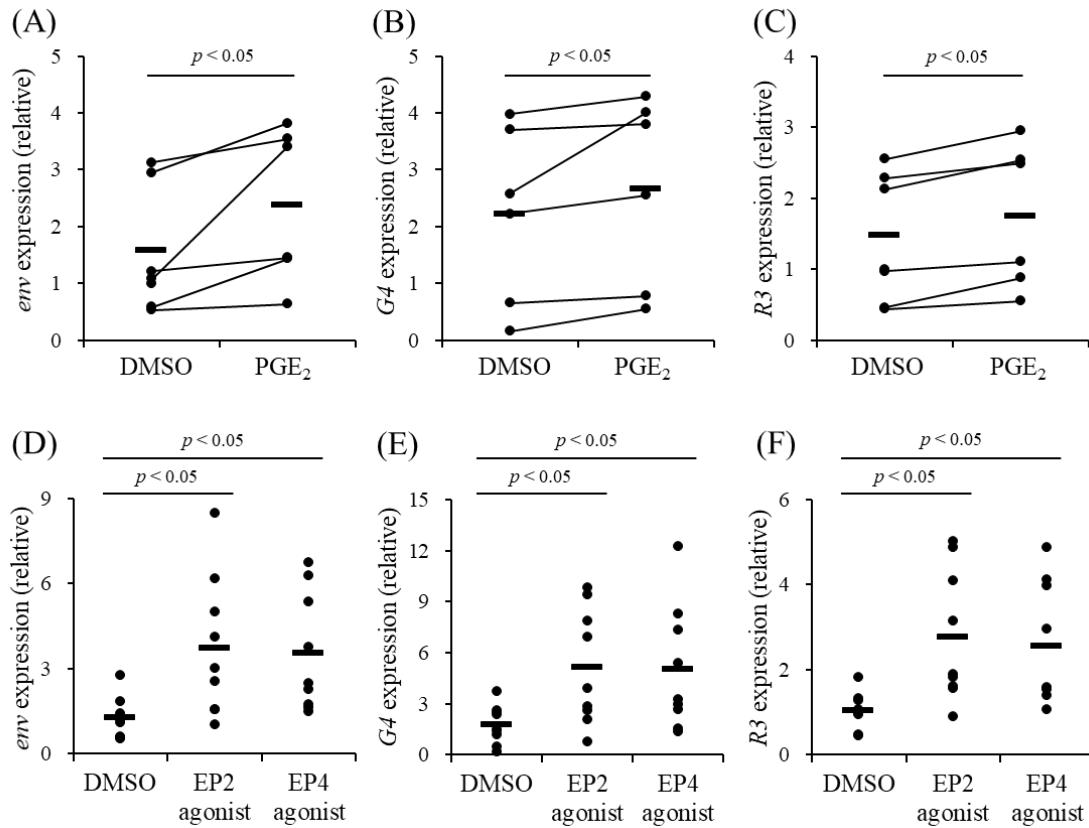


Figure II-6. The upregulation of *env*, *G4*, and *R3* genes by PGE₂. (A–F) PBMCs from BLV-infected cattle (A–C: $n = 6$, D–F: $n = 9$) were cultured with 1 μ M of PGE₂, 1 μ g/mL of EP2 agonist, or 1 μ g/mL of EP4 agonist for 72 h. The gene expression of *env*, *G4*, and *R3* was analyzed by qPCR. Statistical analysis was performed by the Wilcoxon signed-rank test (A–C) and the Steel-Dwass test (D–F).

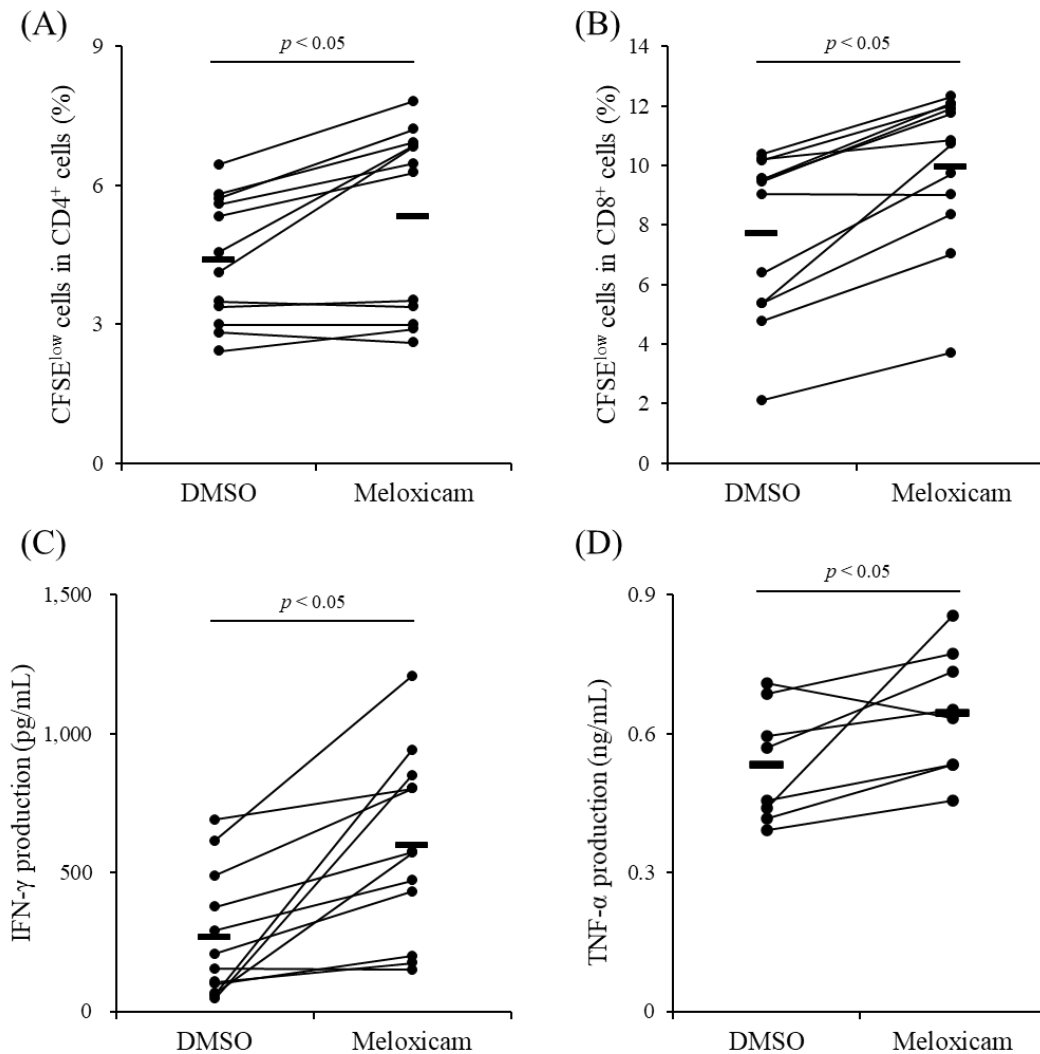


Figure II-7. The activation of Th1 responses by treatment with the COX-2 inhibitor.

(A–D) PBMCs from BLV-infected cattle (A–C: $n = 12$, D: $n = 8$) were cultured with 1 μM of the COX-2 inhibitor in the presence of FLK-BLV for 144 h. The proliferation of CD4⁺ (A) and CD8⁺ (B) cells and the production of IFN- γ (C) and TNF- α (D) were examined by flow cytometry and ELISA, respectively. Statistical analysis was performed by the Wilcoxon signed-rank test.

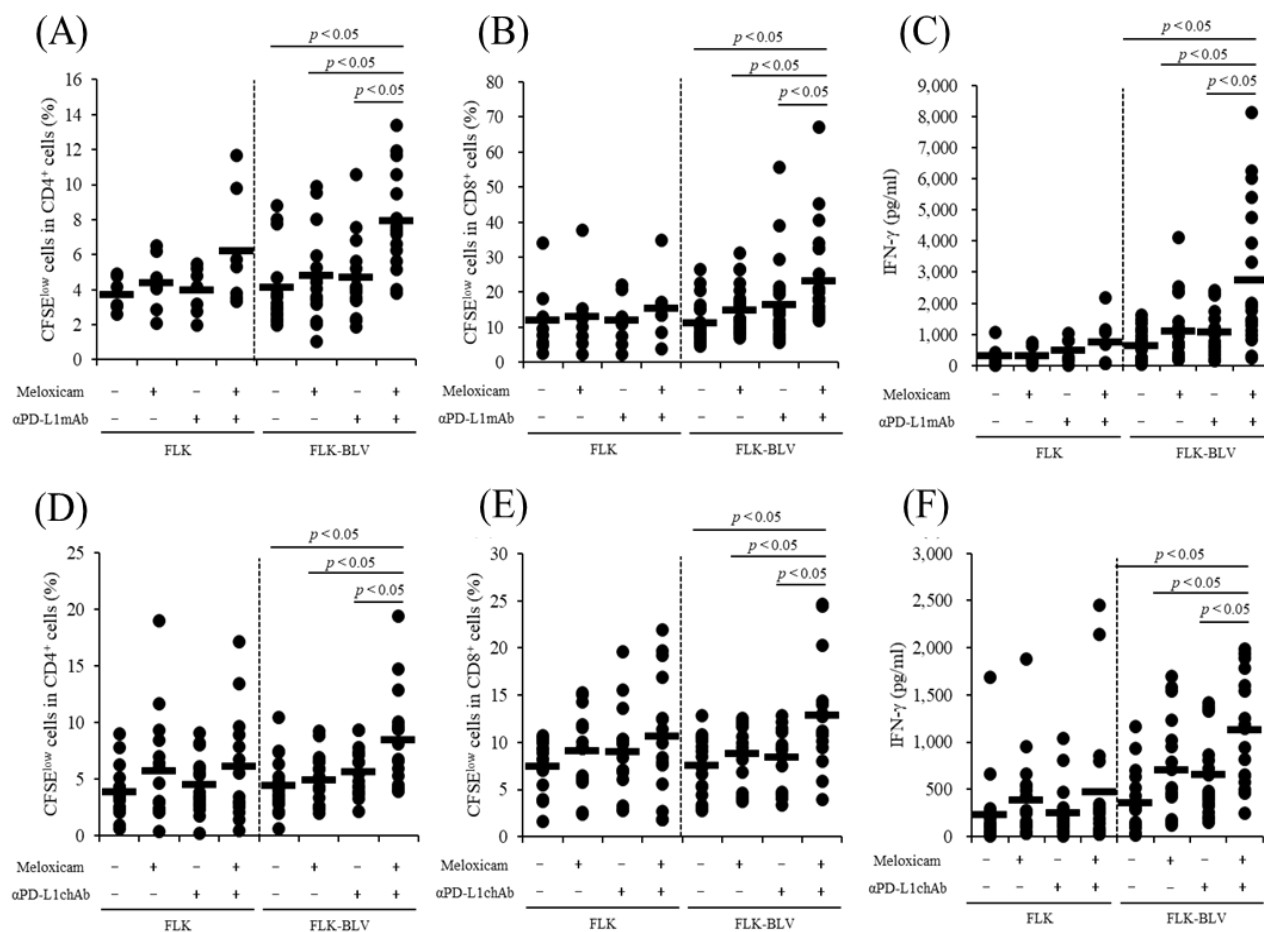


Figure II-8. The enhancement of BLV-specific Th1 responses by the combined treatment. (A–C) PBMCs from BLV-infected cattle were cultured with 1 μ M of the COX-2 inhibitor and 10 μ g/mL of anti-bovine PD-L1 mAb (4G12) in the presence of FLK-BLV for 144 h. FLK was used as a control antigen. The proliferation of CD4⁺ (A, FLK: $n = 7$, FLK-BLV: $n = 15$) and CD8⁺ (B, FLK: $n = 8$, FLK-BLV: $n = 24$) cells and the production of IFN- γ (C, FLK: $n = 7$, FLK-BLV: $n = 20$) were examined by flow cytometry and ELISA, respectively. (D–F) PBMCs from BLV-infected cattle were cultured with 1 μ M of the COX-2 inhibitor and 10 μ g/mL of anti-bovine PD-L1 chAb (Boch4G12) in the presence of FLK-BLV for 144 h. The proliferation of CD4⁺ (D: $n = 16$) and CD8⁺ (E: $n = 16$) cells and the production of IFN- γ (F: $n = 18$) were examined by flow cytometry and ELISA, respectively. (A–F) Statistical analysis was performed by the Steel-Dwass test. α PD-L1 mAb: anti-bovine PD-L1 mAb (4G12), α PD-L1 chAb: anti-bovine PD-L1 chAb (Boch4G12).

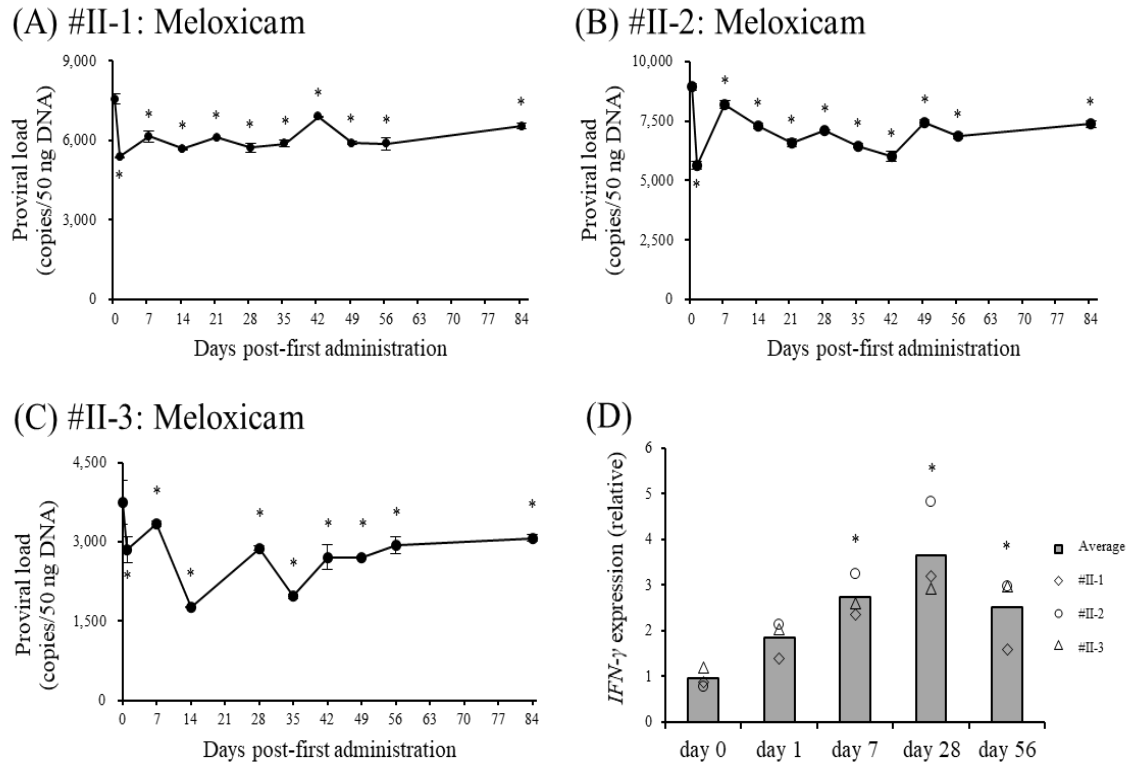
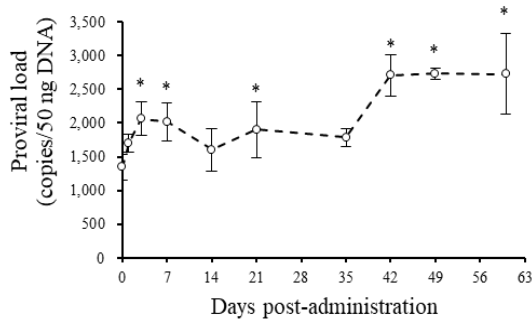
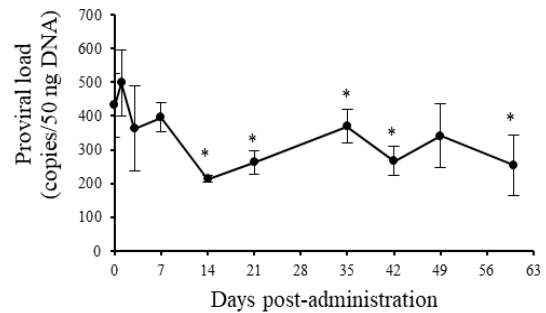


Figure II-9. Clinical tests of the COX-2 inhibitor using BLV-infected cattle. (A–D) Three BLV-infected cattle (animals #II-1–#II-3) were subcutaneously administered 0.5 mg/kg of meloxicam. BLV proviral loads (A–C) and *IFN-γ* expression (D) in PBMCs of animals #II-1–#II-3 were analyzed by qPCR. Statistical significances were determined by the Dunnett test. *: $p < 0.05$ versus day 0.

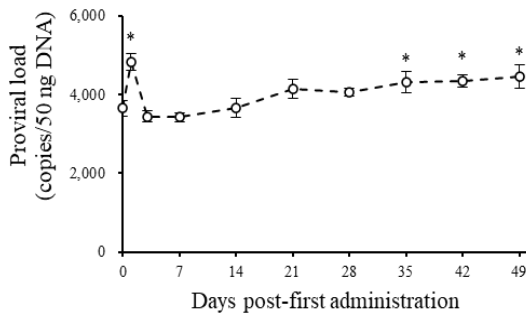
(A) #II-4: Saline



(B) #II-5: Boch4G12



(C) #II-6: Boch4G12



(D) #II-3: Boch4G12 + Meloxicam

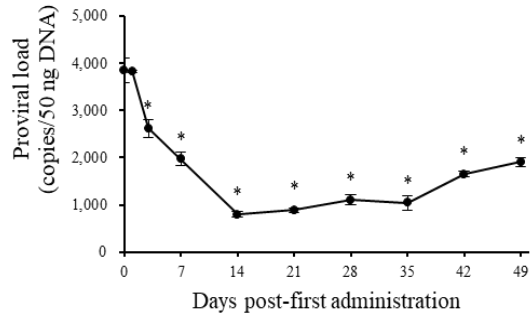


Figure II-10. Clinical tests of the combined treatment using BLV-infected cattle. (A and B) Two BLV-infected cattle (animals #II-4 and #II-5) were intravenously administered 1 mg/kg of anti-bovine PD-L1 chAb (Boch4G12, animal #II-5) or saline (control, animal #II-4). BLV proviral loads in PBMCs of animals #II-4 and #II-5 were analyzed by qPCR. (C and D) Two BLV-infected cattle (animals #II-3 and #II-6) were intravenously administered 1 mg/kg of anti-bovine PD-L1 chAb (Boch4G12). Additionally, animal #II-3 was subcutaneously co-administered 0.5 mg/kg of meloxicam once a week. BLV proviral loads in PBMCs of animals #II-3 and #II-6 were analyzed by qPCR. (A–D) Statistical significances were determined by the Dunnett test. *: $p < 0.05$ versus day 0.

DISCUSSION

In line with disease progression, BLV-specific Th1 response is suppressed, resulting in further disease progression and possible EBL [Konnai *et al.*, 2017]. Previous studies have shown that the suppression of BLV-specific Th1 response is caused by the upregulation of PD-1 and PD-L1 and the increase in the number of Treg cells [Ikebuchi *et al.*, 2010, 2011; Ohira *et al.*, 2016]. In Chapter I, it was demonstrated that PGE₂ suppressed bovine Th1 responses and induced PD-L1 expression *in vitro*. In addition, the treatment with PGE₂ *in vitro* upregulated the expression of *TGF-β1* and *Foxp3* genes in cultured bovine PBMCs. In this chapter, the increase in PGE₂ concentrations in the peripheral blood was observed in BLV-infected cattle. *EP4* and *EP2* expression was also increased in the late stage of BLV infection, whereas the expression of the catabolic enzyme *HPGD* was decreased in PL cattle. Therefore, PGE₂ upregulation might be associated with the induction of PD-L1 expression and Treg cells during BLV infection, leading to the dramatical reduction of BLV-specific Th1 responses.

Monocytes are considered as a major source of PGE₂ production [Passwell *et al.*, 1983]. The expression of *COX2* gene was elevated in PBMCs, CD21⁺ cells, and CD14⁺ cells from PL cattle, and the production capacity of PGE₂ in CD14⁺ cells was higher than that in CD21⁺ cells. These results suggest that CD14⁺ cells are the major cell type producing PGE₂. However, in PL cattle, the number of circulating B cells is dramatically increased [Nieto Farias *et al.*, 2018; Sajiki *et al.*, 2021], and the immunohistochemical analysis in this chapter clearly showed PGE₂ production by tumor B cells in EBL cattle. Therefore, B cells might also act as the main source of PGE₂ secretion in the late stage of BLV infection.

In humans, the *COX2* transcription is promoted by inflammatory cytokines, antigen stimulation, and toll-like receptor signaling via NF-κB activation [Schmedtje *et al.*, 1997; Jobin *et al.*, 1998]. By the stimulation with FLK-BLV, BLV-specific CD4⁺ T cells secrete TNF-α which is a key cytokine to induce *COX2* expression via NF-κB [Jobin *et al.*, 1998]. Based on these data, it is suggested that BLV antigens elevate *COX2* expression via the TNF-α–NF-κB axis in cattle infected with BLV. In addition, the results in this chapter showed *HPGD* downregulation in PL cattle and its negative correlations with BLV proviral loads and serum PGE₂ concentrations. Thus, the coordinate regulation of increased PGE₂ secretion and decreased PGE₂ degradation links to elevated levels of PGE₂ which, in turn, impairs the activation of BLV-specific Th1 responses.

BLV *env* gene encodes an envelope glycoprotein, which is essential for cell-to-cell infection [Johnston *et al.*, 1996; Gatot *et al.*, 1998; Derse *et al.*, 2001; Igakura *et al.*, 2003].

Tax, R3, and G4 are nonstructural proteins which are important for the activation of viral transcription and propagation [Derse, 1987; Van den Broeke *et al.*, 1988; Willems *et al.*, 1993]. A previous paper has shown that PGE₂ induces *tax* expression in PBMCs from BLV-infected cattle [Pyeon *et al.*, 2000], and the results in this chapter revealed that the expression levels of other viral genes, *env*, *G4*, and *R4*, were also increased by PGE₂ via EP2 and EP4 signaling in PBMCs from BLV-infected cattle. It has been reported that binding of PGE₂ to EP2 and EP4 receptors increases intracellular cyclic adenosine monophosphate (cAMP) levels [Kalinski, 2012], that activates protein kinase A (PKA) and downstream transcription factors regulating genes with cAMP-response element (CRE) sites in the promoter. The BLV LTR has a CRE that promotes transcription of BLV genes [Willems *et al.*, 1992; Adam *et al.*, 1994], suggesting that the PGE₂/EP2 and PGE₂/EP4 pathways could induce viral gene transcription through cAMP/PKA/CRE signaling.

CD8⁺ CTLs, which are activated by Th1 cytokines, play a central role in the control of BLV infection. It has been reported that the treatment with COX-2 inhibitors *in vitro* and *in vivo* activates immune responses including T-cell responses as shown in human and murine research [Stolina *et al.*, 2000; Pettersen *et al.*, 2011]. As shown in Chapter I, the treatment with the COX-2 inhibitor promoted Th1-mediated immune reaction in *in vitro* cultures using PBMCs from MAP-infected cattle. In this chapter, the COX-2 inhibitor also activated BLV-specific Th1 responses in PBMC cultures. Remarkably, the administration of the COX-2 inhibitor significantly reduced BLV proviral loads in the infected cattle. Indeed, a previous paper has shown possible benefits of a COX-2 inhibitor celecoxib on the immune function in HIV-infected patients [Pettersen *et al.*, 2011]. However, this is the first to elucidate the therapeutic effects of COX-2 inhibitors on chronic diseases in the field of veterinary medicine.

In the results of this chapter, the treatment with the COX-2 inhibitor alone reduced BLV proviral loads, but not dramatically, presumably due to the upregulation of other immunoinhibitory molecules. The BLV proviral loads of animals #II-1–#II-3 treated with the COX-2 inhibitor alone were extremely high (> 2,000 copies/50 ng DNA). Previous studies have shown that the higher expression of immunoinhibitory molecules, such as PD-L1, LAG-3, cytotoxic T-lymphocyte antigen 4 and Tim-3, is observed in BLV-infected cattle with high proviral loads [Ikebuchi *et al.*, 2011; Okagawa *et al.*, 2012; Konnai *et al.*, 2013; Suzuki *et al.*, 2015]. In addition, the percentage of PD-1⁺LAG-3⁺ cells is increased in CD4⁺ and CD8⁺ T cells at the late stage of BLV infection [Okagawa *et al.*, 2018]. These data suggest that the dual blockade of PGE₂ and other immunoinhibitory molecules is effective to enhance the therapeutic effects on BLV-

infected cattle with high proviral loads. In Chapter II, the effects of monotherapy (Boch4G12 alone) and the combination therapy (Boch4G12 plus meloxicam) were examined using BLV-infected animals. Although the monotherapy had no impact on the infected cow with high proviral loads (animal #II-6), the combined therapy substantially reduced BLV proviral loads to below 2,000 copies/50 ng DNA from day 7 to day 49. Previous studies have shown that positive correlations are observed between BLV proviral loads and vertical/horizontal transmission risks, and the infected cattle with high proviral loads (> 2,000 copies/50 ng DNA) are considered as the major source of BLV transmission within a herd [Mekata *et al.*, 2015a, 2015b; Sajiki *et al.*, 2017]. Hence, the findings in this chapter suggest that the combined treatment on cattle with high proviral loads can be a new strategy for the control of BLV transmission in a herd.

Several recent studies on human cancer have reported a relationship between PGE₂ and the upregulation of other immunoinhibitory molecules, such as PD-1 [Miao *et al.*, 2017; Wang *et al.*, 2018b]. Additionally, treatment co-targeting PGE₂ and PD-1 improves tumor eradication in a murine model [Zelenay *et al.*, 2015]. However, the associations of PGE₂ with immunoinhibitory molecules other than PD-L1 in cattle are still unclear. Future studies are warranted to elucidate these associations using cattle infected with BLV.

Due to the lack of effective therapies, BLV infection is endemic in many countries [VanLeeuwen *et al.*, 2005; Benavides *et al.*, 2013; Murakami *et al.*, 2013; Lee *et al.*, 2016]. Thus, the development of a novel strategy is strongly required for the effective control of BLV infection. The work in Chapter II is a pilot study to examine the potential efficacy of the COX-2 inhibitor and the combined COX-2 and PD-1/PD-L1 inhibition. Although the number of tested animals was limited, the blockade of PGE₂ with or without the PD-1/PD-L1 pathway exhibited antiviral efficacy against BLV. Further experiments using a large number of BLV-infected cattle are required to confirm the efficacy of these novel treatments.

SUMMARY

BLV infection is a chronic viral infection in cattle, and is highly prevalent in many countries, including Japan. The results in Chapter I demonstrated that PGE₂ suppressed Th1 responses in cattle and contributed to the progression of Johne's disease. However, little information was available on the association of PGE₂ with chronic viral infection in cattle.

In Chapter II, kinetic and functional analyses of PGE₂ were performed and the therapeutic potential of COX-2 inhibition was examined in BLV-infected cattle. Both plasma PGE₂ concentrations and the expression of *COX2* mRNA were higher in BLV-infected cattle compared to uninfected cattle. Plasma PGE₂ concentrations were positively correlated with BLV proviral loads. BLV antigen exposure directly increased PGE₂ production from PBMCs of BLV-infected cattle. The transcription of BLV genes, *env*, *G4*, and *R3*, was facilitated by PGE₂/EP2 and PGE₂/EP4 signaling, further suggesting that PGE₂ contributes to the disease progression of BLV infection. In contrast, the COX-2 inhibition activated BLV-specific Th1 responses, such as T-cell proliferation and Th1 cytokine production, *in vitro* and decreased BLV proviral loads *in vivo*. Combined treatment of the COX-2 inhibitor with anti-bovine PD-L1 Ab significantly reduced the BLV proviral loads, suggesting its potential as a novel control strategy against BLV infection. Additional experiments using a larger number of BLV-infected animals are required to support the efficacy of the treatment for clinical application.

CHAPTER III

The enhancement of immunotherapeutic efficacy of anti-PD-L1 antibody in combination with an EP4 antagonist

INTRODUCTION

The PD-1/PD-L1 pathway plays an important role in T-cell exhaustion and is associated with the progression of several cancers and chronic diseases [Okazaki and Honjo, 2007; Blank *et al.*, 2005; Blank and Mackensen, 2007]. In contrast, previous reports have demonstrated that the inhibition of the PD-1/PD-L1 pathway restores the effector functions of exhausted T cells, leading to the enhancement of antitumor immune responses [Iwai *et al.*, 2002; Keir *et al.*, 2007; Dulos *et al.*, 2012]. Therefore, the immunotherapy targeting the PD-1/PD-L1 pathway has become a promising therapy for patients with tumors [Iwai *et al.*, 2017; Ribas and Wolchok, 2018]. Previous studies and the results in Chapter II have shown the therapeutic potential of anti-bovine PD-1/PD-L1 Abs for the treatment of cattle infected with BLV, which is an oncogenic retrovirus of cattle. After the administration of anti-bovine PD-1/PD-L1 chAbs, BLV proviral loads were significantly reduced in the peripheral blood [Nishimori *et al.*, 2017; Okagawa *et al.*, 2017], suggesting that this treatment could contribute to reduce the risk of tumorigenesis associated with BLV infection.

Although the treatment strategy targeting the PD-1/PD-L1 pathway has been approved for cancer treatment in humans, a significant proportion of the patients treated with anti-PD-1/PD-L1 Abs remains less responsive [Gong *et al.*, 2018]. The combination of anti-PD-1/PD-L1 Abs with other therapies is considered as a potential strategy to overcome this issue. PGE₂ is one of the candidate targets for the combined treatment with anti-PD-1/PD-L1 Abs. PGE₂ is an inflammatory mediator, and there are four PGE₂ receptors, EP1, EP2, EP3, and EP4 [Phipps *et al.*, 1991; Sugimoto and Narumiya, 2007]. Previous studies have shown the role of COX-2/PGE₂ in tumor microenvironments [Kobayashi *et al.*, 2018]. The elevated expression of COX-2 is a negative prognostic factor in breast and colorectal cancers [Tomozawa *et al.*, 2000; Denkert *et al.*, 2003]. In the tumor microenvironment, many cell types including tumor cells secrete PGE₂ via COX-2 activation, and PGE₂ promotes the tumor progression via several pathways such as angiogenesis [Rigas *et al.*, 1993; Wang *et al.*, 2004; Wang and Dubois, 2010]. Additionally, PGE₂ affects the immune cells in tumor microenvironments. Specifically, PGE₂ inhibits the activity of Th1 cells, whereas it activates the activity of immunosuppressive cells, such as Treg cells [Kalinski, 2012; Li *et al.*, 2013]. Moreover, previous papers and the results in Chapter I have shown the role of PGE₂ as an inducer of PD-L1 expression. PGE₂ increases PD-L1 expression in murine and bovine models [Prima *et al.*, 2016; Goto *et al.*, 2020], and the treatment with COX-2 inhibitors *in vitro* decreases PD-L1 expression in a murine model [Prima *et al.*, 2016]. Combination

treatment with aspirin, a COX inhibitor, and anti-PD-1 Ab has been shown to exert antitumor activity in several tumor models of mice [Zelenay *et al.*, 2015]. In Chapter II, the combined treatment with anti-bovine PD-L1 Ab and the COX-2 inhibitor significantly enhanced therapeutic efficacy in cattle infected with BLV, although the underlying mechanisms have been unclear.

In Chapter III, based on the observation that serum PGE₂ concentrations were increased after the administration of anti-bovine PD-L1 Ab in BLV-infected cattle, it was hypothesized that the PGE₂ axis may be a mechanism underlying resistance to PD-L1 blockade. To support this hypothesis, the therapeutic potential of the combined treatment of anti-PD-L1 Ab with an EP4 antagonist was examined in bovine PBMC cultures and further investigated in a murine lymphoma model.

MATERIALS AND METHODS

Cells

Peripheral blood samples from uninfected and BLV-infected cattle were collected in several farms in Hokkaido, Japan, and BLV infection was diagnosed as described in Chapter II. Informed consent was obtained from all owners of cattle sampled in Chapter III. All experimental procedures using bovine samples were carried out following approval from the local committee for animal studies at Hokkaido University (approval number: 17-0024). PBMCs were separated from the blood samples as described in Chapter I. For the isolation of CD3⁺ and CD4⁺ cells, PBMCs from BLV-uninfected cattle were incubated with anti-bovine CD3 mAb (MM1A) or anti-bovine CD4 mAb (CC8) at 4°C for 30 min, followed by incubation with anti-mouse IgG₁ MicroBeads (Miltenyi Biotec) at 4°C for 15 min. CD3⁺ and CD4⁺ cells were then sorted from the PBMCs using AutoMACS Pro in accordance with the manufacturer's protocol. The purity of cells, confirmed using FACS Verse, was routinely >90%. PBMCs and isolated CD3⁺ and CD4⁺ cells were cultured in RPMI 1640 medium supplemented with 10% heat-inactivated FCS, 100 U/mL penicillin, 100 µg/mL streptomycin, and 2 mM L-glutamine using 96-well plates as described in previous chapters.

For splenocyte isolation from mice, BALB/c mice (female, eight-week-old) were purchased from Sankyo Labo Service Corporation (Tokyo, Japan) and sacrificed by isoflurane inhalation and cervical dislocation. The spleens were then collected, minced with scissors, digested in RPMI 1640 medium containing 0.2 mg/mL DNase I (Sigma-Aldrich) and 0.67 U/mL research-grade Liberase DL (Sigma-Aldrich) for 30 min at 37°C, and passed through a 100-µm cell strainer (BD Biosciences). The cells were washed twice with PBS and passed through a 40-µm cell strainer (BD Biosciences). The cells were then cultured in RPMI 1640 medium as described above.

EG7, a cell line of murine T-cell lymphoma [Moore *et al.*, 1998], was obtained from the American Type Culture Collection (Manassas, VA, USA) and maintained in RPMI 1640 medium containing 10% heat-inactivated FCS (Sigma-Aldrich), 1% penicillin-streptomycin (FUJIFILM Wako Pure Chemical Corporation, Osaka, Japan), and 0.4 mg/mL G418 (FUJIFILM Wako Pure Chemical Corporation).

Serum samples

Four BLV-infected cattle (animals #II-5, #II-6, #III-1, and #III-2, Table III-1) were intravenously administered with 1 mg/kg anti-bovine PD-L1 chAb (Boch4G12). Serum samples of these animals were obtained on days 0, 1, 3, 7, 14, 28, and 56, and were stored

at -80°C until use.

qPCR

Total RNA extraction and cDNA synthesis were performed as described in Chapter I. To quantitate the expression of *COX2* and *IFN- γ* genes, qPCR was performed as described in Chapter I. *ACTB* was used as a reference gene. Primers used in this chapter are indicated in Table II-1.

ELISA

PGE₂ and IFN- γ concentrations in sera or culture supernatants were measured as described in Chapter I. Mouse IL-2 concentrations in culture supernatants were measured by Mouse IL-2 Matched Antibody Pair Kit (Abcam), according to the manufacturer's protocols.

Flow cytometry

For CD69 expression, after Fc blocking, collected cells were stained for 20 min at 25°C using the following Abs: FITC-conjugated anti-bovine CD4 mAb (CC8), PE-conjugated anti-bovine CD8 mAb (CC63), and Alexa Fluor 647-labeled anti-bovine CD69 mAb (KTSN7A; Kingfisher Biotech). KTSN7A was pre-labeled with a Zenon Alexa Fluor 647 Mouse IgG₁ Labeling Kit. CD69 was used as an activation marker of lymphocytes. The stained cells were then washed twice with PBS containing 1% BSA and analyzed by FACS Verse.

For IFN- γ and TNF- α expression, the collected cells were stained after Fc blocking with FITC-conjugated anti-bovine CD4 mAb (CC8), PerCP/Cy5.5-conjugated anti-bovine CD8 mAb (CC63) and PE-labeled anti-bovine IgM mAb (IL-A30) for 20 min at 25°C . IL-A30 was pre-labeled with a Zenon R-PE Mouse IgG₁ Labeling Kit. After surface staining, the cells were fixed and permeabilized by FOXP3 Fix/Perm Kit (BioLegend, San Diego, CA, USA). Next, the cells were stained with biotinylated anti-bovine IFN- γ mAb (MT307; Mabtech) or biotinylated anti-bovine TNF- α mAb (CC328; Bio-Rad) for 20 min at 25°C . The cells were then washed twice with PBS containing 1% BSA and incubated with APC-conjugated streptavidin (BioLegend) for 20 min at 25°C . After the final staining, the cells were washed twice with PBS containing 1% BSA and analyzed by FACS Verse.

PBMC culture

To analyze the individual effects of EP antagonists, PBMCs from uninfected cattle

were incubated for 1 h with 1 µg/mL of each of the following EP antagonists (Cayman Chemical): EP1 (SC-19220), EP2 (AH6809), EP3 (L-798,106), and EP4 (ONO-AE3-208), and then 250 nM of PGE₂ was added to each culture. The cultures were stimulated by adding 1 µg/mL of anti-bovine CD3 mAb (MM1A) and 1 µg/mL of anti-bovine CD28 mAb (CC220) to each well for 24 h.

To examine the effect of the EP4 agonist, PBMCs from uninfected cattle were incubated with 1 µg/mL of Rivenprost (Cayman Chemical). *IFN-γ* expression after 24 h of incubation without additional stimulation was determined by qPCR as described above, and *IFN-γ* concentrations in culture supernatants after 24 h of incubation with 1 µg/mL of anti-bovine CD3 mAb (MM1A) and 1 µg/mL of anti-bovine CD28 mAb (CC220) were measured by ELISA as described above. Similarly, *IFN-γ* expression in bovine lymphocyte subsets was measured by flow cytometry. PBMCs from uninfected cattle were stimulated by 2 µg/mL of anti-bovine CD3 mAb (MM1A), 2 µg/mL of anti-bovine CD28 mAb (CC220), and 10 ng/mL of recombinant bovine IL-2 (Kingfisher Biotech). Following 19 h of incubation, the cells were incubated with 10 µg/mL of brefeldin A (Sigma-Aldrich) for additional 5 h, and analyzed as describe above. To analyze the effect of anti-PD-L1 Ab and TNF-α on PGE₂ production, PBMCs from uninfected cattle were incubated with 10 µg/mL of anti-bovine PD-L1 chAb (Boch4G12) or 10 ng/mL of bovine recombinant TNF-α (Kingfisher Biotech) for 72 or 24 hours, respectively. Bovine IgG was used as a negative control for Boch4G12, and PBS was used as a vehicle control for bovine recombinant TNF-α. Additionally, to demonstrate whether treatment with anti-PD-L1 Ab promotes TNF-α production, PBMCs from uninfected cattle were incubated with 10 µg/mL of anti-bovine PD-L1 chAb (Boch4G12) in the presence of 2 µg/mL of anti-bovine CD3 mAb (MM1A), 2 µg/mL of anti-bovine CD28 mAb (CC220), and 10 ng/mL of recombinant bovine IL-2. Following 19 h of incubation, the cultures were incubated with 10 µg/mL of brefeldin A for 5 h, after which the cultured cells were collected, and TNF-α expression was measured by flow cytometry as described above. To examine whether the blockade of TNF-α decreases PGE₂ production in the presence of anti-PD-L1 Abs, PBMCs from uninfected cattle were incubated with 172 nM bovine TNF receptor type II (TNFR_{II})-Ig, a decoy receptor for bovine TNF-α [Fujisawa *et al.*, 2019], in the presence of 10 µg/mL of anti-bovine PD-L1 Ab (Boch4G12). Control Ig, which comprised the signal peptide of bovine TNFR_{II} and the Fc domain of bovine IgG₁ [Fujisawa *et al.*, 2019], was used as a negative control for TNFR_{II}-Ig. PBMC cultures were stimulated by adding 1 µg/mL of anti-bovine CD3 mAb (MM1A) and 1 µg/mL of anti-bovine CD28 mAb (CC220) to each well for 72 h.

To examine the effect of the dual blockade of PD-L1 and EPs in cattle, PBMCs from

uninfected or BLV-infected cattle were cultured with 10 µg/mL of anti-bovine PD-L1 chAb (Boch4G12) and 1 µg/mL of each EP antagonist. PBMCs from uninfected cattle were cultured in the presence of 1 µg/mL of anti-bovine CD3 mAb (MM1A) and 1 µg/mL of anti-bovine CD28 mAb (CC220) for 72 h, whereas PBMCs from BLV-infected cattle were cultured in the presence of FLK-BLV for 144 h.

CD3⁺ cell culture

Isolated CD3⁺ cells were cultured with 1 µg/mL of Rivenprost in the presence of 1 µg/mL of anti-bovine CD3 mAb (MM1A) and 1 µg/mL of anti-bovine CD28 mAb (CC220) for 72 h. After incubation, CD69 expression and IFN-γ production were measured by flow cytometry and ELISA, respectively.

Microarray

Isolated CD4⁺ cells were cultured in the presence of 0.5 µg/mL of anti-bovine CD3 mAb (MM1A) and 0.5 µg/mL of anti-bovine CD28 mAb (CC220). Following 18 h of incubation, the cultures were incubated with 1 µg/mL of Rivenprost or DMSO for 4 h. Microarray analysis was performed using Agilent Bos taurus (Bovine) Oligo Microarray v2 (Design ID: 023647, Agilent Technologies, Santa Clara, CA, USA). After incubation, total RNA was extracted using RNeasy Mini Kit (Qiagen, Hilden, Germany) according to the manufacturer's instructions. Synthesis and labelling of cRNA were performed using Low Input Quick Amp Labeling Kit (Agilent Technologies) according to the manufacturer's instructions. The Cy3-labeled cRNA was purified using RNeasy Mini Kit (Qiagen), and hybridization was performed using Gene Expression Hybridization Kit (Agilent Technologies), according to the manufacturers' instructions. The scanning of the hybridized microarray and data analysis were performed using Agilent DNA Microarray Scanner (Agilent Technologies), Feature Extraction software (Agilent Technologies), and GeneSpring (Agilent Technologies), according to the manufacturers' instructions. The microarray procedures from RNA extraction to data analysis were conducted at Hokkaido System Science (Sapporo, Japan). The data obtained from this analysis were deposited in ArrayExpress (E-MTAB-9576, <https://www.ebi.ac.uk/arrayexpress/>).

Splenocyte culture

To examine the effects of PD-L1 blockade on PGE₂ production in mice, splenocytes were cultured with 10 µg/mL of anti-mouse PD-L1 mAb (10F.9G2, rat IgG_{2b}; Bio X Cell, West Lebanon, NH, USA) or 10 µg/mL of rat IgG_{2b} isotype control (LTF-2, Bio X Cell). The cultures were stimulated with or without 10 µg/mL of concanavalin A (Con A, Sigma-

Aldrich) for 72 h. To examine the effect of the dual blockade of PD-L1 and EP4 in mice, splenocytes were cultured with 10 µg/mL of anti-mouse PD-L1 mAb (10F.9G2) and 1 µg/mL of each EP antagonist. Cultures were stimulated by adding 1 µg/mL of anti-mouse CD3e mAb (145-2C11; Thermo Fisher Scientific) to each well for 72 h.

Tumor grafting and tumor growth measurement

Six-week-old male C57BL/6 mice (Japan SLC, Hamamatsu, Japan) were subcutaneously inoculated with EG7 (5×10^6 cells/mouse). The day of EG7 injection was defined as day 0. For the treatment with anti-PD-L1 Abs, mice were intraperitoneally injected with anti-mouse PD-L1 mAb (10F.9G2) (10 mg/kg, sid) on days 7, 10, and 14. For the treatment with EP4 antagonists, mice were orally administered with ONO-AE3-208 (10 mg/kg/day) added to drinking water from day 7 to day 23. Tumor size was monitored at least every other day, starting on day 5, using a caliper until the length or width exceeded 20 mm. Tumor volume was calculated according to the following formula: Tumor volume (mm^3) = (length \times width²)/2. The animal experiments were performed with the approval of the Institutional Animal Care and Use Committee of the Graduate School of Veterinary Medicine at Hokkaido University (approval number: 16-0131). These animals were handled following the Guide for the Care and Use of Laboratory Animals, Graduate School of Veterinary Medicine, Hokkaido University (approved by the Association for Assessment and Accreditation of Laboratory Animal Care International).

Statistical analyses

In Figure III-1, statistical significance was analyzed using the Mann-Whitney *U* test. In Figures III-2–5 and III-6A–C, statistical significances were analyzed using the Wilcoxon signed-rank test for two-group comparisons and the Steel-Dwass test for multiple-group comparisons. In Figures III-6E and III-6F, statistical significances were analyzed using the Tukey's test and the Log-rank test, respectively. In microarray analysis (Table III-2), statistical significances were analyzed using the paired *t* test. All statistical tests were performed using with the MEPHAS program (<http://www.gen-info.osaka-u.ac.jp/MEPHAS/>), or EZR (Saitama Medical Center, Jichi Medical University) that is a graphical user interface for R (The R Foundation for Statistical Computing) [Kanda, 2013]. $p < 0.05$ was considered statistically significant.

Table III-1. Information of cattle administered anti-bovine PD-L1 chAb.

Animal	#II-5	#II-6	#III-1	#III-2
Age	13 months old	76 months old	17 months old	7 months old
Breed	Holstein	Holstein	Holstein	Holstein
Sex	female	female	Female	male
Body weight	295 kg	799 kg	522 kg	267 kg
BLV infection	+	+	+	+
Administration dose	1 mg/kg, <i>i.v.</i>	1 mg/kg, <i>i.v.</i>	1 mg/kg, <i>i.v.</i>	1 mg/kg, <i>i.v.</i>

* The information of animals #II-5 and #II-6 are also shown in Table II-2 in Chapter II.

RESULTS

The increase in serum PGE₂ concentrations with anti-PD-L1 immunotherapy

In Chapter II, the combined treatment of anti-PD-L1 Ab with the COX-2 inhibitor significantly reduced BLV proviral loads in BLV-infected cattle. To elucidate the reason why the combination treatment enhances the efficacy of PD-L1 blockade, the serum samples from BLV-infected cattle administered with anti-bovine PD-L1 chAb (Boch4G12) were firstly analyzed. Serum PGE₂ concentrations were increased after the treatment with anti-bovine PD-L1 chAb (Figures III-1A and B). Therefore, the role of PGE₂ in the blockade of PD-1/PD-L1 interaction was specifically examined in this chapter.

The suppression of T-cell activation via the PGE₂/EP4 pathway

The results in Chapter I revealed that the treatment with PGE₂ suppressed Th1 responses *in vitro*, such as Th1 cytokine production and T-cell proliferation, in cattle. In Chapter III, specific PGE₂ receptors involved in PGE₂-mediated suppression of Th1 responses were further identified using EP antagonists and agonists. PBMCs from uninfected cattle were pre-incubated with each EP antagonist, followed by the incubation with PGE₂ in the presence of anti-bovine CD3 and anti-bovine CD28 mAbs. Pretreatment with the EP4 antagonist inhibited the suppression of IFN- γ production by PGE₂, whereas IFN- γ production was suppressed by PGE₂ in PBMCs pre-treated with the other antagonists (Figure III-2A). Additionally, the treatment with the EP4 agonist significantly impaired IFN- γ expression in PBMCs at both mRNA and protein levels (Figures III-2B and C). The analysis by flow cytometry showed that the EP4 agonist reduced the percentage of IFN- γ ⁺ cells in both the CD4⁺ and CD8⁺ T cells (Figures III-2D and E). Moreover, to examine whether PGE₂ directly suppresses T-cell activity in cattle, isolated CD3⁺ T cells were cultured with the EP4 agonist, and CD69 expression in T cells and IFN- γ production in culture supernatants were measured by flow cytometry and ELISA, respectively. The treatment with the EP4 agonist significantly decreased CD69 expression in CD4⁺ and CD8⁺ T cells and IFN- γ production (Figures III-3A–C). Microarray analysis demonstrated that the treatment with the EP4 agonist downregulated the expression of Th1-related cytokine genes, such as *IL-2*, *IFN- γ* , *TNF- α* , and *IL-12*, in CD4⁺ cells (Figure III-3D, Table III-2). Collectively, these findings suggest that PGE₂ induced by anti-bovine PD-L1 Ab treatment directly impairs T-cell activation via its receptor EP4.

The induction of PGE₂ production by TNF- α

To reveal the mechanism of PGE₂ induction by anti-PD-L1 Ab treatment, bovine PBMCs were cultured with anti-bovine PD-L1 chAb (Boch4G12), which significantly increased *COX2* expression and PGE₂ production *in vitro* (Figures III-4A and B). The PD-1/PD-L1 inhibition using specific Abs reinvigorates exhausted T cells, leading to the increase in Th1 cytokine production from T cells [Keir *et al.*, 2007; Dulos *et al.*, 2012]. Flow cytometric analysis showed that the treatment with anti-bovine PD-L1 chAb (Boch4G12) significantly increased the percentage of TNF- α ⁺ cells in both CD4⁺ and CD8⁺ T cells (Figures III-4C and D). Previous studies have clearly demonstrated that TNF- α induces NF- κ B activation, which is essential for COX-2 upregulation [Jobin *et al.*, 1998; Ghosh and Karin, 2002; Bouwmeester *et al.*, 2004]. Therefore, it was examined whether anti-PD-L1 Ab-induced TNF- α is involved in the observed PGE₂ upregulation. The treatment with bovine recombinant TNF- α significantly induced both *COX2* expression and PGE₂ production in bovine PBMCs (Figures III-4E and F). Interestingly, TNF- α blockade using the decoy receptor TNFRII-Ig decreased PGE₂ secretion in the presence of Boch4G12 (Figure III-4G). Taken together, these data suggest that TNF- α induced by the treatment with anti-PD-L1 Abs enhances PGE₂ production, leading to the impaired efficacy of anti-PD-L1 Ab treatment via PGE₂/EP4 signaling.

The enhancement of Th1 cytokine production by the dual blockade of PD-L1 and EP4

To determine whether the blockade of EP4 enhances the efficacy of anti-PD-L1 Abs *in vitro*, PBMCs from uninfected cattle were cultured with individual EP antagonists in the presence of anti-bovine PD-L1 chAb (Boch4G12). The dual blockade of PD-L1 and EP4 increased IFN- γ production, compared to the other treatment groups (Figure III-5A). In addition, the dual blockade of PD-L1 and EP4 significantly activated BLV-specific IFN- γ production from PBMCs of cattle infected with BLV (Figure III-5B). These results suggest that the combination with EP4 antagonists could be a new strategy to improve the efficacy of anti-PD-L1 Ab treatment in cattle.

The enhancement of antitumor effects by the dual blockade of PD-L1 and EP4

The results obtained from bovine immune cells revealed the new mechanism of anti-PD-L1 Ab resistance and the potential of enhancing Th1 cytokine production by the combined blockade of PD-L1 and EP4. Then, murine splenocytes were used to analyze whether the combined blockade enhances Th1 immune responses in other animal models. Treatment with anti-mouse PD-L1 mAb (10F.9G2) induced PGE₂ secretion from murine splenocytes stimulated with or without Con A (Figures III-6A and B). In addition, the

treatment with the EP4 antagonist increased IL-2 production from murine splenocytes in the presence of anti-mouse PD-L1 mAb (10F.9G2) (Figure III-6C), suggesting that the dual blockade enhanced Th1 responses in not only cattle but also mice. Finally, based on these findings, a mouse lymphoma model was used to evaluate the antitumor effects of the dual blockade as a potent immunotherapy in cancers resistant to the treatment with anti-PD-1/PD-L1 Ab alone. C57BL/6 mice were inoculated with EG7, and the EG7-bearing mice were intraperitoneally injected with anti-mouse PD-L1 mAb (10F.9G2), and were orally administered with the EP4 antagonist (Figure III-6D). Compared to the animals treated with the EP4 antagonist or anti-PD-L1 Ab alone, the tumor volume was significantly reduced in co-administered mice (Figure III-6E). Furthermore, the survival of the combination treatment group was significantly prolonged compared to that of the untreated group (Figure III-6F). Therefore, these results suggest that the dual blockade of PD-L1 and EP4 can be a promising strategy as a novel immunotherapy (Figure III-7A and B).

Table III-2. The change of gene expression in microarray analysis.

GeneSymbol	GeneName	Fold change	p value
IL2	interleukin 2	-2.1255753	0.008147
CCL3	chemokine (C-C motif) ligand 3	-2.0820506	0.004651
TNF	tumor necrosis factor	-2.0492654	0.001460
CSF2	colony stimulating factor 2	-2.0447707	0.005276
IL12A	interleukin 12A	-1.9293255	0.012709
CXCL10	C-X-C motif chemokine ligand 10	-1.8574089	0.019228
CCL20	C-C motif chemokine ligand 20	-1.8484110	0.010516
LTA	lymphotoxin alpha	-1.8189231	0.019710
CCL4	chemokine (C-C motif) ligand 4	-1.7715497	0.000768
FGB	fibrinogen beta chain	-1.7014802	0.026826
IFNB3	interferon, beta 3	-1.5604529	0.043236
CXCL9	C-X-C motif chemokine ligand 9	-1.4785548	0.000302
IFNG	interferon gamma	-1.4232383	0.054541
CREM	cAMP responsive element modulator	2.4109561	0.001597
NR4A3	nuclear receptor subfamily 4 group A member 3	1.9490188	0.029402
NR4A2	nuclear receptor subfamily 4 group A member 2	1.8775752	0.001489
PTGS2	prostaglandin-endoperoxide synthase 2	1.7771128	0.042600
NFKB1	nuclear factor kappa B subunit 1	1.5010872	0.001316
CTLA4	cytotoxic T-lymphocyte associated protein 4	1.1734980	0.011518
PDCD1	programmed cell death 1	1.0657109	0.355153

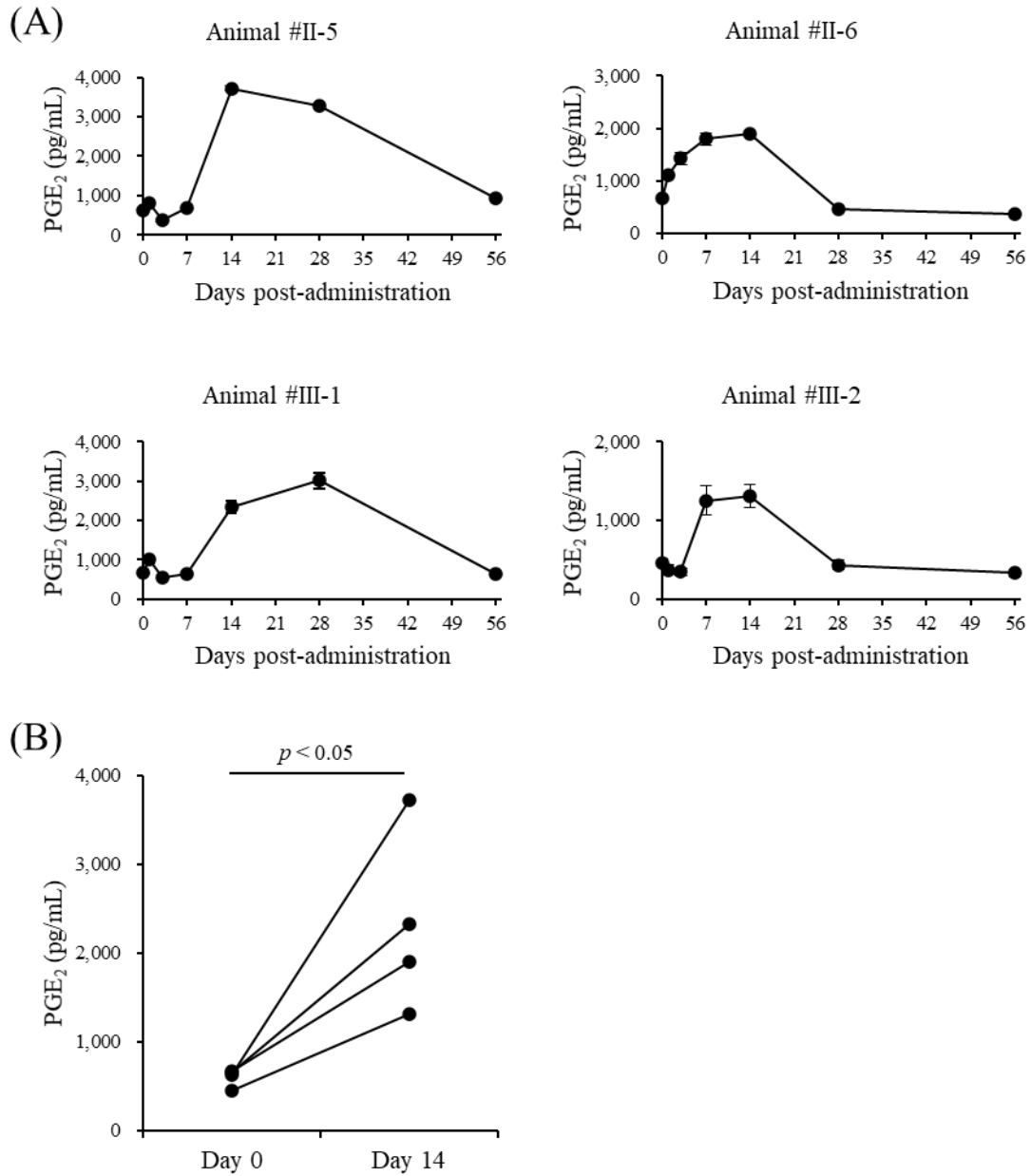


Figure III-1. The increase in serum PGE₂ concentrations after anti-PD-L1 Ab administration. (A and B) BLV-infected cattle (animals #II-5, #II-6, #III-1, and #III-2) were administered 1 mg/kg of anti-bovine PD-L1 chAb (Boch4G12), and serum samples were collected on days 0, 1, 3, 7, 14, 28, and 56 for the measurement of PGE₂ concentrations by ELISA. (B) Statistical significance was determined by the Mann-Whitney *U* test.

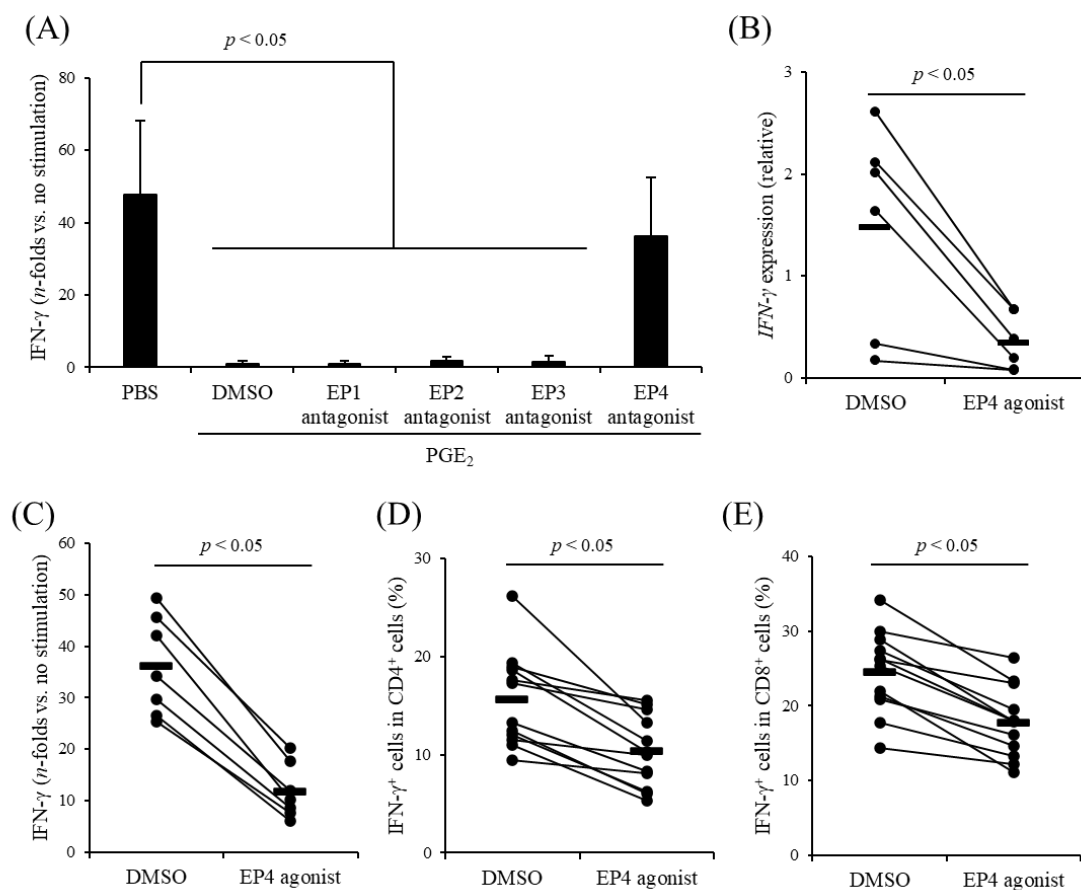


Figure III-2. Functional analysis of EP signaling in bovine PBMCs. (A) Following 1 h of incubation with 1 $\mu\text{g/mL}$ of each EP antagonist, PBMCs from uninfected cattle ($n = 6$) were incubated with 250 nM of PGE₂ in the presence of anti-bovine CD3 and anti-bovine CD28 mAbs for 24 h. IFN- γ concentrations in culture supernatants were determined by ELISA. (B) PBMCs from uninfected cattle ($n = 6$) were cultured with 1 $\mu\text{g/mL}$ of the EP4 agonist for 24 h, and IFN- γ expression was measured by qPCR. (C) PBMCs from uninfected cattle ($n = 7$) were incubated with 1 $\mu\text{g/mL}$ of the EP4 agonist in the presence of anti-bovine CD3 and anti-bovine CD28 mAbs for 24 h. IFN- γ concentrations in culture supernatants were determined by ELISA. (D and E) PBMCs from uninfected cattle ($n = 12$) were incubated with 1 $\mu\text{g/mL}$ of the EP4 agonist in the presence of anti-bovine CD3 and anti-bovine CD28 mAbs and recombinant bovine IL-2 for 24 h. IFN- γ expression in CD4⁺ (D) and CD8⁺ (E) T cells were measured by flow cytometry. (A–E) Statistical significances were determined by the Steel-Dwass test (A) or the Wilcoxon signed-rank test (B–E).

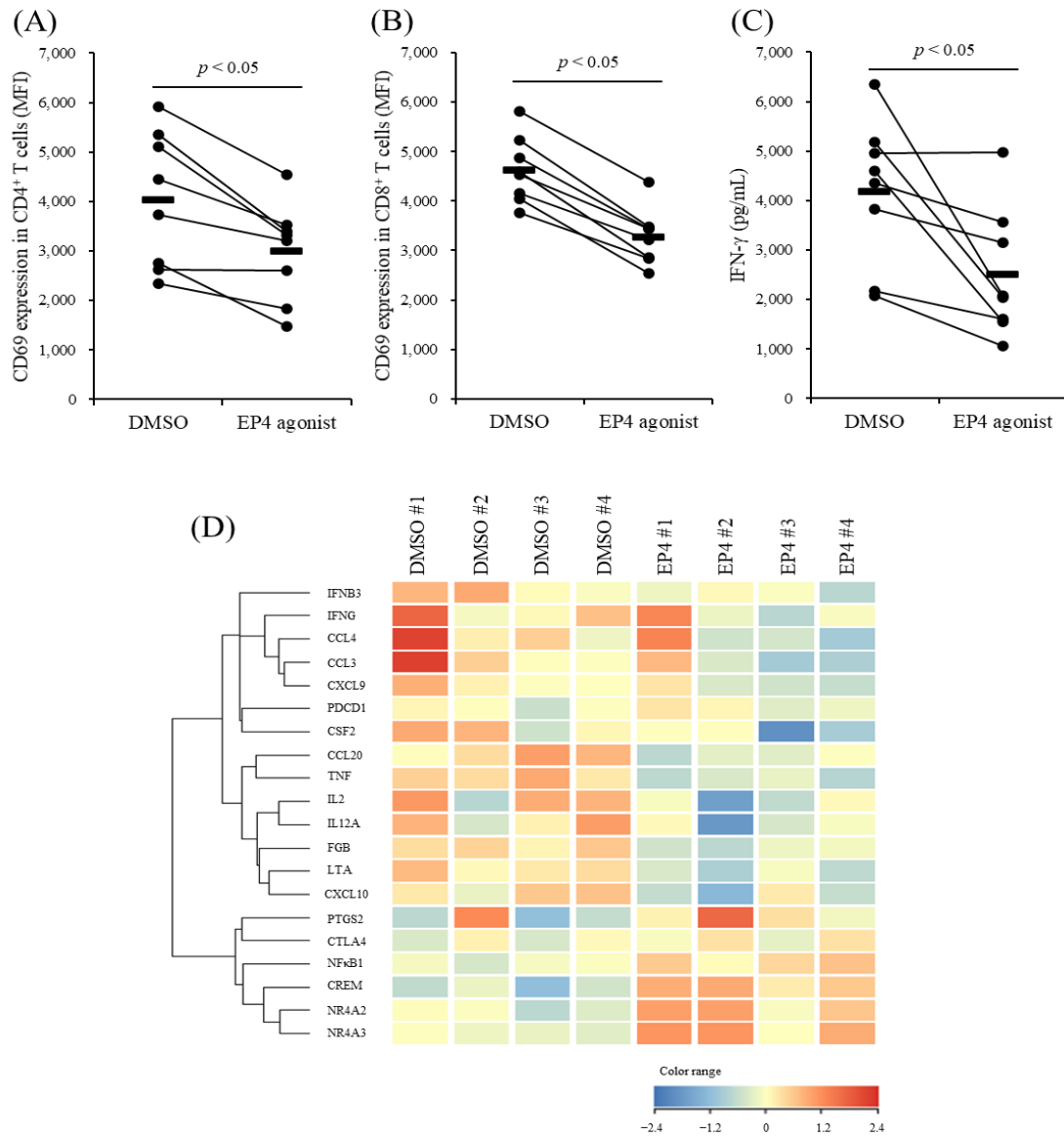


Figure III-3. Functional analysis of EP4 signaling in CD3⁺ cells. (A–C) CD3⁺ T cells isolated from PBMCs of uninfected cattle ($n = 8$) were cultured with 1 $\mu\text{g}/\text{mL}$ of the EP4 agonist in the presence of anti-bovine CD3 and anti-bovine CD28 mAbs. After 72 h, CD69 expression in CD4⁺ (A) and CD8⁺ (B) T cells and IFN- γ production (C) were measured by flow cytometry and ELISA, respectively. Statistical significances were determined by the Wilcoxon signed-rank test. (D) The heat-map for the changes in gene expression in CD4⁺ cells by treatment with 1 $\mu\text{g}/\text{mL}$ of the EP4 agonist. MFI: Mean fluorescence intensity.

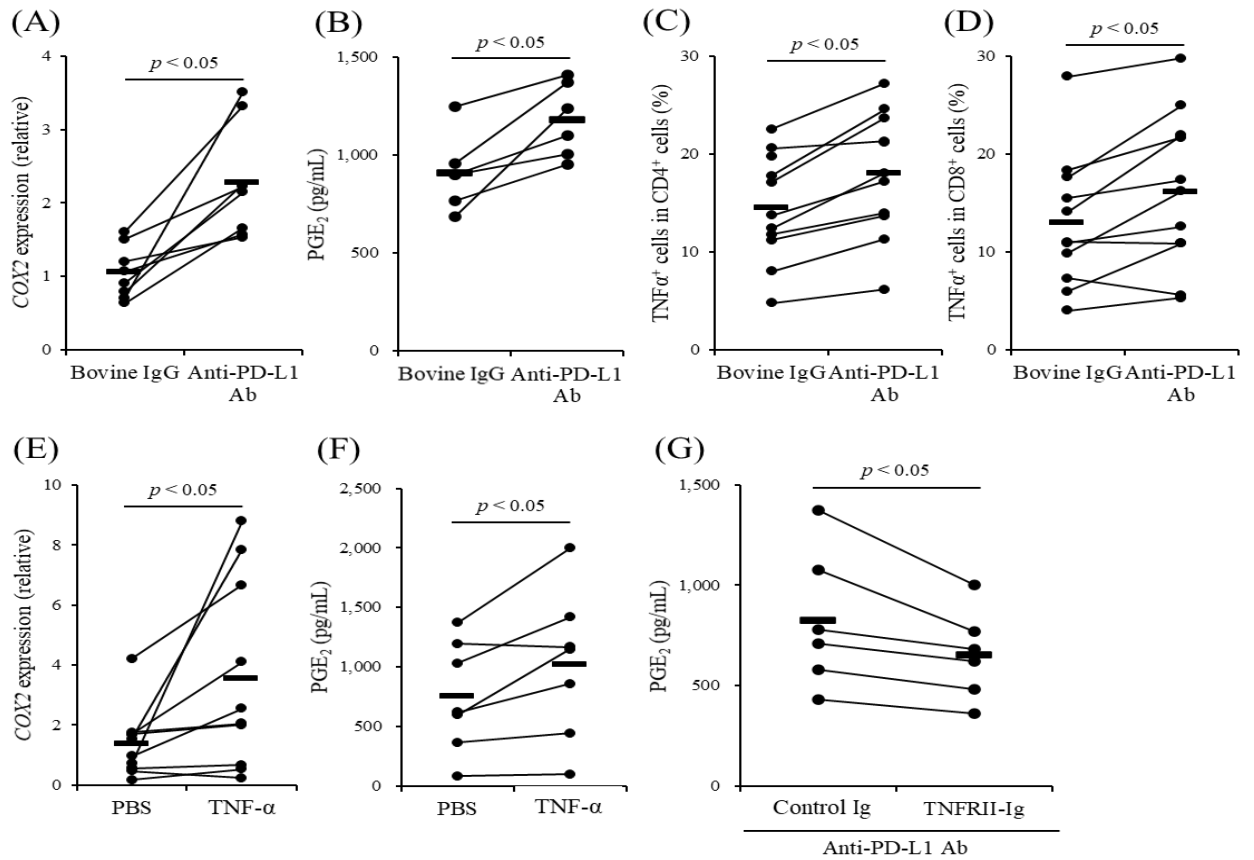


Figure III-4. The upregulation of PGE₂ production by TNF-α. (A and B) PBMCs from BLV-infected cattle were cultured with 10 μg/mL of anti-bovine PD-L1 chAb (Boch4G12) for 72 h, and COX2 expression (A: $n = 8$) and PGE₂ production (B: $n = 6$) were measured by qPCR and ELISA, respectively. Bovine IgG was used as a negative control of Boch4G12. (C and D) PBMCs from uninfected cattle ($n = 11$) were incubated with 10 μg/mL of Boch4G12 in the presence of anti-bovine CD3 and anti-bovine CD28 mAbs and recombinant bovine IL-2 for 24 h. TNF-α expression in CD4⁺ (C) and CD8⁺ (D) T cells were measured by flow cytometry. (E and F) PBMCs from uninfected cattle were cultured with 10 ng/mL of recombinant bovine TNF-α for 24 h, and COX2 expression (E: $n = 10$) and PGE₂ production (F: $n = 7$) were measured by qPCR and ELISA, respectively. PBS was used as a vehicle control. (G) PBMCs from uninfected cattle ($n = 6$) were cultured with 172 nM of TNFRII-Ig in the presence of 10 μg/mL of Boch4G12. Cultures were stimulated by adding anti-bovine CD3 and anti-bovine CD28 mAbs for 72 h. Control Ig was used as a negative control for TNFRII-Ig. PGE₂ production was measured by ELISA. (A–G) Statistical significances were determined by the Wilcoxon signed-rank test.

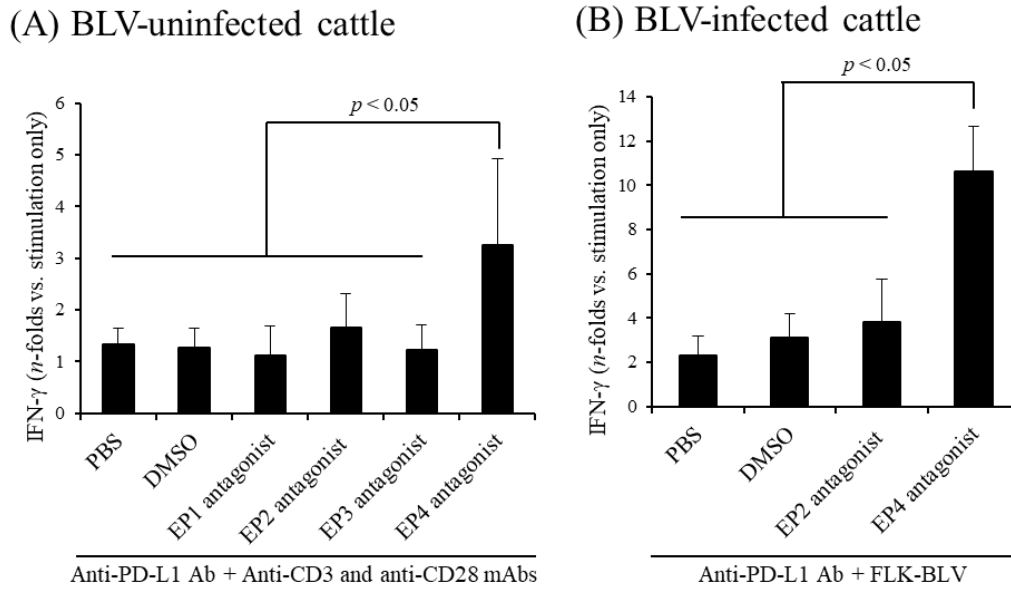


Figure III-5. Functional analysis of the dual blockade of PD-L1 and EP4 in cattle. (A and B) PBMCs from uninfected ($n = 8$) and BLV-infected ($n = 7$) cattle were cultured with 10 $\mu\text{g}/\text{mL}$ of anti-bovine PD-L1 chAb (Boch4G12) and 1 $\mu\text{g}/\text{mL}$ of indicated EP antagonists. PBMCs from uninfected cattle were stimulated by anti-bovine CD3 and anti-bovine CD28 mAbs for 72 h. PBMCs from BLV-infected cattle were stimulated by FLK-BLV for 144 h. After incubation, IFN- γ concentrations in culture supernatants were measured by ELISA. Statistical significances were determined by the Steel-Dwass test.

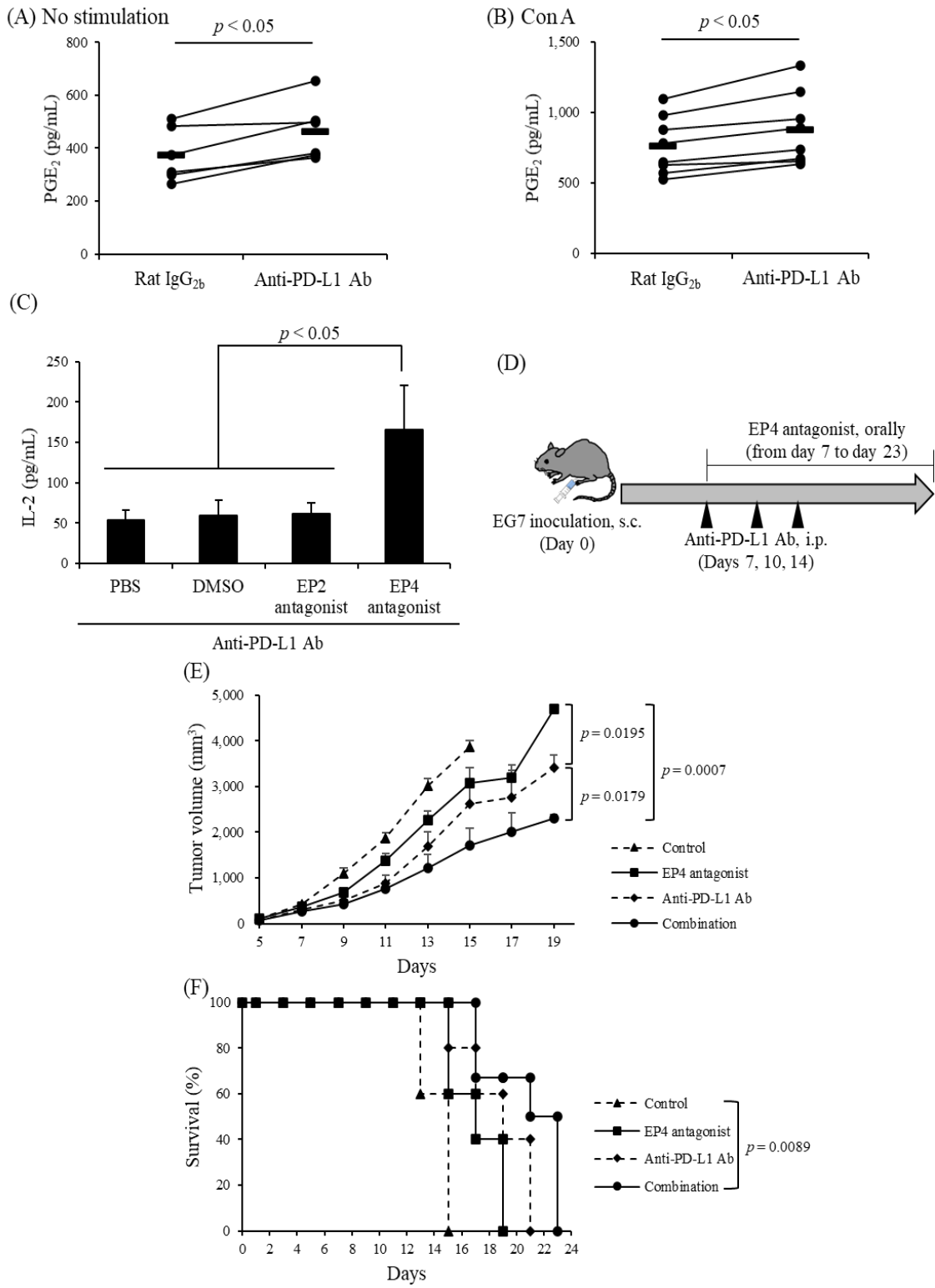


Figure III-6. Functional analysis of the dual blockade of PD-L1 and EP4 in mice. (A and B) Murine splenocytes (A: $n = 6$, B: $n = 8$) were cultured with 10 $\mu\text{g}/\text{mL}$ of anti-mouse PD-L1 mAb (10F.9G2). Cultures were stimulated with or without Con A for 72 h, and PGE_2 concentrations in culture supernatants were measured by ELISA. Statistical significances were determined by the Wilcoxon signed-rank test. (C) Murine splenocytes ($n = 6$) were cultured with 10 $\mu\text{g}/\text{mL}$ of anti-mouse PD-L1 mAb (10F.9G2) and 1 $\mu\text{g}/\text{mL}$ of indicated EP antagonists in the presence of anti-mouse CD3e mAb for 72 h. IL-2 concentrations in culture supernatants were determined by ELISA. Statistical significances were determined by the Steel-Dwass test. (D–F) The evaluation of the anti-tumor effects of the dual blockade in the EG7 mouse model. (D) Experimental design. (E) Tumor growth in each group. Data are presented as means, and the error bars indicate standard errors. Statistical significance was determined by the Tukey's test. (F) The Kaplan-Meier Curve for survival in all groups. Statistical significance was determined by the log-rank test. (D–F) Data are representative of two independent experiments, each performed with 5–8 mice per group.

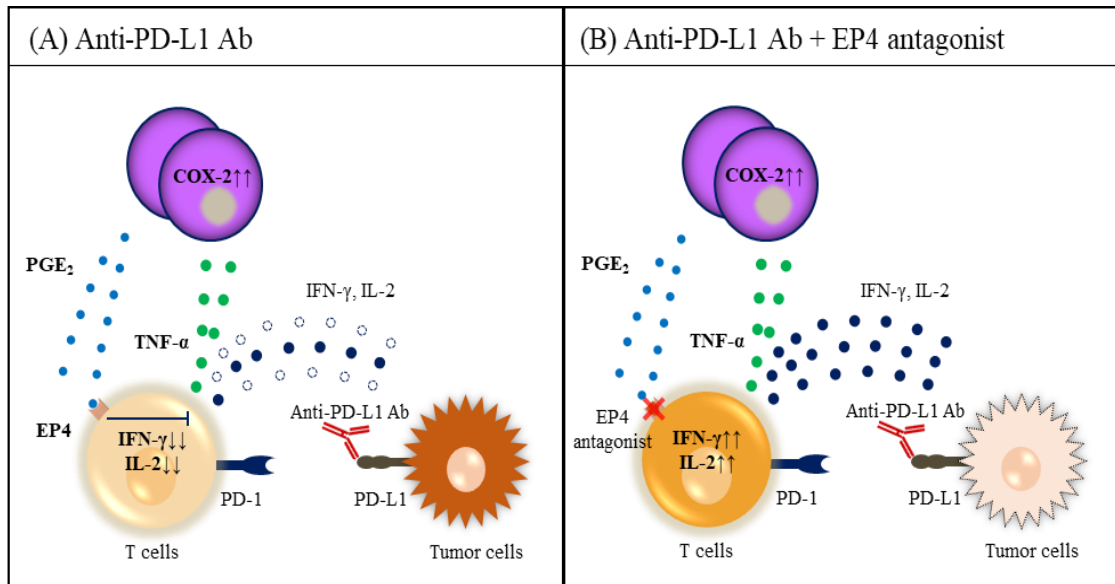


Figure III-7. Graphic abstract of Chapter III. (A) TNF- α induced by anti-PD-L1 Ab treatment promoted PGE₂ production through COX-2 activation, leading to the decrease in Th1 cytokine production via EP4. (B) The combined treatment of anti-PD-L1 Ab with the EP4 antagonist enhanced Th1 cytokine production in a bovine model and antitumor effects in a murine tumor model.

DISCUSSION

Previous studies have recently demonstrated the mechanisms of resistance to cancer immunotherapy [Koyama *et al.*, 2016; Sharma *et al.*, 2017; Nowicki *et al.*, 2018]. For instance, one previous study has shown that therapeutic PD-1 blockade induces the expression of alternative immunoinhibitory molecules, such as Tim-3, which causes resistance to the PD-1/PD-L1 blockade [Koyama *et al.*, 2016]. Therapeutic strategies including anti-PD-1/PD-L1 Abs in the combination with other medicines to overcome resistance are garnering increasing attention. The results shown in Chapter II showed that the combination treatment of PD-1/PD-L1 blockade with COX inhibition enhanced the therapeutic efficacy in a bovine model of chronic viral infection, consistent with results from a previous study in murine tumor models [Zelenay *et al.*, 2015]. However, the underlying mechanism of the observed therapeutic effect by these combination strategies has not been fully elucidated. In Chapter III, a new mechanism of resistance mediated by PGE₂ was proposed using a bovine model (Figure III-7A and B). The results in this chapter showed that the treatment with anti-PD-L1 Ab induced Th1 cytokine production, such as TNF- α , and that PGE₂ induced by TNF- α impaired T-cell activation via EP4. This may partially clarify a reason why the combination treatment enhances the efficacy of PD-1/PD-L1 blockade. Additionally, the therapeutic potential of the combined treatment of anti-PD-L1 Abs with EP4 antagonists was demonstrated in both bovine and murine models. To the best of our knowledge, this is the first study to elucidate the therapeutic efficacy of a dual blockade strategy using anti-PD-L1 Abs and EP4 antagonists *in vivo*. Additional experiments using other murine tumor models are needed to further examine the efficacy of the combined treatment.

Among the four EPs, EP2 and EP4 are involved in PGE₂-mediated immune dysfunction [Sugimoto and Narumiya, 2007; Kalinski, 2012]. In Chapter III, the blockade of EP4, but not EP2, inhibited the regulation of IFN- γ secretion by PGE₂. EP4 represents a high-affinity receptor for PGE₂, whereas EP2 requires significantly higher PGE₂ concentrations for effective signaling [Kalinski, 2012]. Therefore, the differences observed in the results following EP2 and EP4 blockade are presumably due to the difference in the affinity of each receptor. The involvement of EP2 in immune dysfunction should carefully be analyzed in other preclinical models where higher PGE₂ levels are expected during disease progression.

PD-1/PD-L1 blockade using specific Abs restores exhausted T cells, leading to the promotion of Th1 cytokine production, including IFN- γ and TNF- α [Keir *et al.*, 2007; Dulos *et al.*, 2012]. TNF- α not only plays a pivotal role in cellular immunity against

cancer, but also has a cytotoxic effect on tumor cells directly by the induction of apoptosis [Goodsell, 2006; Tamada and Chen, 2006]. Despite the known roles as one of the antitumor cytokines, TNF- α is paradoxically involved in tumor progression in some circumstances [Moore *et al.*, 1999; Balkwill, 2006; Szlosarek *et al.*, 2006]. For instance, serum TNF- α levels are correlated with the progression of several cancers, such as renal cell carcinoma and prostate cancer [Yoshida *et al.*, 2002; Michalaki *et al.*, 2004]. In addition, TNF- α blockade using specific Abs inhibits tumor growth [Scott *et al.*, 2003]. Moreover, several studies have recently demonstrated that the blockade of TNF- α improves the efficacy of PD-1 blockade [Bertrand *et al.*, 2017; Perez-Ruiz *et al.*, 2019]; however, the underlying detailed mechanism remains unclear. In Chapter III, it was revealed that TNF- α was involved in PGE₂ induction under anti-PD-L1 Ab treatment, and that the combined blockade of PD-1/PD-L1 with EP4 improved the efficacy of immunotherapy. This strategy may be more effective than the combined blockade of PD-1/PD-L1 with TNF- α , because the antitumor effects of TNF- α are not inhibited in this combined blockade. Future experiments are necessary to compare the efficacy between the two therapeutic strategies.

PGE₂ signaling via EP4 elevates intracellular cAMP production [Yokoyama *et al.*, 2013]. A previous study has demonstrated that the PGE₂/EP4/cAMP increases Tim-3 expression in a human T cell line [Yun *et al.*, 2019]. Furthermore, previous studies have shown that TIM-3 expression is induced after the blockade of the PD-1/PD-L1 pathway, contributing to the resistance to PD-1/PD-L1 blockade [Koyama *et al.*, 2016; Bertrand *et al.*, 2017]. Thus, PGE₂ upregulation after the PD-1/PD-L1 blockade might also lead to resistance by increasing the expression of other immunoinhibitory molecules.

TNF- α -PGE₂-EP4 axis is a newly identified mechanism of resistance to the immunotherapy targeting PD-1/PD-L1. The novel combined strategy may have a potential to overcome resistance to anti-PD-1/PD-L1 Ab treatment. Future studies using other tumor models in mice as well as other animal models will herald new avenues for cancer treatment.

SUMMARY

Combination therapies are increasingly considered to overcome resistance to immunotherapy targeting immunoinhibitory molecules such as PD-1 and PD-L1. A previous study and the findings in Chapter II have demonstrated that the therapeutic efficacy of anti-PD-L1 Abs is improved by its combining with COX inhibitors, through the regulation of the immunosuppressive eicosanoid PGE₂, although the underlying mechanism is still unclear.

Here, it was revealed that serum PGE₂ concentrations were elevated after anti-PD-L1 Ab administration in BLV-infected cattle and that PGE₂ directly inhibited T-cell activation via EP4. In addition, the treatment with anti-PD-L1 Ab increased TNF- α production, and TNF- α blockade reduced PGE₂ production in the presence of anti-PD-L1 Ab. These results suggest that TNF- α induced by anti-PD-L1 Ab treatment impairs T-cell activation by the increase in PGE₂ production. Additional experiments examining the therapeutic potential of the combined blockade of PD-L1 and EP4 in bovine and murine immune cells revealed that the combined blockade significantly enhanced Th1 cytokine production *in vitro*. Finally, the combined blockade decreased tumor volume and prolonged survival in mice inoculated with EG7, a murine lymphoma cell line. Collectively, these results suggest that TNF- α induced by anti-PD-L1 antibody treatment is involved in T-cell dysfunction via the PGE₂/EP4 pathway, and the dual blockade of PD-L1 and EP4 is considered as a new immunotherapeutic strategy for cancer.

CONCLUSION

Bovine leukemia virus (BLV) infection and Johne's disease are chronic infections of cattle caused by BLV and *Mycobacterium avium* subsp. *paratuberculosis* (MAP), respectively. Although these chronic infections are endemic in many countries including Japan and cause significant economic losses, there is no effective therapeutic method for them. Therefore, the development of a new treatment strategy is strongly required to guarantee the continued supply of livestock and livestock production. Previous studies have shown that T helper (Th) 1-mediated immune response plays a central role in the prevention from the progression of these infections. In addition, previous studies have demonstrated that immunoinhibitory molecules, such as programmed death (PD)-1 and PD-ligand 1 (PD-L1), are associated with the suppression of Th1 responses in line with the disease progression, and the antibody (Ab) treatment targeting these molecules has therapeutic potential against these infections. However, the detailed mechanism of PD-1/PD-L1 upregulation during these infections remains unclear. In the present study, analyses were performed by focusing on prostaglandin E₂ (PGE₂), which has been recently considered as one of the PD-L1 inducers in murine models and human patients. Additionally, the therapeutic effects of cyclooxygenase (COX)-2 inhibition with or without anti-bovine PD-L1 Ab were investigated both *in vitro* and *in vivo*. Furthermore, the antitumor effects of the dual blockade of PD-L1 and a PGE₂ receptor, E prostanoic acid (EP) 4, were examined using a murine lymphoma model.

Chapter I: The suppressive effects of PGE₂ on immune responses were examined using bovine peripheral blood mononuclear cells (PBMCs). Treatment with PGE₂ *in vitro* suppressed Th1 responses and induced PD-L1 expression. The analysis using samples from MAP-infected cattle revealed that PGE₂ concentrations in sera were higher in infected cattle and PGE₂ expression was found in the ileum tissues of the cases with clinical symptoms. In addition, both PGE₂ secretion and PD-L1 expression in PBMCs from MAP-infected cattle were upregulated by the stimulation with MAP antigens. In contrast, the inhibition of PGE₂ production by the COX-2 inhibitor activated MAP-specific Th1 responses, and the activating effects were enhanced by its combination with anti-bovine PD-L1 Ab. These results suggest that PGE₂ is associated with the progression of this infection by suppressing Th1 responses and by inducing PD-L1 expression.

Chapter II: The involvement of PGE₂ in the progression of BLV infection was examined. Plasma PGE₂ concentrations in BLV-infected cattle were increased and positively correlated with the lymphocyte numbers, BLV proviral loads, and PD-L1 expression in B cells. Treatment with the COX-2 inhibitor with or without anti-bovine

PD-L1 Ab invigorated BLV-specific Th1 responses *in vitro*. Interestingly, the administration of the COX-2 inhibitor into BLV-infected cattle reduced BLV proviral loads. These results suggest that the COX-2 inhibitor exerts antiviral activity against BLV *in vivo*. Furthermore, the combined treatment of the COX-2 inhibitor with anti-bovine PD-L1 Ab significantly enhanced antiviral effects, suggesting a potential as a new control strategy for BLV infection.

Chapter III: The underlying mechanism of the combined effect observed in Chapter II was examined. At first, the analysis using samples from BLV-infected cattle treated with anti-bovine PD-L1 Ab revealed that serum PGE₂ concentrations were elevated after the administration with anti-bovine PD-L1 Ab. Therefore, in this chapter, the role of PGE₂ under anti-PD-L1 Ab treatment was elucidated using bovine and murine samples. Treatment with anti-PD-L1 Ab promoted tumor necrosis factor (TNF)- α production, which caused PGE₂ induction via COX-2 activation. In addition, PGE₂ directly suppressed T-cell activity via its receptor EP4. Thus, PGE₂ induced by TNF- α might impair the efficacy of the anti-PD-L1 therapy via EP4. The dual blockade of PD-L1 and EP4 enhanced Th1 cytokine production *in vitro* in both bovine and murine models. Remarkably, the dual blockade exerted significant antitumor effects in mice bearing EG7, a murine lymphoma cell line. These findings suggest that the dual blockade of PD-L1 and EP4 could have a potential for a novel immunotherapy.

In conclusion, this study demonstrates that the suppression of Th1 responses mediated by PGE₂ is a common feature of chronic infections of cattle, and the COX-2 inhibition reactivates antigen-specific Th1 responses in both MAP- and BLV-infected cattle. In addition, the treatment co-targeting the PD-1/PD-L1 pathway and PGE₂ signaling exerts significant antiviral or antitumor activity in BLV-infected cattle or tumor-bearing mice. These results could provide the informative evidences concerning the development of a novel immunotherapy not only in veterinary research but also in human research. Further studies using a large number of animals and other animal models are required to confirm the efficacy of the combination treatment.

ACKNOWLEDGEMENT

I would like to express my deepest appreciation to Dr. Kazuhiko Ohashi, Dr. Satoru Konnai, and Dr. Shiro Murata, Laboratory of Infectious Diseases, Department of Disease Control, Faculty of Veterinary Medicine, Hokkaido University, Sapporo, Japan, Dr. Tomohiro Okagawa and Dr. Naoya Maekawa, Department of Advanced Pharmaceutics, Faculty of Veterinary Medicine, Hokkaido University, for their continuous mentoring, guidance, assistance, and encouragement while this work.

I would like to express my deepest gratitude Dr. Yasuhiko Suzuki, Division of Bioresources, Research Center for Zoonosis Control, Hokkaido University, for his helpful suggestions, valuable advice, and critical review on the manuscript.

I would like to express my sincere appreciation to Dr. Keita Matsuno, Unit of Risk Analysis and Management, Research Center for Zoonosis Control, Hokkaido University, and Dr. Masatoshi Okamatsu, Laboratory of Microbiology, Department of Disease Control, Faculty of Veterinary Medicine, Hokkaido University, for their invaluable advice on the experiments and critical review on the manuscript.

I owe a deep debt of gratitude to Dr. Yasuyuki Mori, Dr. Reiko Nagata, and Dr. Satoko Kawaji, Bacterial and Parasitic Disease Research Division, National Institute of Animal Health, Tsukuba, Japan, for the provision of samples from MAP-infected cattle, their advice, and support throughout the study in Chapter I.

I greatly appreciate Dr. Atsushi Kobayashi and Dr. Erina Minato, Laboratory of Comparative Pathology, Department of Clinical Veterinary Sciences, Faculty of Veterinary Medicine, Hokkaido University, and Dr. Yumiko Kagawa, North Lab, Sapporo, Japan, for their comprehensive supervision on immunohistochemical analyses and helpful supports.

I am deeply grateful to Dr. Junko Kohara, Animal Research Center, Agriculture Research Department, Hokkaido Research Organization, Shintoku, Japan, for her kind assistance in blood collection and cooperation in the clinical experiments using BLV-infected cattle.

I greatly thank Dr. Kensuke Takada and Mr. Zimeng Cai, Laboratory of Molecular Medicine, Department of Applied Veterinary Sciences, Faculty of Veterinary Medicine, Hokkaido University, for their technical assistance and valuable advice throughout the study in Chapter III.

Great appreciation is extended to Dr. Yukinari Kato, Department of Antibody Drug Development, Tohoku University Graduate School of Medicine, Sendai, Japan, Dr. Chie Nakajima, Division of Bioresources, Research Center for Zoonosis Control, Hokkaido

University, Dr. Yoshinori Ikenaka, Laboratory of Toxicology, Department of Environmental Veterinary Sciences, Faculty of Veterinary Medicine, Hokkaido University, Dr. Itabajara da Silva Vaz Junior, Centro de Biotecnologia, Universidade Federal do Rio Grande do Sul, Porto Alegre, Brazil, and Dr. Carlos Logullo, Laboratório Integrado de Bioquímica Hatisaburo Masuda and Laboratório Integrado de Morfologia, NUPEM-UFRJ, Macaé, Brazil, for their technical assistance and valuable advice.

Sincere special thanks are extended to all of colleagues in Laboratory of Infectious Diseases, Department of Disease Control, Faculty of Veterinary Medicine, Hokkaido University for their invaluable help and warm friendship.

I would like to acknowledge to the Japan Society for the Promotion of Science (JSPS) for the fellowship that supported the current studies. I extend my sincere condolences on the death of experimental animals used for this thesis.

I would like to express my strong appreciation to my family and friends for their encouragement and devoted support of my education and research. Finally, I would like to deeply thank all of the people who helped me and this research.

REFERENCES

- Abdelhamed S, Ogura K, Yokoyama S, Saiki I, Hayakawa Y.** 2016. AKT-STAT3 pathway as a downstream target of EGFR signaling to regulate PD-L1 expression on NSCLC cells. *J Cancer* **7**: 1579–1586.
- Adam E, Kerkhofs P, Mammerickx M, Kettmann R, Burny A, Droogmans L, Willems L.** 1994. Involvement of the cyclic AMP-responsive element binding protein in bovine leukemia virus expression *in vivo*. *J Virol* **68**: 5845–5853.
- Alcami A, Koszinowski UH.** 2000. Viral mechanisms of immune evasion. *Trends Microbiol* **8**: 410–418.
- Balkwill F.** 2006. TNF- α in promotion and progression of cancer. *Cancer Metastasis Rev* **25**: 409.
- Bassey EO, Collins MT.** 1997. Study of T-lymphocyte subsets of healthy and *Mycobacterium avium* subsp. *paratuberculosis*-infected cattle. *Infect Immun* **65**: 4869–4872.
- Benavides BB, Cedeño Quevedo DA, Serrano De La Cruz MF.** 2013. Epidemiological study of bovine leukemia virus in dairy cows in six herds in the municipality of Pasto, Nariño. *Rev Lasallista Investig* **10**: 18–26.
- Bertrand F, Montfort A, Marcheteau E, Imbert C, Gilhodes J, Filleron T, Rochaix P, Andrieu-Abadie N, Levade T, Meyer N, Colacios C, Ségui B.** 2017. TNF α blockade overcomes resistance to anti-PD-1 in experimental melanoma. *Nat Commun* **8**: 2256.
- Betz M, Fox SB.** 1991. Prostaglandin E₂ inhibits production of Th1 lymphokines but not of Th2 lymphokines. *J Immunol* **146**: 108–113.
- Blank C, Gajewski TF, Mackensen A.** 2005. Interaction of PD-L1 on tumor cells with PD-1 on tumor-specific T cells as a mechanism of immune evasion: implications for tumor immunotherapy. *Cancer Immunol Immunother* **54**: 307–314.
- Blank C, Kuball J, Voelkl S, Wiendl H, Becker B, Walter B, Majdic O, Gajewski TF,**

Theobald M, Andreesen R, Mackensen A. 2006. Blockade of PD-L1 (B7-H1) augments human tumor-specific T cell responses *in vitro*. *Int J Cancer* **119**: 317–327.

Blank C, Mackensen A. 2007. Contribution of the PD-L1/PD-1 pathway to T-cell exhaustion: an update on implications for chronic infections and tumor evasion. *Cancer Immunol Immunother* **56**: 739–745.

Botti G, Fratangelo F, Cerrone M, Liguori G, Cantile M, Anniciello AM, Scala S, D'Alterio C, Trimarco C, Ianaro A, Cirino G, Caracò C, Colombino M, Palmieri G, Pepe S, Ascierio PA, Sabbatino F, Scognamiglio G. 2017. COX-2 expression positively correlates with PD-L1 expression in human melanoma cells. *J Transl Med* **15**: 46.

Bouwmeester T, Bauch A, Ruffner H, Angrand PO, Bergamini G, Croughton K, Cruciat C, Eberhard D, Gagneur J, Ghidelli S, Hopf C, Huhse B, Mangano R, Michon AM, Schirle M, Schlegl J, Schwab M, Stein MA, Bauer A, Casari G, Drewes G, Gavin AC, Jackson DB, Joberty G, Neubauer G, Rick J, Kuster B, Superti-Furga G. 2004. A physical and functional map of the human TNF-alpha/NF-kappa B signal transduction pathway. *Nat Cell Biol* **6**: 97–105.

Burrells C, Clarke CJ, Colston A, Kay JM, Porter J, Little D, Sharp JM. 1998. Interferon-gamma and interleukin-2 release by lymphocytes derived from the blood, mesenteric lymph nodes and intestines of normal sheep and those affected with paratuberculosis (Johne's disease). *Vet Immunol Immunopathol* **68**: 139–148.

Chen JH, Perry CJ, Tsui YC, Staron MM, Parish IA, Dominguez CX, Rosenberg DW, Kaech SM. 2015. Prostaglandin E₂ and programmed cell death 1 signaling coordinately impair CTL function and survival during chronic viral infection. *Nat Med* **21**: 327–334.

Chen M, Divangahi M, Gan H, Shin DS, Hong S, Lee DM, Serhan CN, Behar SM, Remold HG. 2008. Lipid mediators in innate immunity against tuberculosis: opposing roles of PGE₂ and LXA₄ in the induction of macrophage death. *J Exp Med* **205**: 2791–2801.

Coussens PM. 2004. Model for immune responses to *Mycobacterium avium* subspecies *paratuberculosis* in cattle. *Infect Immun* **72**: 3089–3096.

Denkert C, Winzer KJ, Müller BM, Weichert W, Pest S, Köbel M, Kristiansen G, Reles A, Siegert A, Guski H, Hauptmann S. 2003. Elevated expression of cyclooxygenase-2 is a negative prognostic factor for disease free survival and overall survival in patients with breast carcinoma. *Cancer* **97**: 2978–2987.

Derse D. 1987. Bovine leukemia virus transcription is controlled by a virus encoded trans-acting factor and by cis-acting response elements. *J Virol* **61**: 2462–2471.

Derse D, Hill SA, Lloyd PA, Chung Hk, Morse BA. 2001. Examining human T-lymphotropic virus type 1 infection and replication by cell-free infection with recombinant virus vectors. *J Virol* **75**: 8461–8468.

Dulos J, Carven GJ, van Boxtel SJ, Evers S, Driessen-Engels LJ, Hobo W, Gorecka MA, de Haan AF, Mulders P, Punt CJ, Jacobs JF, Schalken JA, Oosterwijk E, van Eenennaam H, Boots AM. 2012. PD-1 blockade augments Th1 and Th17 and suppresses Th2 responses in peripheral blood from patients with prostate and advanced melanoma cancer. *J Immunother* **35**: 169–178.

Dumais N, Barbeau B, Olivier M, Tremblay MJ. 1998. Prostaglandin E₂ up-regulates HIV-1 long terminal repeat-driven gene activity in T cells via NF-kappaB-dependent and -independent signaling pathways. *J Biol Chem* **273**: 27306–27314.

Dumais N, Bounou S, Olivier M, Tremblay MJ. 2002. Prostaglandin E₂-mediated activation of HIV-1 long terminal repeat transcription in human T cells necessitates CCAAT/enhancer binding protein (C/EBP) binding sites in addition to cooperative interactions between C/EBP β and cyclic adenosine 5'-monophosphate response element binding protein. *J Immunol* **168**: 274–282.

Edwards CK 3rd, Hedegaard HB, Zlotnik A, Gangadharam PR, Johnston RB Jr, Pabst MJ. 1986. Chronic infection due to *Mycobacterium intracellulare* in mice: association with macrophage release of prostaglandin E₂ and reversal by injection of indomethacin, muramyl dipeptide, or interferon-gamma. *J Immunol* **136**: 1820–1827.

Fenwick C, Joo V, Jacquier P, Noto A, Banga R, Perreau M, Pantaleo G. 2019. T-cell exhaustion in HIV infection. *Immunol Rev* **292**: 149–163.

Finlay BB, McFadden G. 2006. Anti-immunology: Evasion of the host immune system by bacterial and viral pathogen. *Cell* **124**: 767–782.

Frie MC, Coussens PM. 2015. Bovine leukemia virus: A major silent threat to proper immune responses in cattle. *Vet Immunol Immunopathol* **163**: 103–114.

Fujisawa S, Konnai S, Okagawa T, Maekawa N, Tanaka A, Suzuki Y, Murata S, Ohashi K. 2019. Effects of bovine tumor necrosis factor alpha decoy receptors on cell death and inflammatory cytokine kinetics: potential for bovine inflammation therapy. *BMC Vet Res* **15**: 68.

Gatot JS, Callebaut I, Mornon JP, Portetelle D, Burny A, Kerkhofs P, Kettmann R, Willems L. 1998. Conservative mutations in the immunosuppressive region of the bovine leukemia virus transmembrane protein affect fusion but not infectivity *in vivo*. *J Biol Chem* **273**: 12870–12880.

Ghosh S, Karin M. 2002. Missing pieces in the NF-kappaB puzzle. *Cell* **109**: S81–S96.

Gong J, Chehrazi-Raffle A, Reddi S, Salgia R. 2018. Development of PD-1 and PD-L1 inhibitors as a form of cancer immunotherapy: a comprehensive review of registration trials and future considerations. *J Immunother Cancer* **6**: 8.

Goodsell DS. 2006. The molecular perspective: tumor necrosis factor. *Oncologist* **11**: 83–84.

Goto S, Konnai S, Okagawa T, Nishimori A, Maekawa N, Gondaira S, Higuchi H, Koiwa M, Tajima M, Kohara J, Ogasawara S, Kato Y, Suzuki Y, Murata S, Ohashi K. 2017. Increase of cells expressing PD-1 and PD-L1 and enhancement of IFN- γ production via PD-1/PD-L1 blockade in bovine mycoplasmosis. *Immun Inflamm Dis* **5**: 355–363.

Goto S, Konnai S, Hirano Y, Kohara J, Okagawa T, Maekawa N, Sajiki Y, Watari K, Minato E, Kobayashi A, Gondaira S, Higuchi H, Koiwa M, Tajima M, Taguchi E, Uemura R, Yamada S, Kaneko MK, Kato Y, Yamamoto K, Toda M, Suzuki Y, Murata S, Ohashi K. 2020b. Upregulation of PD-L1 Expression by Prostaglandin E₂

and the Enhancement of IFN- γ by Anti-PD-L1 Antibody Combined With a COX-2 Inhibitor in *Mycoplasma bovis* Infection. *Front Vet Sci* **7**: 12.

Harizi H, Grosset C, Gualde N. 2003. Prostaglandin E₂ modulates dendritic cell function via EP2 and EP4 receptor subtypes. *J Leukoc Biol* **73**: 756–763.

Harris NB, Barletta RG. 2001. *Mycobacterium avium* subsp. *paratuberculosis* in Veterinary Medicine. *Clin Microbiol Rev* **14**: 489–512.

Hirata T, Narumiya S. 2012. Prostanoids as regulators of innate and adaptive immunity. *Adv Immunol* **116**: 143–174.

Hussain T, Shah SZ, Zhao D, Sreevatsan S, Zhou X. 2016. The role of IL-10 in *Mycobacterium avium* subsp. *paratuberculosis* infection. *Cell Commun Signal* **14**: 29.

Igakura T, Stinchcombe JC, Goon PKC, Taylor GP, Weber JN, Griffiths GM, Tanaka Y, Osame M, Bangham CRM. 2003. Spread of HTLV-I between lymphocytes by virus-induced polarization of the cytoskeleton. *Science* **299**: 1713–1716.

Ikebuchi R, Konnai S, Sunden Y, Onuma M, Ohashi K. 2010. Molecular cloning and expression analysis of bovine programmed death-1. *Microbiol Immunol* **54**: 291–298.

Ikebuchi R, Konnai S, Shirai T, Sunden Y, Murata S, Onuma M, Ohashi K. 2011. Increase of cells expressing PD-L1 in bovine leukemia virus infection and enhancement of anti-viral immune responses *in vitro* via PD-L1 blockade. *Vet Res* **42**: 103.

Ikebuchi R, Konnai S, Okagawa T, Yokoyama K, Nakajima C, Suzuki Y, Murata S, Ohashi K. 2013. Blockade of bovine PD-1 increases T cell function and inhibits bovine leukemia virus expression in B cells *in vitro*. *Vet Res* **44**: 59.

Ikebuchi R, Konnai S, Okagawa T, Yokoyama K, Nakajima C, Suzuki Y, Murata S, Ohashi K. 2014. Influence of PD-L1 cross-linking on cell death in PD-L1-expressing cell lines and bovine lymphocytes. *Immunology* **142**: 551–561.

Iwai Y, Ishida M, Tanaka Y, Okazaki T, Honjo T, Minato N. 2002. Involvement of PD-L1 on tumor cells in the escape from host immune system and tumor immunotherapy

by PD-L1 blockade. *Proc Natl Acad Sci USA* **99**: 12293–12297.

Iwai Y, Hamanishi J, Chamoto K, Honjo T. 2017. Cancer immunotherapies targeting the PD-1 signaling pathway. *J Biomed Sci* **24**: 26.

Jobin C, Morteau O, Han DS, Balfour Sartor R. 1998. Specific NF-kappa B blockade selectively inhibits tumour necrosis factor-alpha-induced COX-2 but not constitutive COX-1 gene expression in HT-29 cells. *Immunology* **95**: 537–543.

Johnston ER, Powers MA, Kidd LC, Radke K. 1996. Peripheral blood mononuclear cells from sheep infected with a variant of bovine leukemia virus synthesize envelope glycoproteins but fail to induce syncytia in culture. *J Virol* **70**: 6296–6303.

Kabeya H, Ohashi K, Onuma M. 2001. Host immune responses in the course of bovine leukemia virus infection. *J Vet Med Sci* **63**: 703–708.

Kalinski P. 2012. Regulation of immune responses by prostaglandin E₂. *J Immunol* **188**: 21–28.

Kanda Y. 2013. Investigation of the freely available easy-to-use software “EZR” for medical statistics. *Bone Marrow Transplant* **48**: 452–458.

Keir ME, Francisco LM, Sharpe AH. 2007. PD-1 and its ligands in T-cell immunity. *Curr Opin Immunol* **19**: 309–314.

Keir ME, Butte MJ, Freeman GJ, Sharpe AH. 2008. PD-1 and its ligands in tolerance and immunity. *Annu Rev Immunol* **26**: 677–704.

Khalifeh MS, Al-Majali AM, Stabel JR. 2009. Role of nitric oxide production in dairy cows naturally infected with *Mycobacterium avium* subsp. *paratuberculosis*. *Vet Immunol Immunopathol* **131**: 97–104.

Kobayashi K, Omori K, Murata T. 2018. Role of prostaglandins in tumor microenvironment. *Cancer Metastasis Rev* **37**: 347–354.

Konnai S, Suzuki S, Shirai T, Ikebuchi R, Okagawa T, Sunden Y, Mingala CN,

Onuma M, Murata S, Ohashi K. 2013. Enhanced expression of LAG-3 on lymphocyte subpopulations from persistently lymphocytotic cattle infected with bovine leukemia virus. *Comp Immunol Microbiol Infect Dis* **36**: 63–69.

Konnai S, Murata S, Ohashi K. 2017. Immune exhaustion during chronic infections in cattle. *J Vet Med Sci* **79**: 1–5.

Koyama S, Akbay EA, Li YY, Herter-Sprrie GS, Buczkowski KA, Richards WG, Gandhi L, Redig AJ, Rodig SJ, Asahina H, Jones RE, Kulkarni MM, Kuraguchi M, Palakurthi S, Fecci PE, Johnson BE, Janne PA, Engelman JA, Gangadharan SP, Costa DB, Freeman GJ, Bueno R, Hodi FS, Dranoff G, Wong KK, Hammerman PS. 2016. Adaptive resistance to therapeutic PD-1 blockade is associated with upregulation of alternative immune checkpoints. *Nat Commun* **7**: 10501.

Larkin J, Chiarion-Sileni V, Gonzalez R, Grob JJ, Cowey CL, Lao CD, Schadendorf D, Dummer R, Smylie M, Rutkowski P, Ferrucci PF, Hill A, Wagstaff J, Carlino MS, Haanen JB, Maio M, Marquez-Rodas I, McArthur GA, Ascierto PA, Long GV, Callahan MK, Postow MA, Grossmann K, Sznol M, Dreno B, Bastholt L, Yang A, Rollin LM, Horak C, Hodi FS, Wolchok JD. 2015. Combined Nivolumab and Ipilimumab or monotherapy in untreated melanoma. *N Engl J Med* **373**: 23–34.

Lee E, Kim EJ, Ratthanophart J, Vitoonpong R, Kim BH, Cho IS, Song JY, Lee KK, Shin YK. 2016. Molecular epidemiological and serological studies of bovine leukemia virus (BLV) infection in Thailand cattle. *Infect Genet Evol* **41**: 245–254.

Lee PP, Yee C, Savage PA, Fong L, Brockstedt D, Weber JS, Johnson D, Swetter S, Thompson J, Greenberg PD, Roederer M, Davis MM. 1999. Characterization of circulating T cells specific for tumor-associated antigens in melanoma patients. *Nat Med* **5**: 677–685.

Li H, Edin ML, Gruzdev A, Cheng J, Bradbury JA, Graves JP, DeGraff LM, Zeldin DC. 2013. Regulation of T helper cell subsets by cyclooxygenases and their metabolites. *Prostaglandins Other Lipid Mediat* **104**: 74–83.

Li L, Katani R, Schilling M, Kapur V. 2016. Molecular epidemiology of *Mycobacterium avium* subsp. *paratuberculosis* on dairy farms. *Annu Rev Anim Biosci* **4**:

155–176.

McLane LM, Abdel-Hakeem MS, Wherry EJ. 2019. CD8 T Cell Exhaustion During Chronic Viral Infection and Cancer. *Annu Rev Immunol* **37**: 457–495.

Mekata H, Sekiguchi S, Konnai S, Kirino Y, Honkawa K, Nonaka N, Horii Y, Norimine J. 2015a. Evaluation of the natural perinatal transmission of bovine leukaemia virus. *Vet Rec* **176**: 254.

Mekata H, Sekiguchi S, Konnai S, Kirino Y, Horii Y, Norimine J. 2015b. Horizontal transmission and phylogenetic analysis of bovine leukemia virus in two districts of Miyazaki, Japan. *J Vet Med Sci* **77**: 1115–1120.

Miao J, Lu X, Hu Y, Piao C, Wu X, Liu X, Huang C, Wang Y, Li D, Liu J. 2017. Prostaglandin E₂ and PD-1 mediated inhibition of antitumor CTL responses in the human tumor microenvironment. *Oncotarget* **8**: 89802–89810.

Michalaki V, Syrigos K, Charles P, Waxman J. 2004. Serum levels of IL-6 and TNF-alpha correlate with clinicopathological features and patient survival in patients with prostate cancer. *Br J Cancer* **90**: 2312–2316.

Moore MW, Carbone FR, Bevan MJ. 1998. Introduction of soluble protein into the class I pathway of antigen processing and presentation. *Cell* **54**: 777–785.

Moore RJ, Owens DM, Stamp G, Arnott C, Burke F, East N, Holdsworth H, Turner L, Rollins B, Pasparakis M, Kollias G, Balkwill F. 1999. Mice deficient in tumor necrosis factor-alpha are resistant to skin carcinogenesis. *Nat Med* **5**: 828–831.

Morita I. 2002. Distinct functions of COX-1 and COX-2. *Prostaglandins Other Lipid Mediat* **68-69**: 165175.

Murakami K, Kobayashi S, Konishi M, Kameyama K, Tsutsui T. 2013. Nationwide survey of bovine leukemia virus infection among dairy and beef breeding cattle in Japan from 2009–2011. *J Vet Med Sci* **75**: 1123–1126.

Nataraj C, Thomas DW, Tilley SL, Nguyen MT, Mannon R, Koller BH, Coffman

TM. 2001. Receptors for prostaglandin E₂ that regulate cellular immune responses in the mouse. *J Clin Invest* **108**: 1229–1235.

Nieto Farias MV, Souza FN, Lendez PA, Martínez-Cuesta L, Santos KR, Della Libera AMMP, Ceriani MC, Dolcini GL. 2018. Lymphocyte proliferation and apoptosis of lymphocyte subpopulations in bovine leukemia virus-infected dairy cows with high and low proviral load. *Vet Immunol Immunopathol* **206**: 41–48.

Nishimori A, Konnai S, Okagawa T, Maekawa N, Ikebuchi R, Goto S, Sajiki Y, Suzuki Y, Kohara J, Ogasawara S, Kato Y, Murata S, Ohashi K. 2017. *In vitro* and *in vivo* antiviral activity of an anti-programmed death-ligand 1 (PD-L1) rat-bovine chimeric antibody against bovine leukemia virus infection. *PLoS One* **12**: e0174916.

Norby B, Bartlett PC, Byrem TM, Erskine RJ. 2016. Effect of infection with bovine leukemia virus on milk production in Michigan dairy cows. *J Dairy Sci* **99**: 2043–2052.

Nowicki TS, Hu-Lieskovan S, Ribas A. 2018. Mechanisms of resistance to PD-1 and PD-L1 blockade. *Cancer J* **24**: 47–53.

Ohira K, Nakahara A, Konnai S, Okagawa T, Nishimori A, Maekawa N, Ikebuchi R, Kohara J, Murata S, Ohashi K. 2016. Bovine leukemia virus reduces anti-viral cytokine activities and NK cytotoxicity by inducing TGF- β secretion from regulatory T cells. *Immun Inflamm Dis* **4**: 52–63.

Okagawa T, Konnai S, Ikebuchi R, Suzuki S, Shirai T, Sunden Y, Onuma M, Murata S, Ohashi K. 2012. Increased bovine Tim-3 and its ligand expressions during bovine leukemia virus infection. *Vet Res* **43**: 45.

Okagawa T, Konnai S, Nishimori A, Ikebuchi R, Mizorogi S, Nagata R, Kawaji S, Tanaka S, Kagawa Y, Murata S, Mori Y, Ohashi K. 2016a. Bovine immunoinhibitory receptors contribute to suppression of *Mycobacterium avium* subsp. *paratuberculosis*-specific T-cell responses. *Infect Immun* **84**: 77–89.

Okagawa T, Konnai S, Deringer JR, Ueti MW, Scoles GA, Murata S, Ohashi K, Brown WC. 2016b. Cooperation of PD-1 and LAG-3 contributes to T-cell exhaustion in *Anaplasma marginale*-infected cattle. *Infect Immun* **84**: 2779–2790.

Okagawa T, Konnai S, Nishimori A, Maekawa N, Ikebuchi R, Goto S, Nakajima C, Kohara J, Ogasawara S, Kato Y, Suzuki Y, Murata S, Ohashi K. 2017. Anti-bovine programmed death-1 rat–bovine chimeric antibody for immunotherapy of bovine leukemia virus infection in cattle. *Front Immunol* **8**: 650.

Okagawa T, Konnai S, Nishimori A, Maekawa N, Goto S, Ikebuchi R, Kohara J, Suzuki Y, Yamada S, Kato Y, Murata S, Ohashi K. 2018. Cooperation of PD-1 and LAG-3 in the exhaustion of CD4⁺ and CD8⁺ T cells during bovine leukemia virus infection. *Vet Res* **49**: 50.

Okazaki T, Honjo T. 2007. PD-1 and PD-1 ligands: from discovery to clinical application. *Int Immunol* **19**: 813–824.

Ooshiro M, Konnai S, Katagiri Y, Afuso M, Arakaki N, Tsuha O, Murata S, Ohashi K. 2013. Horizontal transmission of bovine leukemia virus from lymphocytotic cattle, and beneficial effects of insect vector control. *Vet Rec* **173**: 527.

Orlik O, Splitter GA. 1996. Progression to persistent lymphocytosis and tumor development in bovine leukemia virus (BLV)-infected cattle correlates with impaired proliferation of CD4⁺ T cells in response to *gag*- and *env*- encoded BLV proteins. *J Virol* **70**: 7584–7593.

Passwell J, Levanon M, Davidsohn J, Ramot B. 1983. Monocyte PGE₂ secretion in Hodgkin's disease and its relation to decreased cellular immunity. *Clin Exp Immunol* **51**: 61–68.

Pauken KE, Wherry EJ. 2015. Overcoming T cell exhaustion in infection and cancer. *Trends Immunol* **36**: 265–276.

Perez-Ruiz E, Minute L, Otano I, Alvarez M, Ochoa MC, Belsue V, de Andrea C, Rodriguez-Ruiz ME, Perez-Gracia JL, Marquez-Rodas I, Llacer C, Alvarez M, de Luque V, Molina C, Teijeira A, Berraondo P, Melero I. 2019. Prophylactic TNF blockade uncouples efficacy and toxicity in dual CTLA-4 and PD-1 immunotherapy. *Nature* **569**: 428–432.

Pettersen FO, Torheim EA, Dahm AE, Aaberge IS, Lind A, Holm M, Aandahl EM, Sandset PM, Taskén K, Kvale D. 2011. An exploratory trial of cyclooxygenase type 2 inhibitor in HIV-1 infection: downregulated immune activation and improved T cell-dependent vaccine responses. *J Virol* **85**: 6557–6566.

Phipps RP, Stein SH, Roper RL. 1991. A new view of prostaglandin E regulation of the immune response. *Immunol Today* **12**: 349–352.

Prima V, Kaliberova LN, Kaliberov S, Curiel DT, Kusmartsev S. 2016. COX2/mPGES1/PGE₂ pathway regulates PD-L1 expression in tumor associated macrophages and myeloid-derived suppressor cells. *Proc Natl Acad Sci USA* **144**: 1117–1122.

Pyeon D, Diaz FJ, Splitter GA. 2000. Prostaglandin E₂ increases bovine leukemia virus *tax* and *pol* mRNA levels via cyclooxygenase 2: regulation by interleukin-2, interleukin-10, and bovine leukemia virus. *J Virol* **74**: 5740–5745.

Rathnaiah G, Zinniel DK, Bannantine JP, Stabel JR, Gröhn YT, Collins MT, Barletta RG. 2017. Pathogenesis, molecular genetics, and genomics of *Mycobacterium avium* subsp. *paratuberculosis*, the etiologic agent of Johne's disease. *Front Vet Sci* **4**: 187.

Ribas A, Wolchok JD. 2018. Cancer immunotherapy using checkpoint blockade. *Science* **359**: 1350–1355.

Ricciotti E, FitzGerald GA. 2013. Prostaglandins and inflammation. *Arterioscler Thromb Vasc Biol* **31**: 986–1000.

Riches JC, Davies JK, McClanahan F, Fatah R, Iqbal S, Agrawal S, Ramsay AG, Gribben JG. 2013. T cells from CLL patients exhibit features of T-cell exhaustion but retain capacity for cytokine production. *Blood* **121**: 1612–1621.

Rigas B, Goldman IS, Levine L. 1993. Altered eicosanoid levels in human colon cancer. *J Lab Clin Med* **122**: 518–523.

Rodríguez SM, Florins A, Gillet N, de Brogniez A, Sánchez-Alcaraz MT, Boxus M,

- Boulanger F, Gutiérrez G, Trono K, Alvarez I, Vagnoni L, Willems L.** 2011. Preventive and therapeutic strategies for bovine leukemia virus: lessons for HTLV. *Viruses* **3**: 1210–1248.
- Sagata N, Yasunaga T, Tsuzuku-Kawamura J, Ohishi K, Ogawa Y, Ikawa Y.** 1985. Complete nucleotide sequence of the genome of bovine leukemia virus: its evolutionary relationship to other retroviruses. *Proc Natl Acad Sci USA* **82**: 677–681.
- Sajiki Y, Konnai S, Nishimori A, Okagawa T, Maekawa N, Goto S, Nagano M, Kohara J, Kitano N, Takahashi T, Tajima M, Mekata H, Horii Y, Murata S, Ohashi K.** 2017. Intrauterine infection with bovine leukemia virus in pregnant dam with high viral load. *J Vet Med Sci* **79**: 2036–2039.
- Sajiki Y, Konnai S, Okagawa T, Maekawa N, Nakamura H, Kato Y, Suzuki Y, Murata S, Ohashi K.** 2021. A TLR7 agonist activates bovine Th1 response and exerts antiviral activity against bovine leukemia virus. *Dev Comp Immunol* **114**: 103847.
- Schmedtje JF Jr, Ji YS, Liu WL, DuBois RN, Runge MS.** 1997. Hypoxia induces cyclooxygenase-2 via the NF-kappaB p65 transcription factor in human vascular endothelial cells. *J Biol Chem* **272**: 601–608.
- Schwartz I, Levy D.** 1994. Pathobiology of bovine leukemia virus. *Vet Res* **25**: 521–536.
- Scott KA, Moore RJ, Arnott CH, East N, Thompson RG, Scallon BJ, Shealy DJ, Balkwill FR.** 2003. An anti-tumor necrosis factor-alpha antibody inhibits the development of experimental skin tumors. *Mol Cancer Ther* **2**: 445–451.
- Seidel JA, Otsuka A, Kabashima K.** 2018. Anti-PD-1 and Anti-CTLA-4 therapies in cancer: mechanisms of action, efficacy, and limitations. *Front Oncol* **8**: 86.
- Sharma P, Hu-Lieskovan S, Wargo JA, Ribas A.** 2017. Primary, adaptive, and acquired resistance to cancer immunotherapy. *Cell* **168**: 707–723.
- Sierro S, Romero P, Speiser DE.** 2011. The CD4-like molecule LAG-3, biology and therapeutic applications. *Expert Opin Ther Targets* **15**: 91–101.

Sohal JS, Singh SV, Tyagi P, Subhodh S, Singh PK, Singh AV, Narayanasamy K, Sheoran N, Singh Sandhu K. 2008. Immunology of mycobacterial infections: with special reference to *Mycobacterium avium* subspecies *paratuberculosis*. *Immunobiology* **231**: 585–598.

Stabel JR. 2006. Host responses to *Mycobacterium avium* subsp. *paratuberculosis*: a complex arsenal. *Anim Heal Res Rev* **7**: 61–70.

Stolina M, Sharma S, Lin Y, Dohadwala M, Gardner B, Luo J, Zhu L, Kronenberg M, Miller PW, Portanova J, Lee JC, Dubinett SM. 2000. Specific inhibition of cyclooxygenase 2 restores antitumor reactivity by altering the balance of IL-10 and IL-12 synthesis. *J Immunol* **164**: 361–370.

Subbaramaiah K, Telang N, Ramonetti TJ, Araki R, DeVito B, Weksler BB, Dannenberg JA. 1996. Transcription of cyclooxygenase-2 is enhanced in transformed mammary epithelial cells. *Cancer Res* **56**: 4424–4429.

Sugimoto Y, Narumiya S. 2007. Prostaglandin E receptors. *J Biol Chem* **282**: 11613–11617.

Suzuki S, Konnai S, Okagawa T, Ikebuchi R, Nishimori A, Kohara J, Mingala CN, Murata S, Ohashi K. 2015. Increased expression of the regulatory T cell-associated marker CTLA-4 in bovine leukemia virus infection. *Vet Immunol Immunopathol* **163**: 115–124.

Szlosarek P, Charles KA, Balkwill FR. 2006. Tumour necrosis factor-alpha as a tumour promoter. *Eur J Cancer* **42**: 745–750.

Tamada K, Chen L. 2006. Renewed interest in cancer immunotherapy with the tumor necrosis factor superfamily molecules. *Cancer Immunol Immunother* **55**: 355–362.

Thommen DS, Schumacher TN. 2018. T cell dysfunction in cancer. *Cancer Cell* **33**: 547–562.

Tomozawa, S, Tsuno NH, Sunami E, Hatano K, Kitayama J, Osada T, Saito S,

Tsuruo T, Shibata Y, Nagawa H. 2000. Cyclooxygenase-2 overexpression correlates with tumour recurrence, especially haematogenous metastasis, of colorectal cancer. *Br J Cancer* **83**: 324–328.

Topalian SL, Hodi FS, Brahmer JR, Gettinger SN, Smith DC, McDermott DF, Powderly JD, Carvajal RD, Sosman JA, Atkins MB, Leming PD, Spigel DR, Antonia SJ, Horn L, Drake CG, Pardoll DM, Chen L, Sharfman WH, Anders RA, Taube JM, McMiller TL, Xu H, Korman AJ, Jure-Kunkel M, Agrawal S, McDonald D, Kollia GD, Gupta A, Wigginton JM, Sznol M. 2012. Safety, activity, and immune correlates of anti-PD-1 antibody in cancer. *N Engl J Med* **366**: 2443–2454.

Van den Broeke A, Cleuter Y, Chen G, Portetelle D, Mammerickx M, Zagury D, Fouchard M, Coulombel L, Kettmann R, Burny A. 1988. Even transcriptionally competent proviruses are silent in bovine leukemia virus induced sheep tumor cells. *Proc Natl Acad Sci USA* **85**: 9263–9267.

VanLeeuwen JA, Forsythe L, Tiwari A, Chartier R. 2005. Seroprevalence of antibodies against bovine leukemia virus, bovine viral diarrhoea virus, *Mycobacterium avium* subspecies *paratuberculosis*, and *Neospora caninum* in dairy cattle in Saskatchewan. *Can Vet J* **46**: 56–58.

Vassiliou E, Jing H, Ganea D. 2003. Prostaglandin E₂ inhibits TNF production in murine bone marrow-derived dendritic cells. *Cell Immunol* **223**: 120–132.

Vila-del Sol V, Fresno M. 2005. Involvement of TNF and NF- κ B in the transcriptional control of cyclooxygenase-2 expression by IFN- γ in macrophages. *J Immunol* **174**: 2825–2833.

Wang D, Wang H, Shi Q, Katkuri S, Walhi W, Desvergne B, Das SK, Dey SK, DuBois RN. 2004. Prostaglandin E₂ promotes colorectal adenoma growth via transactivation of the nuclear peroxisome proliferator-activated receptor delta. *Cancer Cell* **6**: 285–295.

Wang D, DuBois RN. 2010. Eicosanoids and cancer. *Nat Rev Cancer* **10**: 181–193.

Wang D, DuBois RN. 2013. An inflammatory mediator, prostaglandin E₂, in colorectal

cancer. *Cancer J* **19**: 502–510.

Wang D, DuBois RN. 2016. The role of prostaglandin E₂ in tumor associated immunosuppression. *Trends Mol Med* **22**: 1–3.

Wang JC, Xu Y, Huang ZM, Lu XJ. 2018a. T cell exhaustion in cancer: mechanisms and clinical implications. *J Cell Biochem* **119**: 4279–4286.

Wang J, Zhang L, Kang D, Yang D, Tang Y. 2018b. Activation of PGE₂/EP2 and PGE₂/EP4 signaling pathways positively regulate the level of PD-1 in infiltrating CD8⁺ T cells in patients with lung cancer. *Oncol Lett* **15**: 552–558.

Waris D, Siddiqui A. 2005. Hepatitis C virus stimulates the expression of cyclooxygenase-2 via oxidative stress: role of prostaglandin E₂ in RNA replication. *J Virol* **79**: 9725–9734.

Weiss DJ, Evanson OA, de Souza C, Abrahamsen MS. 2005. A critical role of interleukin-10 in the response of bovine macrophages to infection by *Mycobacterium avium* subsp. *paratuberculosis*. *Am J Vet Res* **66**: 721–726.

Weiss DJ, Evanson OA, Souza CD. 2006. Mucosal immune response in cattle with subclinical Johne's disease. *Vet Pathol* **43**: 127–135.

Wherry EJ. 2011. T cell exhaustion. *Nat Immunol* **12**: 492–499.

Wherry EJ, Kurachi M. 2015. Molecular and cellular insights into T cell exhaustion. *Nat Rev Immunol* **15**: 486–499.

Willems L, Kettmann R, Chen G, Portetelle D, Burny A, Derse D. 1992. A cyclic AMP-responsive DNA-binding protein (CREB2) is a cellular transactivator of the bovine leukemia virus long terminal repeat. *J Virol* **66**: 766–772.

Willems L, Kettmann R, Dequiedt F, Portetelle D, Vonèche V, Cornil I, Kerkhofs P, Burny A, Mammerickx M. 1993. *In vivo* infection of sheep by bovine leukemia virus mutants. *J Virol* **67**: 4078–4085.

Windsor PA, Whittington RJ. 2010. Evidence for age susceptibility of cattle to Johne's disease. *Vet J* **184**: 37–44.

Yang Y, Fan W, Mao Y, Yang Z, Lu G, Zhang R, Zhang H, Szeto C, Wang C. 2016. Bovine leukemia virus infection in cattle of China: association with reduced milk production and increased somatic cell score. *J Dairy Sci* **99**: 3688–3697.

Yao C, Sakata D, Esaki Y, Li Y, Matsuoka T, Kuroiwa K, Sugimoto Y, Narumiya S. 2009. Prostaglandin E₂-EP4 signaling promotes immune inflammation through Th1 cell differentiation and Th17 cell expansion. *Nat Med* **15**: 633–640.

Ye B, Liu X, Li X, Kong H, Tian L, Chen Y. 2015. T-cell exhaustion in chronic hepatitis B infection: current knowledge and clinical significance. *Cell Death Dis* **6**: e1694.

Yokoyama U, Iwatsubo K, Umemura M, Fujita T, Ishikawa Y. 2013. The prostanoid EP4 receptor and its signaling pathway. *Pharmacol Rev* **65**: 1010–1052.

Yoshida N, Ikemoto S, Narita K, Sugimura K, Wada S, Yasumoto R, Kishimoto T, Nakatani T. 2002. Interleukin-6, tumour necrosis factor alpha and interleukin-1beta in patients with renal cell carcinoma. *Br J Cancer* **86**:1396–1400.

Yun SJ, Lee B, Komori K, Lee MJ, Lee BG, Kim K, Park S. 2019. Regulation of TIM-3 expression in a human T cell line by tumor-conditioned media and cyclic AMP-dependent signaling. *Mol Immunol* **105**: 224–232.

Zelenay S, van der Veen AG, Böttcher JP, Snelgrove KJ, Rogers N, Acton SE, Chakravarty P, Girotti MR, Marais R, Quezada SA, Sahai E, Reis e Sousa C. 2015. Cyclooxygenase-dependent tumor growth through evasion of immunity. *Cell* **162**: 1257–1270.

SUMMARY IN JAPANESE

和文要旨

牛伝染性リンパ腫 (旧名:牛白血病) およびヨーネ病は、日本で広く蔓延しているウシの慢性感染症である。家畜伝染病予防法に定められたウシの監視伝染病のうち、牛伝染性リンパ腫は最も発生頭数が多く、次いでヨーネ病が 2 番目に多い。そのため、両疾病は日本の畜産業に甚大な被害をもたらす家畜衛生上の重大な課題とみなされているが、現在有効なワクチンや治療法が存在せず、新規制御法の開発が強く望まれている。先行研究において、免疫抑制因子 programmed death (PD)-1 および PD-ligand 1 (PD-L1) を介した T 細胞の疲弊化が、牛伝染性リンパ腫ウイルス (BLV) やヨーネ菌の免疫回避機構の一つであることが示された。一方で抗 PD-L1 抗体などの抗体薬は、PD-1/PD-L1 経路を阻害することで病原体特異的な免疫応答を活性化させることから、BLV 感染症およびヨーネ病に対する新規制御法となる可能性が示された。しかしながら、両疾病の病態進行に伴い、PD-1 や PD-L1 等の免疫抑制因子の発現が誘導される機序はいまだ解明されていない。

PD-1/PD-L1 の発現誘導機序を解明するため本研究では、プロスタグランジン E₂ (PGE₂) に着目した。PGE₂ は、アラキドン酸からシクロオキシゲナーゼ (COX)-2 を含む様々な酵素を介して合成される生理活性物質であり、炎症の誘導に関与するとともに免疫抑制作用を持つことが知られている。また近年、ヒトやマウスの研究において、PGE₂ が PD-1 や PD-L1 を含む免疫抑制因子の発現を制御することが示された。しかしながら獣医学領域において、PGE₂ の免疫抑制作用と感染症の病態形成との関連はほとんど報告がなかったことから、本稿では、まずウシにおける PGE₂ の機能解析およびウシの慢性感染症における PGE₂ の動態解析を行った。また、PGE₂ 産生を阻害する COX-2 阻害剤に着目し、単剤および抗 PD-L1 抗体との併用における治療効果を *in vitro* および *in vivo* にて評価した。さらに、COX-2 阻害剤と抗 PD-L1 抗体の併用によって治療効果が増強された詳細な機序の解明を行った。

第 1 章:ウシにおける PGE₂ の免疫抑制作用および PGE₂ とヨーネ病の関連を解析した。まず PGE₂ の機能解析として、ウシの末梢血単核球 (PBMC) を PGE₂ 存在下で培養したところ、PGE₂ は PBMC からの T helper (Th) 1 サイトカイン産生および T 細胞の増殖能を強く抑制し、免疫抑制因子 PD-L1 の発現を誘導することが示された。このことより、PGE₂ がウシにおいて免疫抑制に関与することが明らかとなった。さらにヨーネ病罹患牛では、血中 PGE₂ 量が増加し、回腸病変部での PGE₂ 発現が亢進していた。一方で、COX-2 阻害剤を用いて PGE₂ の産生を阻害するとヨーネ菌特異的 Th1 応答が活性化されたことから、PGE₂ がヨーネ病の病態進行に伴う免疫抑制に関与することが示唆された。

第2章:BLV感染症とPGE₂の関連を示すために、BLV感染牛におけるPGE₂の動態解析を行った。その結果、BLV感染症の病態進行に伴い、血中PGE₂量が増加することおよび血中PGE₂量がリンパ球数、プロウイルス量およびB細胞におけるPD-L1発現率と正の相関関係にあることが明らかとなった。次に、COX-2阻害剤の治療効果を*in vitro*および*in vivo*で評価した。BLV感染牛由来PBMCをCOX-2阻害剤存在下で培養したところ、COX-2阻害剤がBLV特異的なTh1サイトカイン産生ならびにT細胞増殖を活性化することが示された。また、COX-2阻害剤と抗PD-L1抗体を併用すると、特異的なTh1応答がさらに増強されることも明らかとなった。これら結果をもとに、BLV感染牛に対して「COX-2阻害剤単剤」あるいは「COX-2阻害剤と抗PD-L1抗体の併用」の臨床試験を実施し、抗ウイルス効果を評価した。その結果、COX-2阻害剤は単剤でも有意にBLV感染牛のプロウイルス量を減少させた。さらに併用法は、抗PD-L1抗体単剤では効果が認められないような病態が重度に進行したBLV感染牛に対しても、強い抗ウイルス効果(最大80%減少)を示した。以上より、COX-2阻害剤は単剤および抗PD-L1抗体との併用においてウシの慢性感染症に対する新規制御法として有用である可能性が示された。

第3章:第2章において抗PD-L1抗体およびCOX-2阻害剤の併用によって治療効果が増強された機序を解明するために、抗PD-L1抗体単剤で治療されたBLV感染牛由来の検体を解析した。その結果、抗PD-L1抗体投与後、血中PGE₂濃度が有意に増加することが示された。抗PD-L1抗体治療下に誘導されたPGE₂の役割を解明するために解析を行ったところ、PGE₂が受容体E prostanoïd (EP) 4を介してT細胞の活性を直接抑制することおよび抗PD-L1抗体処置により産生されたTh1サイトカインの一種であるtumor necrosis factor (TNF)- α によってPGE₂産生が誘導されることが明らかになった。以上より、TNF- α によって誘導されたPGE₂が受容体EP4を介して抗PD-L1抗体の治療効果を減弱させている可能性が示唆された。これらの結果をもとに、抗PD-L1抗体とEP4阻害剤の併用法の治療効果の評価を行った。抗PD-L1抗体とEP4阻害剤の併用は、ウシのPBMCおよびマウスの脾細胞からのTh1サイトカイン産生を有意に増加させた。さらにマウスのリンパ腫モデルを用いた試験では、抗腫瘍効果の増強が確認されたことから、本治療戦略が動物種によらず適応可能であることが示唆された。

本研究により、PGE₂はウシの慢性感染症に共通して認められる免疫回避機構の一つであることが示唆された。PD-1/PD-L1経路およびCOX-2/PGE₂/EP4経路を標的とした併用療法が、生体内において抗ウイルス免疫を活性化することが明らかとなり、BLV感染症に対する新規制御法となりうることを示した。本併用療法は、マウスリンパ腫モデルにおいても抗腫瘍効果を増強させたことから、ヒトを含む様々な医療分野への応用が期待される。今後は、より大規模な、もしくはより多くの動物モデルを用いた臨床試験を行い、本研究を基にした新規治療法の効果を詳細に検討する必要がある。